

Hydroacoustic Evaluation of Downstream Fish Passage at John Day Dam in 2002



R.A. Moursund
K.D. Ham
P.S. Titzler

FINAL REPORT
March 2003

Prepared for
the U.S. Army Corps of Engineers
Portland District
Portland, Oregon
under Contract DACW57-00-D-0009
Task Order No. 08



LEGAL NOTICE

This report was prepared by Battelle Memorial Institute (Battelle) as an account of sponsored research activities. Neither Client nor Battelle nor any person action on behalf of either:

MAKES ANY WARRANTY OR REPRESENTATION, EXPRESS OR IMPLIED, with respect to the accuracy, completeness, or usefulness of the information contained in this report, or that the use of any information, apparatus, process, or composition disclosed in this report may not infringe privately owned rights; or

Assumes any liabilities with respect to the use of, or for damages resulting from the use of, any information, apparatus, process, or composition disclosed in this report.

Reference herein to any specific commercial product, process, or service by trade name, trademark, manufacture or otherwise, does not necessarily constitute or imply its endorsement, recommendation, or favoring by Battelle. The views and opinions of authors expressed herein do not necessarily state or reflect those of Battelle.

Hydroacoustic Evaluation of Downstream Fish Passage at John Day Dam in 2002

R.A. Moursund
K.D. Ham
P.S. Titzler

FINAL REPORT
March 2003

Prepared for
the U.S. Army Corps of Engineers
Portland District
Portland, Oregon
under Contract DACW57-00-D-0009

Battelle, Pacific Northwest Division
PO Box 999
Richland, Washington 99352

Executive Summary

Battelle Pacific Northwest Division conducted this study in 2002 for the U.S. Army Corps of Engineers – Portland District (Corps) to evaluate downstream fish passage at John Day Dam. The goal of this fixed-location hydroacoustic study was to estimate fish passage efficiency (FPE) for 12-h (0% daytime and 60% nighttime) and 24-h (constant 30%) spill treatments. The objectives of this study were to 1) estimate the proportion of smolts passing through each passage route for each spill treatment and per proportion of discharge, 2) estimate spatial and temporal differences in juvenile salmonid passage through each route during the two spill treatments, and 3) estimate fish guidance efficiency (FGE) at a modified extended-length submersible bar screen (ESBS) installed in turbine unit 7 and at the remaining units with submersible traveling screens (STS).

The passage monitoring period extended from 18 April to 15 July. The transition from spring to summer occurred 6 June when the dominant species in the Smolt Monitoring Program switched from spring chinook to fall chinook. The installation and operation of the ESBS was delayed until 22 May, after which operation continued through the study period. Each turbine unit and spill bay was sampled with fixed-aspect hydroacoustic sampling techniques. Split-beam transducers were deployed at each deployment type (spill bay, turbine unit guided or unguided passage) with redundancy, where possible, to help characterize the influence of operational differences on the acoustic screen model across the dam. Passage estimates were made from spatial and temporal expansions of fish traces identified by automated tracking software.

Each spill treatment was randomly assigned to the first or last 2 consecutive days within 4-day blocks. Of 21 complete blocks within the study period, 7 were dropped because actual spill levels were well outside of scheduled levels; therefore, only 9 blocks during spring and 5 blocks during summer were used. Blocks with spill levels roughly equivalent to scheduled spill levels were retained to reflect typical operational limitations and to provide a conservative estimate of treatment differences. Spill treatment differences were tested by ANOVA.

FPE during the 12-h spill treatment condition was significantly higher than during the 24-h spill treatment condition (Table S.1). Sixty percent spill at night provided high spill passage efficiency (SPE), and the tendency of smolts to pass via the spillway at night maximized the benefit of increased SPE. Lower nighttime FGE also suggests that efforts to improve SPE at night would have greater-than-proportional effect on FPE for an entire treatment day. The benefit of daytime spill was minimal because daytime fish guidance was high in all treatments. Differences among spill treatments in FGE, SPE, and SPS were not significant in either spring or summer. Our results suggest that passage through non-turbine routes will be maximized by spilling more water during twilight hours to compensate for low FGE during that time.

Table S.1. Mean Fish Passage Metric Values (\pm 95% confidence intervals based on measurement uncertainty) by Season and by Spill Treatment

Metric	Spring		Summer	
	12-h	24-h	12-h	24-h
FPE	93.8 (\pm 2.5)	89.3 (\pm 2.4)	91.6 (\pm 1.0)	88.0 (\pm 0.9)
SPE	78.2 (\pm 5.6)	72.2 (\pm 5.2)	58.4 (\pm 11.0)	60.9 (\pm 11.5)
SPS	2.90 (\pm 0.30)	2.68 (\pm 0.26)	2.10 (\pm 0.30)	2.30 (\pm 0.32)
FGE	69.5 (\pm 12.6)	55.0 (\pm 9.9)	73.3 (\pm 12.6)	61.7 (\pm 10.6)

The occurrence of spill levels outside the treatment ranges provided an opportunity to fit relationships to passage metrics versus actual spill percent. The confounding of spill percent with day and night periods of the planned experimental treatments remains, but relationships illustrate the trade-off between SPE and SPS. As spill percent increases, SPE increases and SPS decreases. The trend in SPE rises rapidly from 0% at 0% spill to approximately 70% at 30% spill and then rises only gradually to 90% at 60% spill.

Hydroacoustic estimates of FGE were 66% for both spring and summer, but a strong diel trend was evident at both STS and ESBS (Table S.2). FGE was lower at night, regardless of screen type. However, ESBS guided a greater proportion of fish than did STS during all seasons and diel periods. In addition, diel trends showed that while the ESBS consistently performed better than the STS intakes, the greatest differences were at night.

Table S.2. Mean FGE (\pm 95% confidence intervals based on measurement uncertainty) by Screen Type, Season, and Diel Period

Screen Type	Spring		Summer	
	Day	Night	Day	Night
STS	86.5 (\pm 2.4)	65.7 (\pm 3.8)	81.9 (\pm 1.8)	45.9 (\pm 2.2)
ESBS	93.2 (\pm 1.0)	86.1 (\pm 1.7)	89.5 (\pm 1.2)	64.8 (\pm 1.7)

Acknowledgments

We sincerely acknowledge the cooperation, assistance, and hard work of the following:

U.S. Army Corps of Engineers staff:

Dan Feil and Mike Langeslay for project oversight; Bob Cordie and Miro Zyndol for their research coordination activities; Don Kumm and all the John Day Dam riggers for their outstanding support and suggestions at the dam; Dick Leatherbury, Mike Colesar, for project administration and engineering; John Day Dam control room operators for hourly dam operations; Don Hibbs, Larry Lawrence, Denise Reynolds, and Chip Pearson for dive coordination and safety; and Paul Williams for supplying the spill gate hydraulic rating curves.

Battelle staff:

Fenton Khan for field installation, repairs, and data management for the field season; Susan Thorsten for tireless server administration, data management, and backups; Eric Robinson for database management and support; Traci Degerman for illustrations and for acting as data sentry; Matt Bleich, Bill Markham, Nate Phillips, and Rhett Zufelt for installation support; and Chris Cook and John Serkowski for providing the computational fluid dynamics model runs and visualizations of the spillway.

Mevatec staff:

Peter Johnson led the team with Carl Shilt, Mike Hanks, and Charlie Escher providing system setup. Kiel Bouchard and Shon Zimmerman were super technicians. Kathy Chandler, Julie Cowart, Chris Holzer, and Keri Taylor were deployment technicians and manual trackers. Daniel Hunt, Nichole Brege, Jeffrey McEwen, Jason Cooper, and Brian Rice were system monitors at the project.

Subcontractors:

John Skalski provided statistical support and guidance. Global Diving and Salvage, Inc., installed and removed the powerhouse transducers. Dive Safety Consulting, Inc., provided the on-site dive safety officer. Honald Crane, Inc., provided on-site mobile crane and boom truck support. The Dalles Ironworks provided mount fabrication as well as on-site welding.

Oregon State University:

Cliff Pereira provided many helpful suggestions on the analysis and display of statistical relationships among spill treatments.

NOAA Fisheries:

Dean Brege and Randy Absolon generously shared early 2002 fyke net results.

U.S. Geological Survey, Biological Resources Division:

John Beeman provided the latest radio telemetry study reports through 2001.

Contents

Executive Summary.....	iii
Acknowledgments.....	v
1.0 Introduction.....	1.1
1.1 Background.....	1.1
1.2 Study Goals and Objectives.....	1.1
1.3 Relevance to the Biological Opinion.....	1.2
1.4 Study Site Description.....	1.2
1.5 Report Organization.....	1.3
2.0 Methods.....	2.1
2.1 Study Design.....	2.1
2.2 Hydroacoustic Sampling System.....	2.1
2.3 Powerhouse Sampling.....	2.2
2.3.1 STS Intake Deployment.....	2.3
2.3.2 ESBS Intake Deployment.....	2.4
2.4 Spillway Sampling.....	2.6
2.4.1 Spill Bay Deployment.....	2.6
2.5 Data Processing.....	2.7
2.5.1 Dam Operations.....	2.7
2.5.2 Autotracking.....	2.7
2.5.3 Detectability and Effective Beam Widths.....	2.8
2.5.4 Spatial and Temporal Expansion.....	2.8
2.6 Data Analysis.....	2.9
2.6.1 Organization.....	2.9
2.6.2 Performance Measures.....	2.9
3.0 Results.....	3.1
3.1 Study Conditions.....	3.1
3.1.1 River Discharge and Temperature.....	3.1
3.1.2 Species Composition and Run Timing.....	3.2
3.1.3 Dam Operations.....	3.3

3.2	General Fish Passage	3.5
3.2.1	Seasonal Fish Passage Metrics	3.5
3.2.2	Daily Trends	3.5
3.2.3	Seasonal Diel Passage	3.9
3.2.4	Seasonal Horizontal Distributions	3.11
3.2.5	Continuous Spill Curves	3.14
3.2.6	FGE by Screen Type	3.16
3.2.7	Fish Trajectories	3.18
3.3	Treatment Effects	3.22
3.3.1	Analysis of Variance	3.24
3.3.2	Fish Passage Metrics by Treatment	3.28
3.3.3	Diel Trends by Treatment	3.30
3.3.4	Horizontal Distribution by Treatment	3.35
3.3.5	Vertical Distributions by Treatment	3.38
4.0	Discussion	4.1
4.1	Study Conditions	4.1
4.2	General Fish Passage	4.1
4.2.1	Fish Passage Efficiency	4.1
4.2.2	Spill Passage	4.4
4.2.3	Screens	4.4
4.3	Spill Treatment Effects	4.5
4.3.1	Performance Metrics	4.6
4.3.2	Synthesis of Spill Treatment and Screen Results	4.6
5.0	Conclusions	5.1
6.0	References	6.1
	Appendix A: Statistical Methods for Hydroacoustic Data Analysis at John Day Dam 2002	A.1
	Appendix B: Equipment Diagrams	B.1
	Appendix C: System Setup and Calibration	C.1
	Appendix D: Autotracker Parameters	D.1
	Appendix E: Post Tracking Filters	E.1
	Appendix F: Effective Beam Widths	F.1
	Appendix G: Spill Bay Hydraulics	G.1
	Appendix H: Hourly Spill by Block	H.1
	Appendix I: Raw Data	on CD

Figures

1.1	Plan View of John Day Dam.....	1.3
2.1	Plan View of the Powerhouse Showing each System and Transducer Location.....	2.3
2.2	a) Side View of the Intake Transducer Mount and Cage; b) Front View of the Mount.....	2.4
2.3	a) STS Transducer Aiming Angles and Sampling Volume; b) ESBS Transducer Aiming Angles and Sampling Volume	2.5
2.4	a) Dry Deployment of the ESBS and Transducer Position; b) Split-Beam Transducer and Its Mount Attached to the Top Frame Tube.....	2.5
2.5	Plan View of the Spillway Showing each System and Transducer Locations.....	2.6
2.6	Spillway Transducer Mount Deployment.	2.7
3.1	Daily River Discharge and Temperature for 2002 and the 10-yr Average.	3.1
3.2	Species Composition Data from the John Day Dam Smolt Monitoring Facility.....	3.2
3.3	John Day Dam Smolt Monitoring Program Passage Index and Hydroacoustic Estimates of Run Timing.....	3.2
3.4	Hydroacoustic Estimates Plotted Versus John Day Dam Smolt Monitoring Program Passage Index.....	3.3
3.5	Hourly Dam Operations.....	3.4
3.6	Actual Spill Levels and the Nominal Treatments for the Study.	3.4
3.7	Fish Passage Efficiency (FPE) in Spring and Summer.....	3.6
3.8	Spill Passage Efficiency (SPE) in Spring and Summer.	3.6
3.9	Spill Passage Effectiveness (SPS) in Spring.....	3.6
3.10	Fish Guidance Efficiency (FGE) in Spring and Summer.....	3.7
3.11	Daily Fish Passage Efficiency (FPE) Trend across the Season.	3.7
3.12	Daily Spill Passage Efficiency (SPE) Trend across the Season.....	3.8
3.13	Daily Spill Passage Effectiveness (SPS) Trend across the Season.	3.8

3.14 Daily Fish Guidance Efficiency (FGE) Trend for the Entire Powerhouse across the Season.	3.9
3.15 Diel Passage during the Spring	3.10
3.16 Diel Passage during the Summer.	3.11
3.17 Horizontal Distribution of Fish Passage and Flow during the Spring.....	3.12
3.18 Horizontal Distribution of Fish Passage and Flow during the Summer.....	3.13
3.19 Spring Fish Guidance Efficiency (FGE) by Powerhouse Unit.	3.14
3.20 Summer Fish Guidance Efficiency (FGE) by Powerhouse Unit.....	3.14
3.21 Fish Passage Efficiency vs. Percent Spill by Season and Diel Period.	3.15
3.22 Spill Passage Efficiency vs. Percent Spill by Season and Diel Period.	3.15
3.23 Spill Passage Effectiveness vs. Percent Spill by Season and Diel Period.....	3.16
3.24 Fish Guidance Efficiency vs. Continuous Percent Spill by Season and Diel Period.	3.16
3.25 Comparison of FGE for STS Intakes vs. the ESBS Intake.	3.17
3.26 FGE by Screen Type by Block.	3.17
3.27 Diel Trends of the ESBS and STS in Spring.....	3.18
3.28 Diel Trends of the ESBS and STS in Summer.....	3.18
3.29 Fish Trajectories at an STS Deployment.	3.19
3.30 Fish Trajectories at the ESBS Deployment.....	3.19
3.31 Speeds of Fish and CFD Flow for a 3-, 6-, and 9-ft Gate Opening at the Spillway.....	3.20
3.32 Plunge (the angle in degrees below horizontal) of Fish and CFD Flow for a 3-, 6-, and 9-ft Gate Opening at the Spillwayl.	3.20
3.33 Fish and Flow at the Spillway with a 2-ft (left) and 3-ft (right) Gate Opening	3.21
3.34 Fish and Flow at the Spillway with a 4-ft (left) and 5-ft (right) Gate Opening.	3.21
3.35 Fish and Flow at the Spillway with a 6-ft (left) and 7-ft (right) Gate Opening	3.21
3.36 Fish and Flow at the Spillway with an 8-ft (left) and 9-ft (right) Gate Opening	3.22
3.37 Fish Passage Efficiency (FPE) by Block.	3.23

3.38 Spill Passage Efficiency (SPE) by Block..... 3.23

3.39 Spill Passage Effectiveness (SPS) by Block. 3.24

3.40 Fish Guidance Efficiency (FGE) by Block. 3.24

3.41 a) FPE ANOVA Results, b) SPE ANOVA Results, c) SPS ANOVA Results,
d) FGE ANOVA Results, 3.27

3.42 Fish Passage Efficiency (FPE) by Treatment for the Selected Blocks. 3.29

3.43 Spill Passage Efficiency (SPE) by Treatment for the Selected Blocks..... 3.29

3.44 Spill Passage Effectiveness (SPS) by Treatment for the Selected Blocks. 3.30

3.45 Fish Guidance Efficiency (FGE) by Treatment for the Selected Blocks. 3.30

3.46 Diel Passage during the Spring 12-h Spill Treatment for the Nine Selected Blocks. 3.31

3.47 Diel Passage during the Spring 24-h Spill Treatment for the Nine Selected Blocks. 3.32

3.48 Diel Passage during the Summer 12-h Spill Treatment for Five Selected Blocks..... 3.33

3.49 Diel Passage during the Summer 24-h Spill Treatment for Five Selected Blocks..... 3.34

3.50 Horizontal Passage and Flow Distribution in Spring during the Day and by Treatment
for the Nine Selected Blocks included in the Statistical Comparison of Treatments..... 3.35

3.51 Horizontal Passage and Flow Distribution in Spring during the Night and by Treatment
for the Nine Selected Blocks included in the Statistical Comparison of Treatments 3.36

3.52 Horizontal Passage and Flow Distribution in Summer during the Day and by Treatment
for the Five Selected Blocks included in the Statistical Comparison of Treatments. 3.37

3.53 Horizontal Passage and Flow Distribution in Summer during the Night and by Treatment
for the Nine Selected Blocks..... 3.38

3.54 Vertical Distribution of Guided Fish at STS Units in Spring (left) and Summer (right)..... 3.39

3.55 Vertical Distribution of Unguided Fish at STS Units in Spring (left) and Summer (right)..... 3.39

3.56 Vertical Distribution of Guided Fish at the ESBS Unit in Spring (left) and Summer (right) 3.39

3.57 Vertical Distribution of Unguided Fish at the ESBS Unit in Spring (left) and Summer (right)..... 3.40

3.58 Vertical Distribution of Fish Passing in Spill at a 1-ft Spill Gate Opening in Spring (left) and
Summer (right)..... 3.40

3.59 Vertical Distribution of Fish Passing in Spill at a 2-ft Spill Gate Opening in Spring (left) and Summer (right) 3.40

3.60 Vertical Distribution of Fish Passing in Spill at a 3-ft Spill Gate Opening in Spring (left) and Summer (right) 3.41

3.61 Vertical Distribution of Fish Passing in Spill at a 4-ft Spill Gate Opening in Spring (left) and Summer (right) 3.41

3.62 Vertical Distribution of Fish Passing in Spill at a 5-ft Spill Gate Opening in Spring (left) and Summer (right) 3.41

3.63 Vertical Distribution of Fish Passing in Spill at a 6-ft Spill Gate Opening in Spring (left) and Summer (right) 3.42

3.64 Vertical Distribution of Fish Passing in Spill at a 7-ft Spill Gate Opening in Summer Only 3.42

3.65 Vertical Distribution of Fish Passing in Spill at an 8-ft Spill Gate Opening in Spring (left) and Summer (right) 3.42

3.66 Vertical Distribution of Fish Passing in Spill at All Spill Gate Openings Combined in Spring (left) and Summer (right) 3.43

4.1 Hydroacoustic and Fyke Net Daily Estimates of Fish Guidance Efficiency at Unit 7B 4.4

4.2 Hypothetical Diagram of FPE for an All-ESBS Powerhouse Scenario in Spring. 4.7

4.3 Hypothetical Diagram of FPE for an All-ESBS Powerhouse Scenario in Summer. 4.7

Tables

2.1	Spill Schedule during Study Period with Two-Day Treatment Periods (12-h 0% daytime / 60% nighttime spill and 24-h 30% spill) Randomly Assigned to the First or Last Half of Each Four-Day Block..	2.2
3.1	Mean Actual Spill Levels by Season and Diel Period for the Periods Used in the Statistical Comparison of Treatments.....	3.5
3.2	ANOVA Results for Fish Passage Efficiency (FPE) in Spring for the Nine Selected Blocks.....	3.25
3.3	ANOVA Results for Spill Passage Efficiency (SPE) in Spring for the Nine Selected Blocks.....	3.23
3.4	ANOVA Results for Spill Passage Effectiveness (SPS) in Spring for the Nine Selected Blocks ...	3.23
3.5	ANOVA Results for Fish Guidance Efficiency (FGE) in Spring for the Nine Selected Blocks	3.23
3.6	ANOVA Results for Fish Passage Efficiency (FPE) in Summer for the Five Selected Blocks	3.24
3.7	ANOVA Results for Spill Passage Efficiency (SPE) in Summer for the Five Selected Blocks.....	3.24
3.8	ANOVA Results for Spill Passage Effectiveness (SPS) in Summer for the Five Selected Blocks .	3.24
3.9	ANOVA Results for Fish Guidance Efficiency (FGE) in Summer for the Five Selected Blocks ...	3.24
4.1	Summary of Fixed Location Hydroacoustic Fish Passage Studies from 1988 to 2002	4.3
4.2	Summary of Radio Tag Studies from 1984 to 2000	4.5

1.0 Introduction

This report presents results of a two-part hydroacoustic study of juvenile salmonid passage funded by the Portland District of the U.S. Army Corps of Engineers and conducted at John Day Dam by a team of researchers led by Battelle, Pacific Northwest Division. One part of the study was a comparison of the effect of 12- and 24-h spill treatments. The other was a study of fish guidance efficiency at a unit where modified extended-length submersible bar screens were being tested. The District funded other parallel research on juvenile salmonids in 2002, including a radio telemetry study by the U.S. Geological Survey, Biological Resources Division (USGS BRD) and a fyke net study of fish guidance efficiency by the National Oceanic and Atmospheric Administration, National Marine Fisheries Service (NOAA Fisheries).

1.1 Background

The U.S. Army Corps of Engineers (Corps) is committed to improving fish passage and increasing survival rates for fish passing its hydroelectric projects on the Columbia River. At John Day Dam, this strategy has entailed the use of spill, and the design and testing of a turbine intake extended-length submersible bar screen (ESBS) juvenile bypass system (JBS). Surface collection may also be successful at John Day Dam, either as an augmentation or replacement of the JBS system.

Basic information on fish passage is critical for identifying potential improvements. A first step in improving juvenile migrant passage is to determine current passage rates through available passage routes. Such baseline data are necessary to determine what, where, and how to implement passage improvements. Conversely, without detailed information on fish behavior and distributions across space and time, successful improvements in fish passage efficiency (FPE) are unlikely.

Route-specific survival-rate data for John Day Dam are sparse. However, non-turbine passage routes are generally considered to be safer than turbine passage routes. Intake screens installed at the powerhouse guide fish away from the turbines and into a juvenile bypass system. Spill is generally considered to be a relatively benign passage route; however, higher spill levels can cause the total dissolved gas concentration to quickly exceed levels harmful to fish. Therefore, the benefits of spill are limited. Accurate passage estimates for all routes, when combined with route-specific survival estimates, are necessary to estimate project survival. These data are necessary to evaluate any operational or fish facility modifications.

Data from previous passage route studies have been compiled and summarized in a synthesis report (Anglea et al. 2001). This report provided a compendium of passage route estimates from hydroacoustic and radio telemetry methods from 1980 to 2000. Four fyke net studies have also estimated fish guidance efficiency at this project in 1985, 1986, 1996, and 1999 (Brege et al. 1987, 1997, 2001; Krcma et al. 1986).

1.2 Study Goals and Objectives

The goal of this study was to collect critical information for the Corps' spill passage program to optimize project passage. Specifically, the goal was to determine if downstream migrants would benefit

from 24-h spill at John Day Dam. Specific objectives for this study were to:

- Estimate the proportion of juvenile salmon passing the dam through each passage route, and in relation to discharge
- Test for significant differences in fish passage efficiency, spill passage efficiency/effectiveness, and fish guidance efficiency for the 12-h and 24-h spill treatments
- Present the horizontal and vertical distributions of fish passage at the spillway and powerhouse by diel period, spill level, and spill treatment
- Compare fish guidance efficiency of an ESBS to that of standard-length submersible traveling screens (STS)
- Present the temporal passage patterns for the turbine and spillway for the two spill treatments.

1.3 Relevance to the Biological Opinion

The 2000 Biological Opinion (National Marine Fisheries Service 2000) actions relating to John Day Dam directed the Corps to “continue 24-hour spill investigations to determine juvenile passage and survival benefits” (Actions 54 and 71), and continue “development and investigations of extended submerged intake screens...to optimize guidance and safe passage” (Action 73). This study addresses those actions. The operating criteria identified in the 2002 Fish Passage Plan included 12-hour spill from 6:00 p.m. to 6:00 a.m., at 60% of the outflow up to the total dissolved gas limit. Those criteria define the 12-h treatment condition for this study, against which a 24-h spill treatment was tested. At the time the Biological Opinion was released, the dam was configured with standard-length screens at all 16 main units. The installation of prototype modified ESBS screens in Unit 7 provided the opportunity to evaluate ESBS fish passage performance relative to the STS screens.

1.4 Study Site Description

John Day Dam, located at Columbia River mile 215.6, includes a navigation lock, a spillway with 20 bays, and a 1,975 ft (602 m) long powerhouse comprised of 16 turbines and 4 skeleton bays (Figure 1.1). Standard-length submersible traveling screens (STS) were in all units, except for unit 7, which contained a modified ESBS. A juvenile fish facility is located on the Oregon shore. Turbine units are numbered 1-16 from south to north. Each turbine unit is divided into three intakes, identified as A, B, and C, beginning from the north. With each intake 20 ft (6.1 m) wide, the effective opening for fish passage of an entire turbine unit was 60 ft (18.3 m). Spill bays are numbered from the Washington shore, north to south. Each spill bay opening was 50 ft (15.2 m) across.

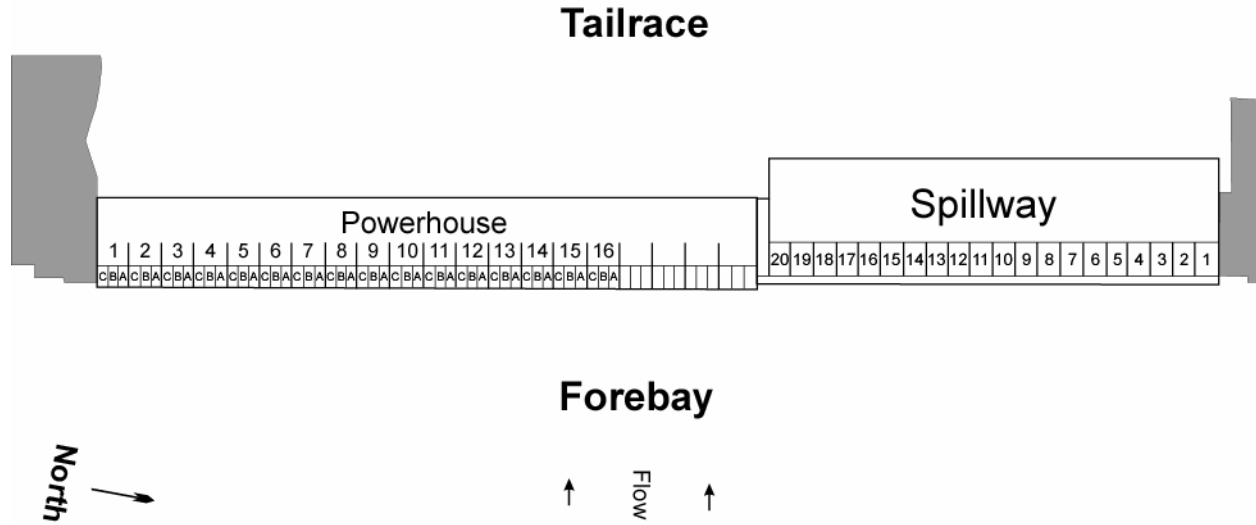


Figure 1.1. Plan View of John Day Dam Powerhouse Units 17-20. The unnumbered spaces at the north end of the powerhouse are skeleton bays that do not pass water or fish.

1.5 Report Organization

This report has several sections. The study and explanation of the research are put into context in Section 1, the Introduction. Section 2, Methods, describes the equipment used and sampling scheme. Section 3 provides results. Section 3.1, “Study Conditions,” describes the environmental and operational characteristics during the 2002 study. Section 3.2, “General Fish Passage,” reports on fish passage efficiency and other project-wide fish passage metrics. Section 3.3, “Spill Treatment Effects,” examines in detail the relationship of spill levels with fish passage. Section 4, the Discussion, interprets these results in relation to current and prior research. Section 5, the Conclusions, wraps up all the information in the context of the questions of interest. Section 6 is References.

Appendix A provides the statistical methods used for data analysis. Appendix B provides schematics of the hydroacoustic equipment used. Appendix C lists calibrations and other specifications for each transducer. Appendix D defines the parameters needed by the autotracker software to process raw sonar data files. Appendix E lists post tracking filters used to filter the data. Appendix F shows the effective beam widths used in this study, which were calculated from a detectability model. Appendix G shows the Spill Bay Hydraulics - flow field output and transducer sampling volume - provided by a dynamic flow model (Flow3D™) which was run for each spill gate opening. Appendix H shows the hourly spill proportions for each four-day block of the study. Appendix I, which is provided on the CD that accompanies the final report, provides the hourly data in comma separated value format.

2.0 Methods

Fixed-aspect hydroacoustic methods were used to estimate fish passage through all routes. Single-beam and split-beam transducers were deployed to estimate fish passage rates and distributions. This approach uses the acoustic screen model to determine passage rates. At each type of passage route (spill bay, turbine or juvenile bypass system), split-beam transducer deployments were used to estimate the average backscattering cross-section of fish for detectability modeling and the direction of fish travel through sampling volumes to assess the assumptions of the acoustic screen model. The transducer sampling volumes were strategically aimed to minimize ambiguity in ultimate fish passage routes and the potential for multiple detections. Hourly estimates of passage through individual routes were combined to evaluate passage performance across varied spatial and temporal scales of interest and in relation to flow.

2.1 Study Design

Spill was manipulated for the purpose of this study. A randomized block design was used with 4-day blocks. A treatment was in place for 2 days and was assigned to either the first or last half of a block. Treatments were either 12-h spill (0% daytime with 60% nighttime) or 24-h spill (constant 30%) (Table 2.1). Each treatment day began at 0600 h and ended at 0559 h. Nighttime extended from 1900 h through 0559 h. Data collection occurred from 18 April through 15 July, 2002. The null and alternate hypotheses for testing may be stated as follows.

H₀: Project passage during 24-h spill does not differ from that during 12-h spill.

H_A: Project passage during 24-h spill differs from that during 12-h spill.

2.2 Hydroacoustic Sampling System

Single-beam data collection employed five Precision Acoustic Systems, Inc. (PAS) single-beam multiplexed systems. Split-beam data collection included three PAS split-beam systems. All of these systems operated at 420 kHz. The single-beam data collection system consisted of Harp-1B Single-Beam Data Acquisition/Signal Processing Software installed on a personal computer controlling a PAS-103 Multi-Mode Scientific Sounder. The PAS-103 sounder then operated multiple PAS 420 kHz single-beam transducers deployed in turbine units or spill bays. The split-beam data collection system required Harp-SB Split-Beam Data Acquisition/Signal Processing Software controlling a PAS-103 Split-Beam Multi-Mode Scientific Sounder. The PAS-103 Sounder then communicated with a PAS-203 Split-Beam Remote 4-Channel Transducer Multiplexer. Finally, the PAS-203 Remote Transducer Multiplexer multiplexed a maximum of four PAS 420 kHz Split-Beam Transducers deployed at a turbine unit or spill bay. Appendix B describes the equipment layout in detail. Appendix C describes the calibration for each system.

Table 2.1. Spill Schedule during Study Period with Two-Day Treatment Periods (12-h 0% daytime / 60% nighttime spill and 24-h 30% spill) Randomly Assigned to the First or Last Half of Each Four-Day Block. The block numbering is based on a preseason schedule that starts at block 3 to retain consistency with other concurrent fish passage studies at John Day Dam in 2002.

Date	%Spill	Block	Date	%Spill	Block	Date	%Spill	Block
18-Apr	0 day / 60 night	3	18-May	30 day / 30 night	10	17-Jun	30 day / 30 night	18
19-Apr	0 day / 60 night	3	19-May	30 day / 30 night	10	18-Jun	30 day / 30 night	18
20-Apr	30 day / 30 night	3	20-May	30 day / 30 night	11	19-Jun	0 day / 60 night	18
21-Apr	30 day / 30 night	3	21-May	30 day / 30 night	11	20-Jun	0 day / 60 night	18
22-Apr	0 day / 60 night	4	22-May	0 day / 60 night	11	21-Jun	0 day / 60 night	19
23-Apr	0 day / 60 night	4	23-May	0 day / 60 night	11	22-Jun	0 day / 60 night	19
24-Apr	30 day / 30 night	4	24-May	0 day / 60 night	12	23-Jun	30 day / 30 night	19
25-Apr	30 day / 30 night	4	25-May	0 day / 60 night	12	24-Jun	30 day / 30 night	19
26-Apr	30 day / 30 night	5	26-May	30 day / 30 night	12	25-Jun	30 day / 30 night	20
27-Apr	30 day / 30 night	5	27-May	30 day / 30 night	12	26-Jun	30 day / 30 night	20
28-Apr	0 day / 60 night	5	28-May	30 day / 30 night	13	27-Jun	0 day / 60 night	20
29-Apr	0 day / 60 night	5	29-May	30 day / 30 night	13	28-Jun	0 day / 60 night	20
30-Apr	30 day / 30 night	6	30-May	0 day / 60 night	13	29-Jun	0 day / 60 night	21
1-May	30 day / 30 night	6	31-May	0 day / 60 night	13	30-Jun	0 day / 60 night	21
2-May	0 day / 60 night	6	1-Jun	0 day / 60 night	14	1-Jul	30 day / 30 night	21
3-May	0 day / 60 night	6	2-Jun	0 day / 60 night	14	2-Jul	30 day / 30 night	21
4-May	30 day / 30 night	7	3-Jun	30 day / 30 night	14	3-Jul	0 day / 60 night	22
5-May	30 day / 30 night	7	4-Jun	30 day / 30 night	14	4-Jul	0 day / 60 night	22
6-May	0 day / 60 night	7	5-Jun	30 day / 30 night	15	5-Jul	30 day / 30 night	22
7-May	0 day / 60 night	7	6-Jun	30 day / 30 night	15	6-Jul	30 day / 30 night	22
8-May	0 day / 60 night	8	7-Jun	0 day / 60 night	15	7-Jul	30 day / 30 night	23
9-May	0 day / 60 night	8	8-Jun	0 day / 60 night	15	8-Jul	30 day / 30 night	23
10-May	30 day / 30 night	8	9-Jun	0 day / 60 night	16	9-Jul	0 day / 60 night	23
11-May	30 day / 30 night	8	10-Jun	0 day / 60 night	16	10-Jul	0 day / 60 night	23
12-May	30 day / 30 night	9	11-Jun	30 day / 30 night	16	11-Jul	0 day / 60 night	24
13-May	30 day / 30 night	9	12-Jun	30 day / 30 night	16	12-Jul	0 day / 60 night	24
14-May	0 day / 60 night	9	13-Jun	30 day / 30 night	17	13-Jul	30 day / 30 night	24
15-May	0 day / 60 night	9	14-Jun	30 day / 30 night	17	14-Jul	30 day / 30 night	24
16-May	0 day / 60 night	10	15-Jun	0 day / 60 night	17	15-Jul	0 day / 60 night	25
17-May	0 day / 60 night	10	16-Jun	0 day / 60 night	17			

2.3 Powerhouse Sampling

Three single-beam and two split-beam systems were used to monitor the turbine intakes. One intake within each of the 16 units was randomly selected and monitored, except for unit 7. Unit 7 had the modified ESBS and was sampled with fyke nets from the b slot; hydroacoustic sampling also took place in the b slot. Pairs of transducers were placed within each randomly selected intake (Figure 2.1). 6° single-beam transducers were deployed at units 1A, 2B, 3C, 4C, 5A, 6B, 8A, 9C, 10A, 13A, 14C, 15B, and 16B. 6° split-beam transducers were deployed at units 7B, 11B, and 12C. Single-beam systems sampled at a rate of 25 pings per second, slow multiplexing 1 transducer at 59- or 74-second intervals, 6 times per hour. The STS split-beam systems in Units 11B and 12C sampled at a rate of 25 pings per second, slow multiplexing 1 transducer at 89-second intervals, 10 times per hour. The ESBS split-beam system in Unit 7B sampled at a rate of 25 pings per second, slow multiplexing 1 transducer at 177-second intervals, 10 times per hour. The STS and ESBS intakes were not sampled with identical deployments. The next two sections describe the deployments and their rationale.

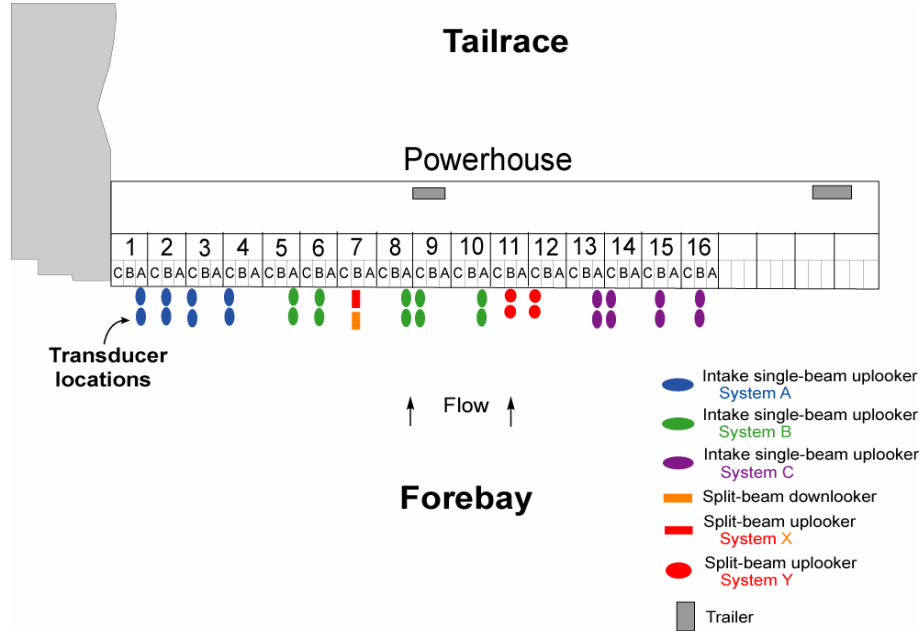


Figure 2.1. Plan View of the Powerhouse Showing each System and Transducer Location

2.3.1 STS Intake Deployment

Intake transducer mounts (Figure 2.2) were designed to fit between the trash rack vertical members, which were spaced approximately 5.5” apart. This design allowed divers to secure the mount to the trash rack from the forebay side of the trash racks. This strategy eliminated the need for more costly and time-consuming penetration dives. Transducer, mount, and cable assemblies were sent down with the diver. The diver then pushed the mount between the vertical trash rack members and secured them to a horizontal member via an existing drain hole. Prior to each transducer mount deployment, a 73’2” long by 2” diameter schedule 40 PVC pipe was deployed through trash rack drain holes that run the entire vertical length of the trash rack. Each PVC pipe was cut so that the bottom end sat just above the head of the transducer. The PVC pipes provided a way to route and protect the telemetry cables from debris and trash raking.

STS intake deployments consisted of two either single-beam or split-beam transducers, mounted at an elevation of 129 ft. One of the two transducers in each intake was intended to sample guided fish and was aimed up and above the STS screen tip at approximately 35° from the plane of the trash rack and looking downstream. Guided transducer aiming angles were adjusted within 33-42° of the plane of the trash rack to minimize noise (multi-path) and avoid unwanted structure (the screen tip) in the sample volume. The second transducer, intended to sample the unguided fish, was aimed up, but below the STS screen tip at approximately 63° from the plane of the trash rack (Figure 2.32a). Unguided transducer aiming angles ranged from 58-64° after adjustments to minimize noise and unwanted structure in the sample volume.

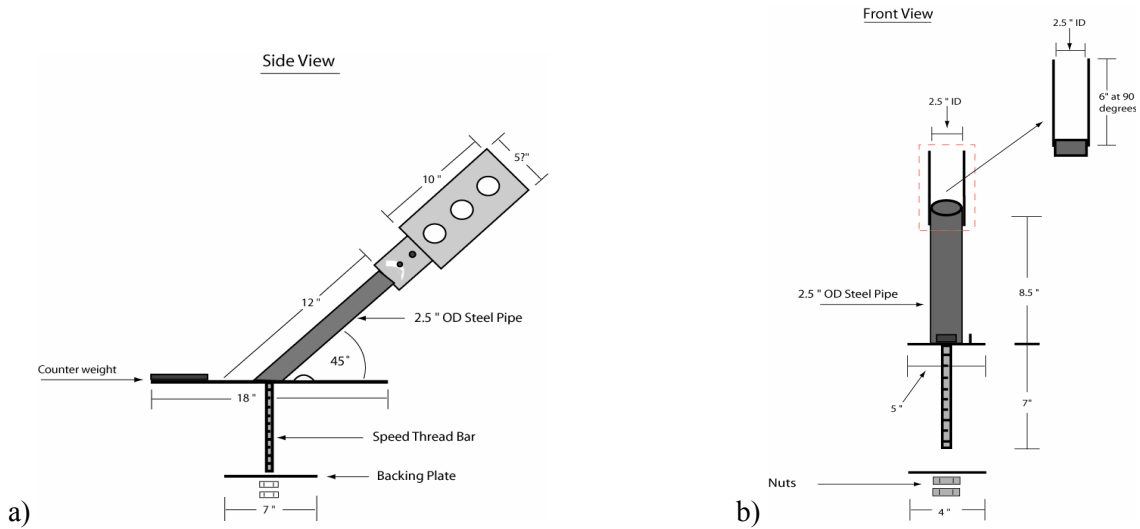


Figure 2.2. a) Side View of the Intake Transducer Mount and Cage; b) Front View of the Mount

2.3.2 ESBS Intake Deployment

At turbine unit 7, the ESBS screen was monitored by two split-beam transducers. A transducer for guided fish was aimed upward in front of the screen, and a transducer for unguided fish was aimed downward from just behind the screen (Figure 2.3b). The fact that the ESBS is twice as long as the STS made the trash rack mount impractical for monitoring unguided fish. The ESBS was not deployed during the optimization study (Ploskey et al. 2002), so both transducers were attached to rotators and optimal aiming angles were determined at deployment. The guided transducer was housed in the same mount as the STS transducers and was deployed in a similar manner, at an elevation of 129 ft. and aimed up and above the screen tip at 37° from the plane of the trash rack. The unguided transducer was attached to the ESBS support frame via a clamping mount (Figure 2.4), and was aimed 53° from vertical downward behind the screen. This put the wide, distal part of the beam where fish were expected to pass, which maximized detectability.

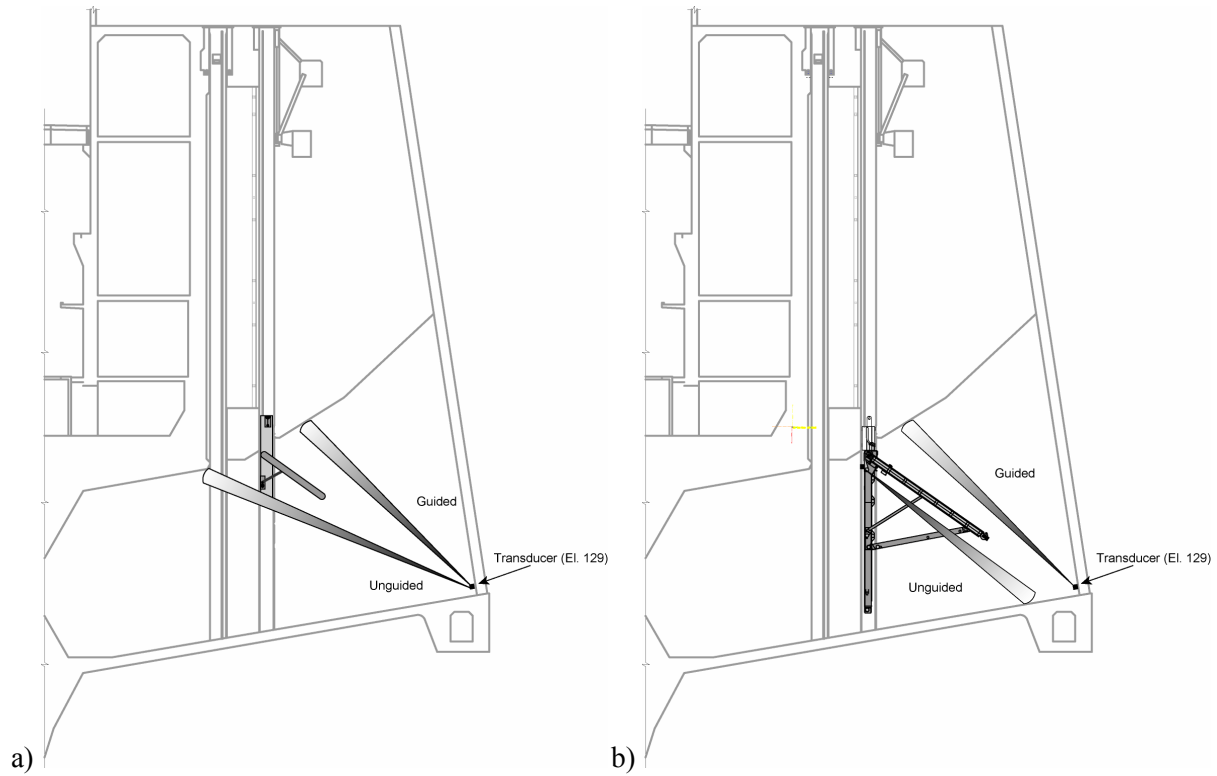


Figure 2.3. a) STS Transducer Aiming Angles and Sampling Volume; b) ESBS Transducer Aiming Angles and Sampling Volume

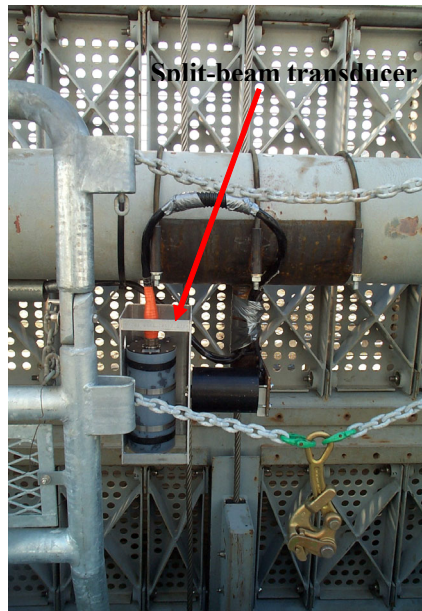


Figure 2.4. a) Dry Deployment of the ESBS and Transducer Position; b) Split-Beam Transducer and Its Mount Attached to the Top Frame Tube

2.4 Spillway Sampling

One split-beam and two single-beam systems were used to monitor the spillway. Every spill bay was monitored, except for bays 1 and 18 (Figure 2.5). The spill pattern for this year did not include spill bay 1, and mechanical failure of the spillway gantry crane prevented installation at bay 18. Each mount was offset in either a north (n), middle (m), or south (s) position to reduce any bias caused by non-uniform distribution within each bay. 10° single-beam transducers were deployed at spill bays 2n, 4s, 5n, 7n, 8s, 10s, 11s, 12n, 13n, 14s, 15m, 16n, 17n, 19m, and 20n. The middle position became unavailable for use after the gantry crane failure as we were able to lift only one of the roadway slabs with a mobile crane. 10° split-beam transducers were deployed at spill bays 3n, 6m, and 9n. The single-beam systems sampled at a rate of 25 pings per second, slow multiplexing each transducer at 74- or 85-second intervals, 6 times per hour. The split-beam system sampled at a rate of 25 pings per second, slow multiplexing each transducer at 118-second intervals, 10 times per hour.

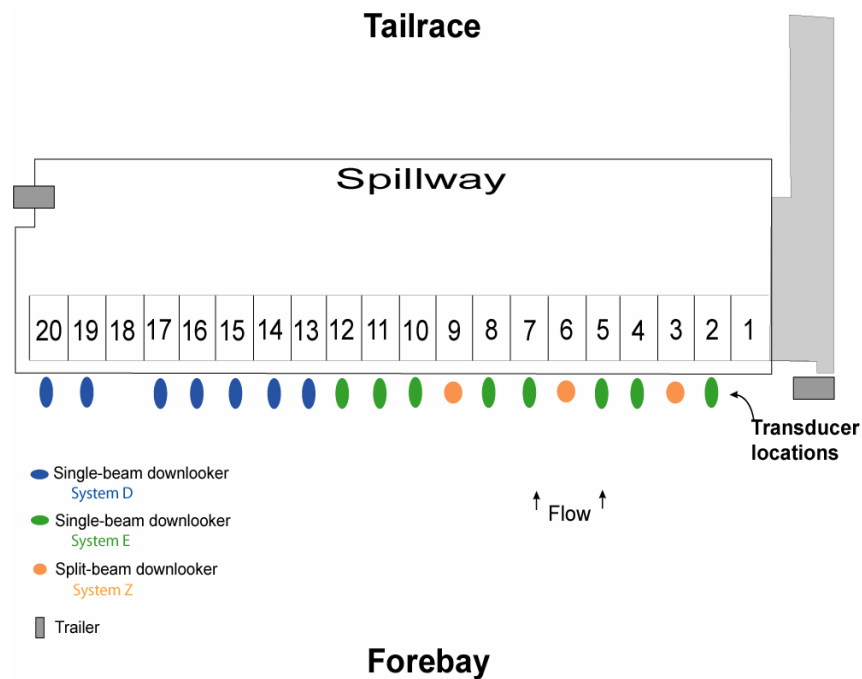


Figure 2.5. Plan View of the Spillway Showing each System and Transducer Locations

2.4.1 Spill Bay Deployment

All single-beam and split-beam transducers were deployed from poles mounted on the downstream side of the stop log slots in the spillway (Figure 2.6). From an elevation of 258 ft., they were aimed 2° downstream from vertical, putting the beam as close to the tainter gate as possible. Sampling volumes as close as possible to the tainter gate assured that fish were committed to passage when detected.

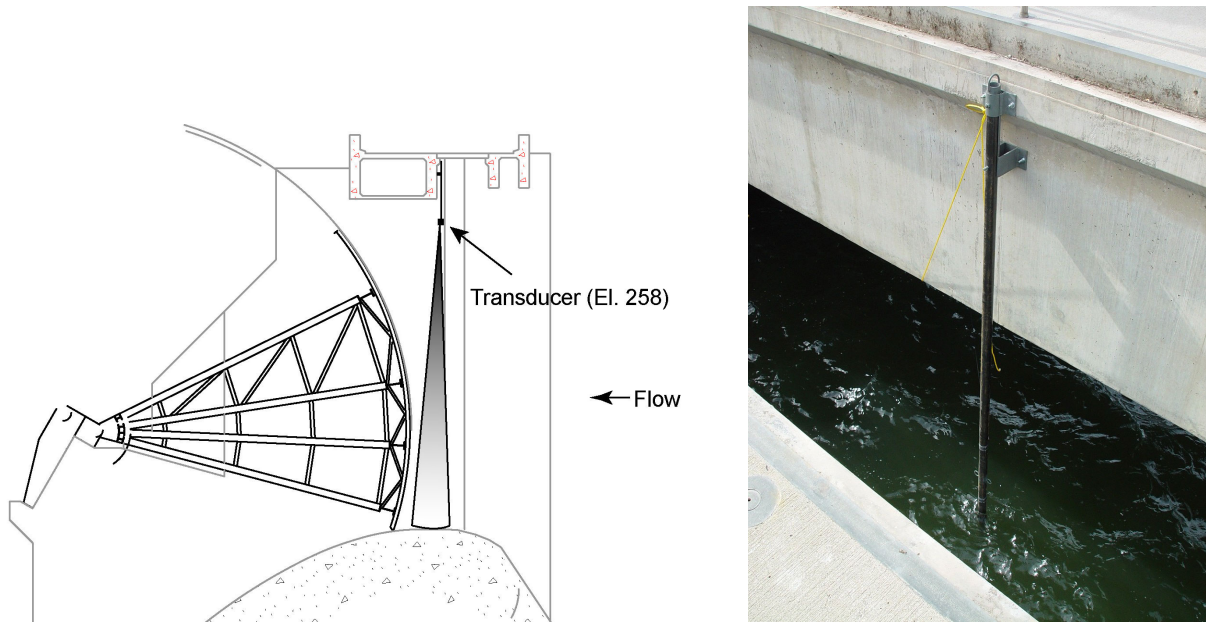


Figure 2.6. Spillway Transducer Mount Deployment. Both the single- and split-beam transducers were mounted in identical configurations.

2.5 Data Processing

2.5.1 Dam Operations

Dam operations data were collected on an hourly basis (24/7) as paper printouts from the control room. Data were manually entered by different technicians into two separate spreadsheets, which were compared to expose transcription errors. Unmatched entries in the two datasets were checked against the original sheets to verify the correct value. The corrected dam operations data was loaded into the database and associated with the fish passage data.

2.5.2 Autotracking

The data produced by both single- and split-beam transducers were processed with autotracking software, which was initially developed by the Portland District and received major revision by Battelle in 2001. The autotracker identifies linear features in echograms. Linear traces that meet minimum criteria are saved as tracks. These criteria were based upon fields contained in the track statistics output by the autotracker and are described in detail in Appendix D. Additional filters eliminate tracks that do not match the criteria established for fish committed to passing. These post-tracking filters were developed to eliminate tracks having characteristics inconsistent with a smolt-sized fish committed to passing the dam by the monitored route. The parameters used are described in Appendix E. The filtered tracks estimate the number of fish passing the sample volume covered by the effective beam of a transducer.

2.5.3 Detectability and Effective Beam Widths

Split-beam data of smolt movements (e.g., trajectory and speed distributions) through the beam were used as an input to a detectability model. The detectability model also originated from the Portland District. The detectability model simulates individual echoes for fish passing through a transducer beam. The fish movement and echo characteristics are simulated to match those measured in split-beam transducers. A simulated fish is tabulated as detected if enough echoes in a series exceed a minimum number of consecutive echoes and echo strength. The proportion of fish detected in the beam is used to compute an effective beam width. The effective beam width more accurately quantifies how well a beam is able to detect fish than the nominal beam width. Effective beam widths are computed for each meter because track characteristics such as angle and speed can change with distance from the transducer.

Effective beam widths correct the spatial expansion factors for the detectability of fish described in the following section. Appendix F shows the effective beam widths used under each operational condition of this study. For regions that contain too few fish to comprise a reasonable statistical sample on the spillway, hydraulic model data is often used to estimate values needed for detectability modeling. In 2002, hydraulic information was available at the spillway, but the increased coverage of the split-beam transducers provided sufficient coverage at all spill gate openings and ranges so that hydraulic information was not required for detectability modeling. The data from a computational fluid dynamics model of the spillway are shown in Appendix G. No hydraulic information was available for the powerhouse at the time of this report.

2.5.4 Spatial and Temporal Expansion

Under the acoustic screen model, the number of tracks within the beam is expanded spatially and temporally to estimate total passage through a single passage route. Detected fish are adjusted for detectability and expanded for space and time not sampled. Hourly passage was estimated by expanding the fish that passed through the beam for the cross-sectional area sampled (Equation 1) and sampled fraction per hour (Equation 2). All remaining analyses and response variables derive from these fundamental data. Appendix I is a comma-delimited matrix of the raw hourly passage data and is included on the CD with this report.

$$W_{ij} = \frac{I_j}{2R_i \tan\left(\frac{\theta_j}{2}\right)} \quad (1)$$

where,

W_{ij} is the i^{th} weighted fish at the j^{th} location

I_j is the width (m) at the j^{th} location

R_i is the midrange (m) of the i^{th} fish

θ_j is the effective beam width of the transducer at the j^{th} location

$$X_{jh} = \left(\frac{K}{k} \right) \sum_{i=1}^{n_{jh}} W_{ijh} \quad (2)$$

where,

X_{jh} is the fish passage at the j^{th} location in the h^{th} hour

W_{ijh} is the i^{th} weighted fish at the j^{th} location in the h^{th} hour

n_{jh} is the number of fish at the j^{th} location in the h^{th} hour

K is the total number of sampling intervals in the hour

k is the number of intervals sampled in the hour.

2.6 Data Analysis

Data analysis consisted of estimating fish passage and integrating that with flow and other conditions for specific time periods and passage routes. These general analysis results were then summarized to address specific questions of interest. Care has been taken to account for both spatial and temporal variation in the sampling. The variances were calculated and carried through to the final estimates. The detailed statistical methods are contained in Appendix A.

2.6.1 Organization

The analysis is divided into sections based on the scope of inference for each section. General fish passage estimates are presented for each season in the first section. Treatment effects are dealt with in the next section. The planned treatment analysis of the stratified random block design was an analysis of variance (ANOVA). A series of ANOVAs were run on the various fish passage metrics such as fish passage efficiency, spill passage efficiency, and spill passage effectiveness. Graphical presentations were used to illustrate treatment effects on metrics for smaller time scales, such as trends among days or blocks.

2.6.2 Performance Measures

The following fish passage metric terms are used extensively in this report. Understanding of the definitions presented here is critical for interpretation of the results of the study. Fish passage efficiency (FPE) is the proportion of fish that passed through non-turbine routes at the dam as a whole (Equation 3). Spill passage efficiency (SPE) is the proportion of fish that passed via the spillway (Equation 4). Both FPE and SPE are unitless ratios that are reported as a percentage to avoid confusion with spill effectiveness. Spill passage effectiveness (SPS) is the ratio of the proportion of fish passing over the spillway vs. the proportion of water passing over the spillway (Equation 5). It is intended to describe the effectiveness that a particular passage route has at passing fish per unit of water. If fish passed the spillway in the same proportion as water, then SPS would equal 1. Fish guidance efficiency (FGE) is the percentage of fish guided into the juvenile bypass system by the intake screens (Equation 6). It is intended to be a measure of screen performance.

$$FPE \equiv \frac{X_{guided} + X_{spillway}}{X_{guided} + X_{unguided} + X_{spillway}} \quad (3)$$

$$SPE \equiv \frac{X_{spillway}}{X_{guided} + X_{unguided} + X_{spillway}} \quad (4)$$

$$SPS \equiv \frac{SPE}{Q_{spillway} / (Q_{powerhouse} + Q_{spillway})} \quad (5)$$

$$FGE \equiv \frac{X_{guided}}{X_{guided} + X_{unguided}} \quad (6)$$

where,

X is the fish passage estimate for the subscripted route

Q is the flow of water through that route.

Estimation of FGE using two transducers requires that fish tracks counted in the guided sample volume are not counted again in the unguided sample volume. A cut-off point for guided fish is set at a distance from the transducer beyond which a fish is presumed to be guided by the screen. The screen itself is downstream of the sample volume, so the cut-off point is determined by estimating whether extrapolated fish trajectories will encounter the screen. Beam locations relative to the screen are illustrated in Figure 2.3. Where flow information is available, extrapolations are made under the assumption that fish will travel in the same direction as flow. Insufficient flow information was available for turbines at John Day Dam, so cutoffs are based only on extrapolation of fish trajectories. Error in the estimation of the cut-off point could result in over- or under-estimation of guided fish passage. Inaccurate estimates of guided fish passage would bias estimates of FGE. Biased estimates of FGE would have the potential to bias FPE, SPE, and SPS.

3.0 Results

The presentation of results begins with environmental conditions of the study, such as river flow and run timing by species. Next, seasonal (spring and summer) estimates of fish passage are described. This includes seasonal and daily trends, but not operational treatments. The last section deals exclusively with the analysis of the operational treatments. The statistics used and inferences drawn from the two sections are distinct.

3.1 Study Conditions

The environmental and dam operational characteristics during the 2002 study are described in this section. These data set the stage and context for the fish passage results that follow. In general, river flows were about average; however, the peak flows arrived late with the peak runoff occurring in the summer study period.

3.1.1 River Discharge and Temperature

River discharge during the study period averaged 274 kcfs, which was 87% of the 10-yr average. The minimum discharge was 171 kcfs on May 12. The maximum discharge was 384 kcfs on June 6. Spring had lower flows (77% of the 10-yr average) than summer (101% of the 10-yr average). Spill averaged 86 kcfs (108% of the 10-yr average) with a low of 38 kcfs on May 2 and a high of 196 kcfs on June 5. Spill was slightly below average during the spring and slightly above average during the summer. River temperature increased steadily over the study period, averaging 13.7°C with the low and high at the beginning and end of the study period, respectively (Figure 3.1).

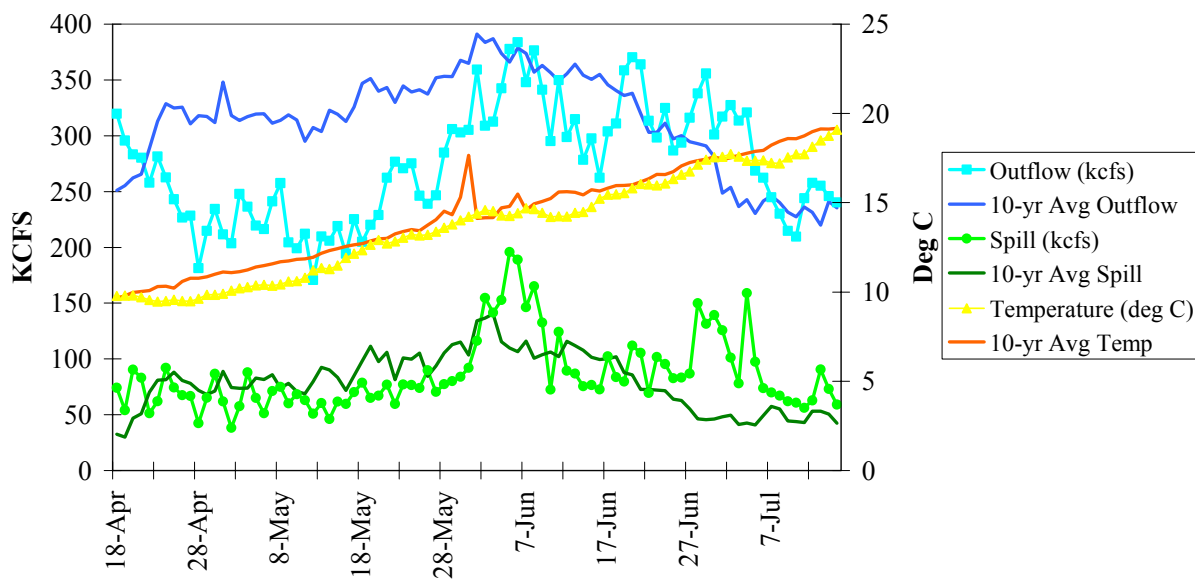


Figure 3.1. Daily River Discharge and Temperature for 2002 (lines with markers) and the 10-yr Average (lines only). Data from DART (www.cbr.washington.edu).

3.1.2 Species Composition and Run Timing

Species composition and run timing data for juvenile salmonids are presented below. The division of spring and summer for the analyses in this report was based on the transition of dominance of the run from yearling chinook to subyearling chinook on June 6. During spring, 55% of the downstream migrants were yearling chinook, 24% were sockeye, and 13% were steelhead as indicated by smolt monitoring data from the sampling site at John Day Dam. The remainder of the run consisted of coho and subyearling chinook smolts. During summer, 91% of the downstream migrants were subyearling chinook (Figure 3.2). The John Day Dam smolt monitoring program passage index for all species combined and hydroacoustic estimates show similar run timing (Figure 3.3 and Figure 3.4).

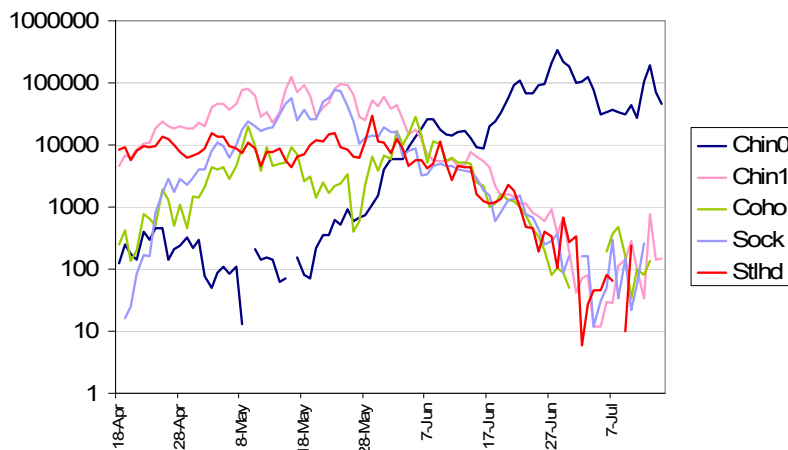


Figure 3.2. Species Composition Data from the John Day Dam Smolt Monitoring Facility. Data from DART (www.cbr.washington.edu).

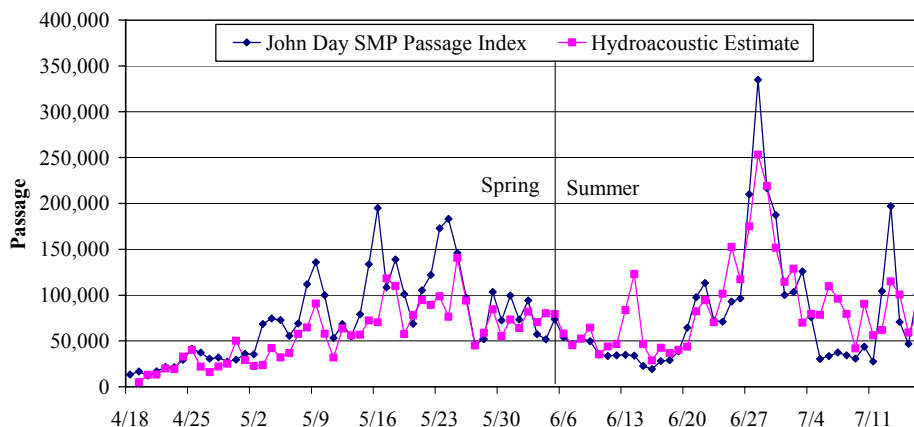


Figure 3.3. John Day Dam Smolt Monitoring Program Passage Index and Hydroacoustic Estimates of Run Timing

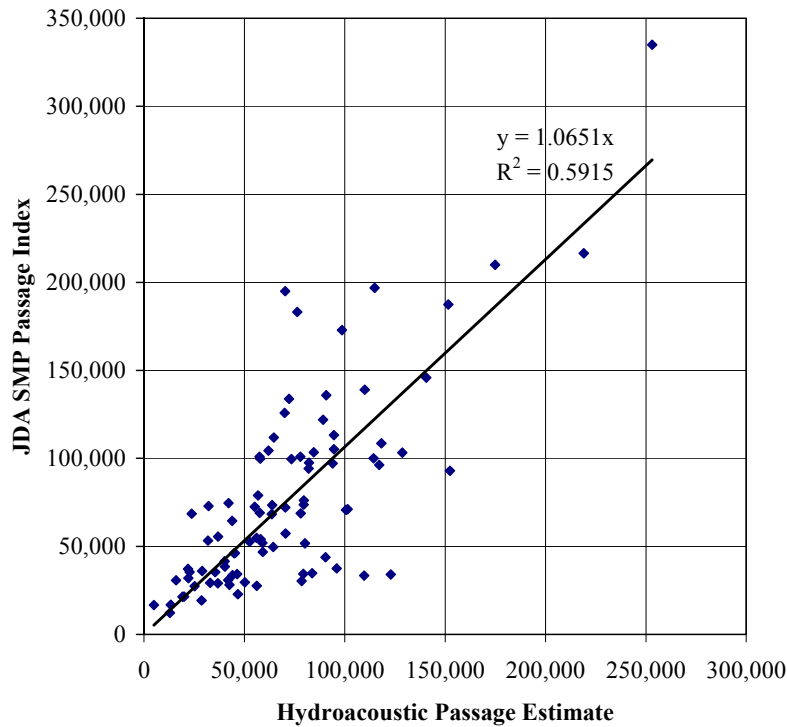


Figure 3.4. Hydroacoustic Estimates Plotted Versus John Day Dam Smolt Monitoring Program Passage Index (correlation, $R^2 = 0.59$)

3.1.3 Dam Operations

Hourly dam operations data illustrate the range of operations at the dam. Both powerhouse and spillway discharge reflect the spill treatment schedule. Recall that spill treatments were either 12-h spill (0% daytime with 60% nighttime) or 24-h spill (constant 30%), with each treatment in place for the first or last half of 4-day blocks. Forebay elevation was nearly constant, varying only between 263 and 264 ft (Figure 3.5).

The spill treatments were generally met in the spring until the beginning of summer. Mean flows are plotted by block in Figure 3.6 to show when spill treatments were met, when they were not met, and when they were nearly met. Block numbering is derived from the pre-season treatment schedule. We chose to include in statistical comparisons both those blocks where treatments were met and those where they were nearly met. The inclusion of blocks that did not exactly meet the target spill levels may reduce statistical power to differentiate among treatments, but it makes inferences from statistical tests more broadly applicable to realistic dam operations. Graphs of the hourly dam operation conditions of each block are included as Appendix H. The overall achievement in meeting the spill treatment goals is shown in the mean spill levels (Table 3.1). It is particularly important for interpreting the results sections that follow to note that some spill did occur during the scheduled 0% spill periods.

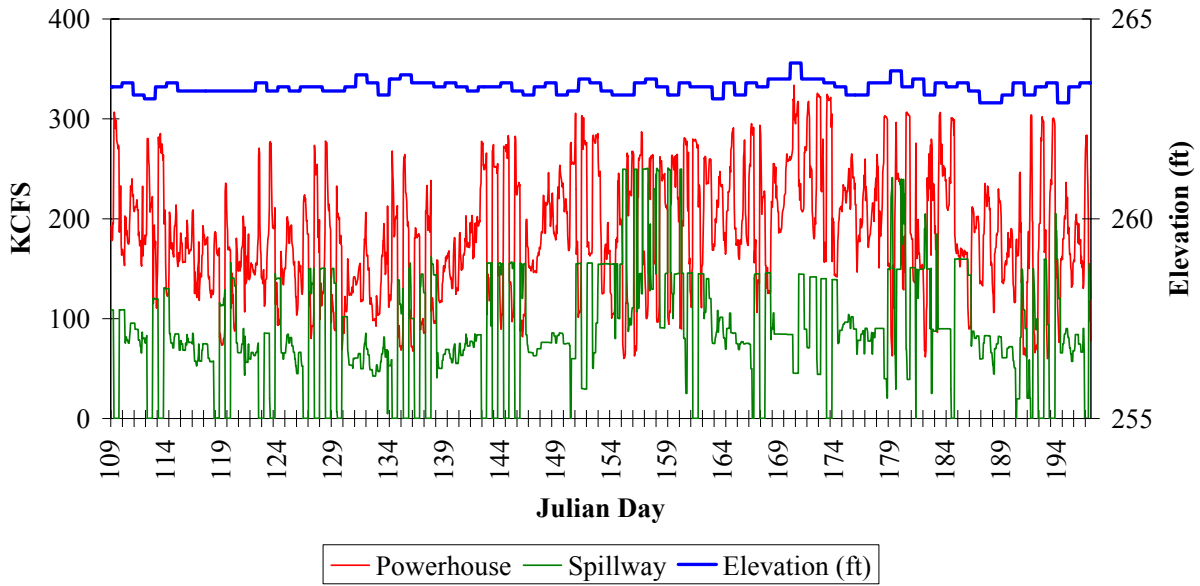


Figure 3.5. Hourly Dam Operations

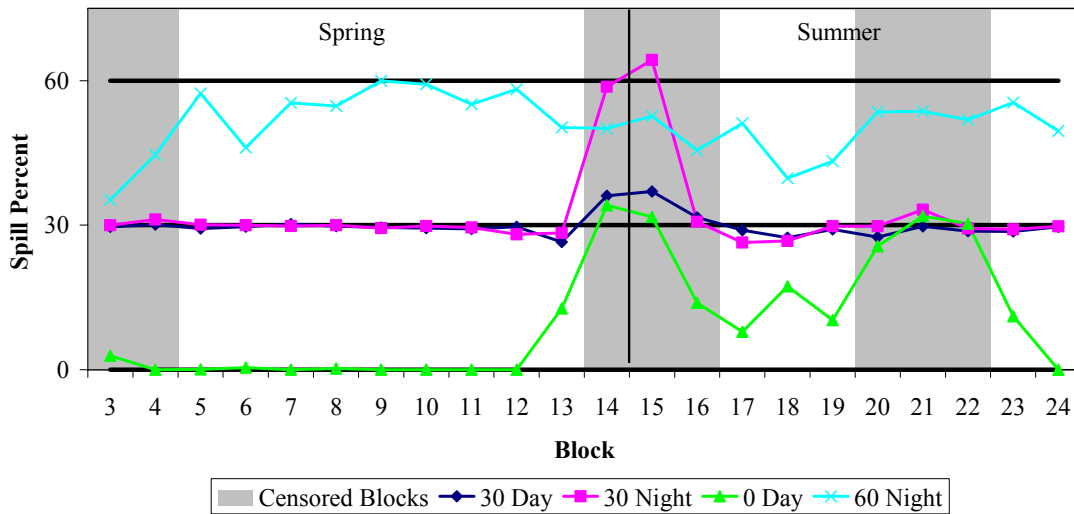


Figure 3.6. Actual Spill Levels and the Nominal Treatments for the Study. Planned spill levels were 0%, 30%, or 60%. Blocks not used in the statistical comparison of treatments are shown in gray.

Table 3.1. Mean Actual Spill Levels by Season and Diel Period for the Periods Used in the Statistical Comparison of Treatments

Season	Diel Period	Nominal Treatment	Actual Spill
Spring	Day	0%	6%
Spring	Day	30%	31%
Spring	Night	60%	51%
Spring	Night	30%	36%
Summer	Day	0%	18%
Summer	Day	30%	30%
Summer	Night	60%	49%
Summer	Night	30%	32%

3.2 General Fish Passage

This section describes fish passage at the dam over the entire sampling season. The intent is to illustrate the influence that varying river conditions and species composition may have, independent of spill treatments. Fish passage metrics are based on actual dam operations. All blocks are included, without regard to whether spill treatment conditions were met. The influence of spill treatments cannot be eliminated, so the reader should be aware that it may be evident in this section, especially in diel trends. This section will break metrics out by season (spring|summer) and diel period (day|night). The statistical analysis of the treatment blocks are addressed in the next section.

3.2.1 Seasonal Fish Passage Metrics

These metrics are calculated for spring and summer, and day and night separately. No treatments or blocks are taken into account. Fish passage efficiency (FPE) was $92 \pm 1\%$ in spring, and $89 \pm 1\%$ in summer (Figure 3.7). Overall spill passage efficiency (SPE) was $78 \pm 1\%$ in spring and $67 \pm 1\%$ in summer (Figure 3.8). Overall spill passage effectiveness (SPS) was 2.7 ± 0.1 in spring and 2.3 ± 0.1 in summer (Figure 3.9). Fish guidance efficiency (FGE) was consistently lower at night than during the day ($49 \pm 3\%$ vs. $81 \pm 3\%$, respectively) and averaged at $66 \pm 2\%$ in both spring and summer (Figure 3.10). Both the ESBS and STS units were combined for these estimates.

3.2.2 Daily Trends

Trends in fish passage metrics across the entire sampling season are shown in this section. No block or treatment effects are considered in the computation of the confidence intervals; however, the selected blocks used in the analysis of the next section are shown simply to avoid the need for duplicating these graphics and to make the reader aware of their potential influence. The fish passage metrics were relatively constant during the season (Figure 3.11 through Figure 3.14).

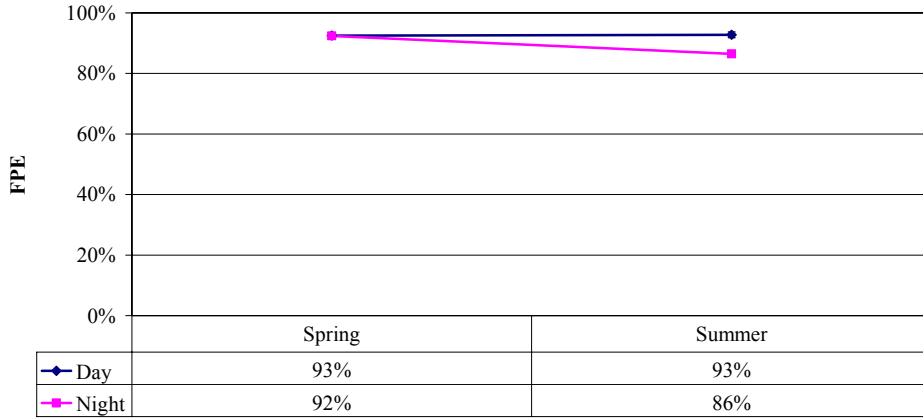


Figure 3.7. Fish Passage Efficiency (FPE) in Spring and Summer. Error bars are 95% confidence intervals based on measurement uncertainty (Equation A29, Appendix A).

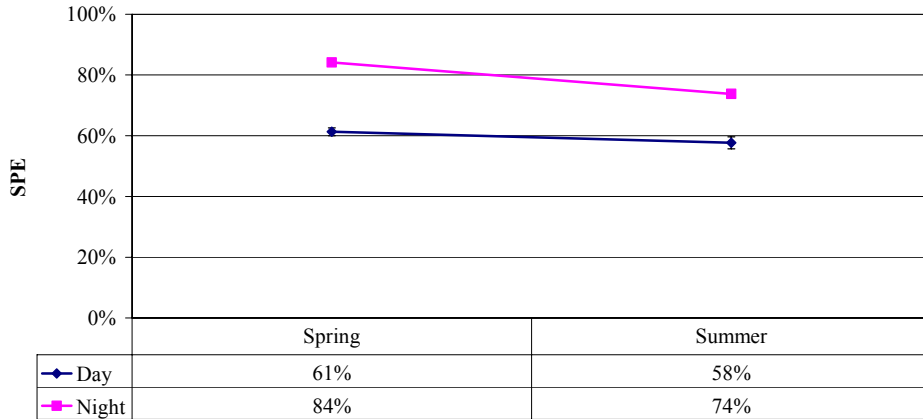


Figure 3.8. Spill Passage Efficiency (SPE) in Spring and Summer. Error bars are 95% confidence intervals based on measurement uncertainty (Equation A29, Appendix A).

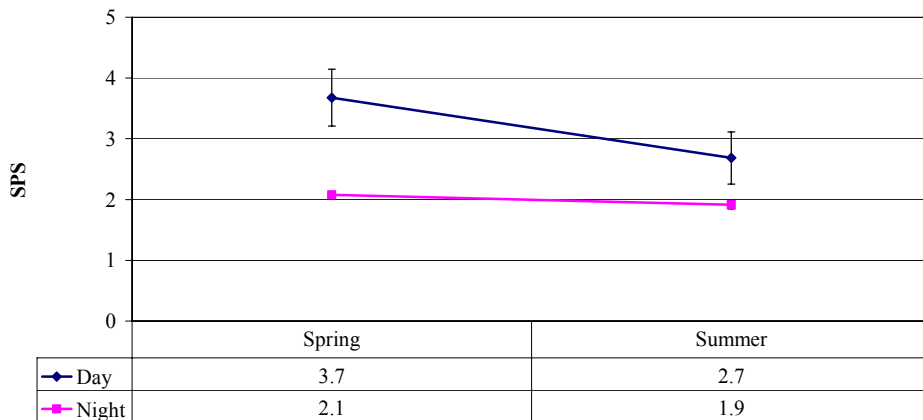


Figure 3.9. Spill Passage Effectiveness (SPS) in spring. Error bars are 95% confidence intervals based on measurement uncertainty (Equation A29, Appendix A).

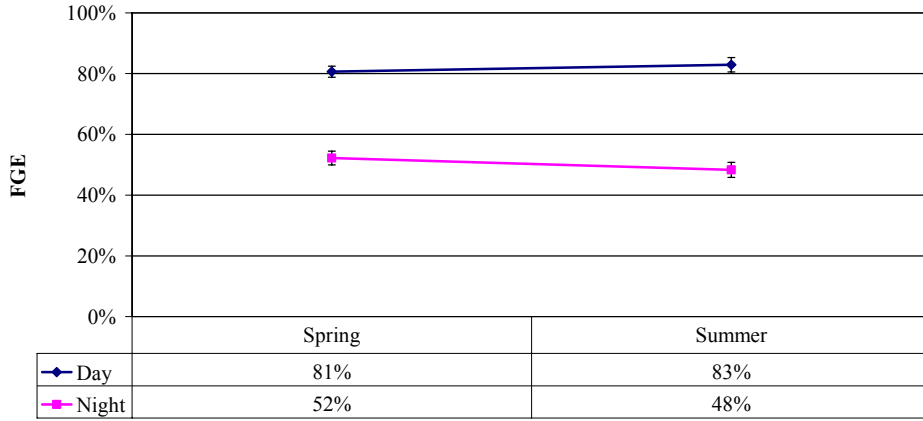


Figure 3.10. Fish Guidance Efficiency (FGE) in Spring and Summer. Error bars are 95% confidence intervals based on measurement uncertainty (Equation A29, Appendix A).

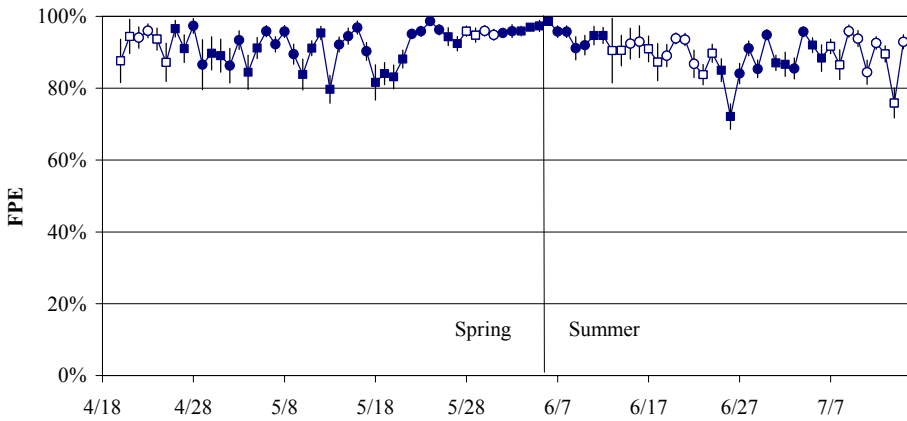


Figure 3.11. Daily Fish Passage Efficiency (FPE) Trend across the Season. The selected treatment periods used in further analyses are shown as solid symbols. Circles indicate days of the 12-h spill treatment, and squares indicate days of the 24-h spill treatment. Error bars are 95% confidence intervals based on measurement uncertainty (Equation A29, Appendix A).

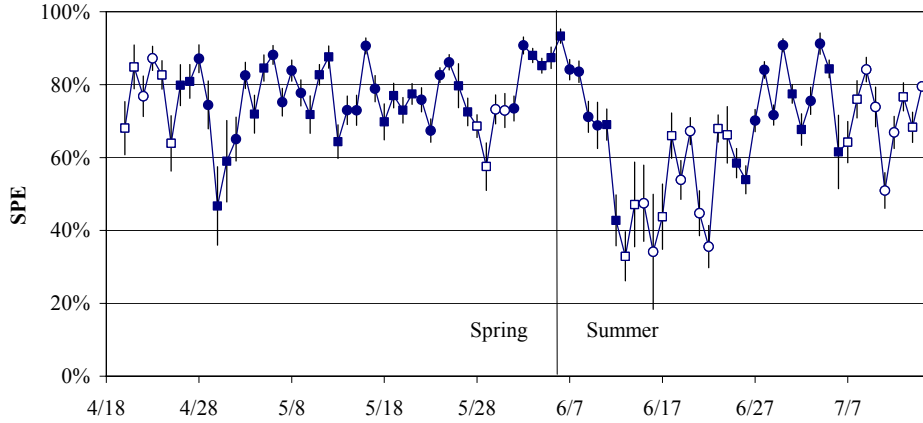


Figure 3.12. Daily Spill Passage Efficiency (SPE) Trend across the Season. The selected treatment periods used in further analyses are shown as solid symbols. Circles indicate days of the 12-h spill treatment, and squares indicate days of the 24-h spill treatment. Error bars are 95% confidence intervals based on measurement uncertainty (Equation A29, Appendix A).

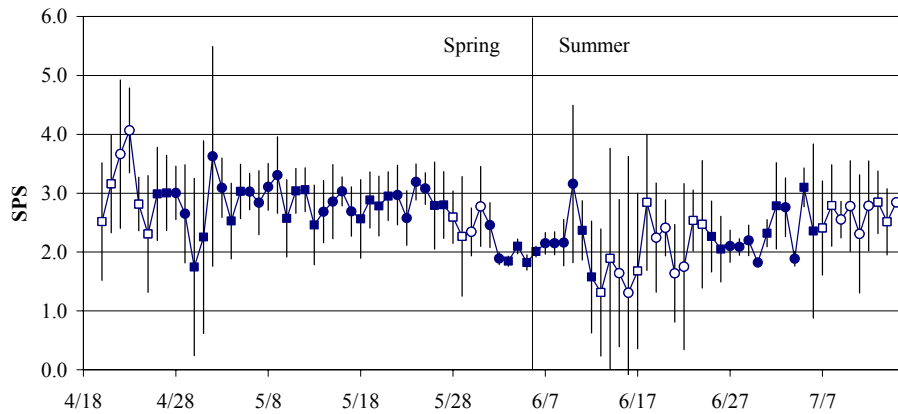


Figure 3.13. Daily Spill Passage Effectiveness (SPS) Trend across the Season. The selected treatment periods used in further analyses are shown as solid symbols. Circles indicate days of the 12-h spill treatment, and squares indicate days of the 24-h spill treatment. Error bars are 95% confidence intervals based on measurement uncertainty (Equation A29, Appendix A).

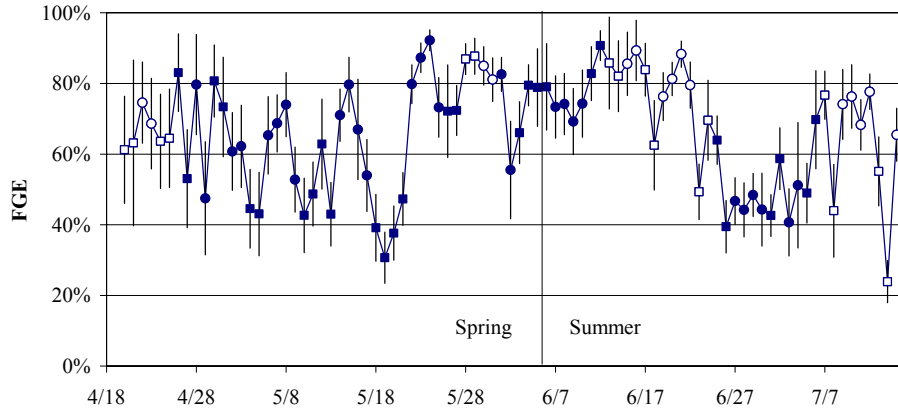


Figure 3.14. Daily Fish Guidance Efficiency (FGE) Trend for the Entire Powerhouse across the Season. STS and ESBS are combined. The selected treatment periods used in further analyses are shown as solid symbols. Circles indicate days of the 12-h spill treatment, and squares indicate days of the 24-h spill treatment. Error bars are 95% confidence intervals based on measurement uncertainty (Equation A29, Appendix A).

3.2.3 Seasonal Diel Passage

Passage trends over the 24-hour day revealed the influence of spill proportion manipulations related to the treatments and fish passage behavior. The specific effects of spill treatments are addressed in Section 3.3. The majority of passage occurred during the nighttime hours in both spring and summer (Figure 3.15 and Figure 3.16). The greater tendency of the summer run to pass unguided through the powerhouse is also clear.

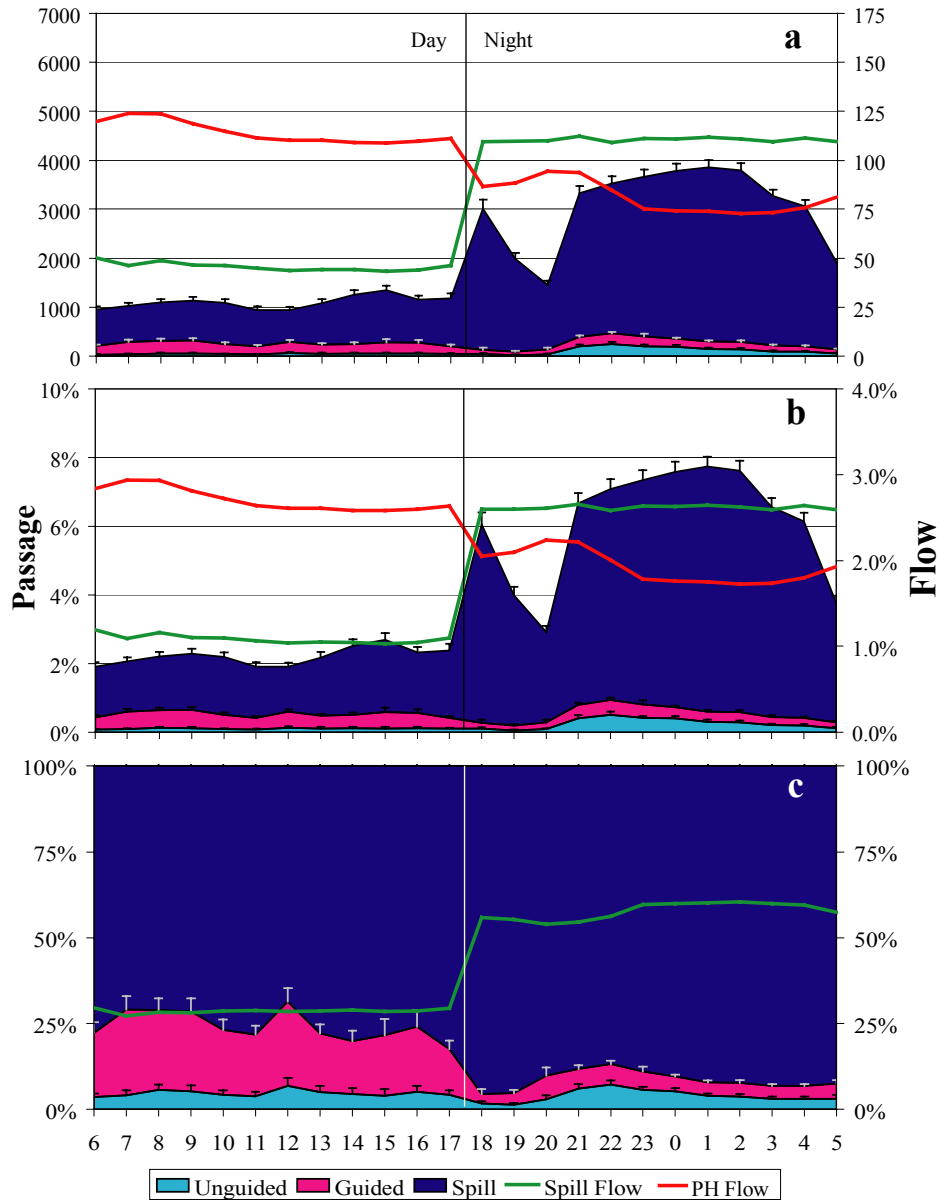


Figure 3.15. Diel Passage during the Spring. All spill treatments were pooled. Passage is expressed as fish/h and flow as kcfs (a), proportion of total (b), and proportion within the hour (c). Error bars are 95% confidence intervals based on measurement uncertainty (Equation A29, Appendix A).

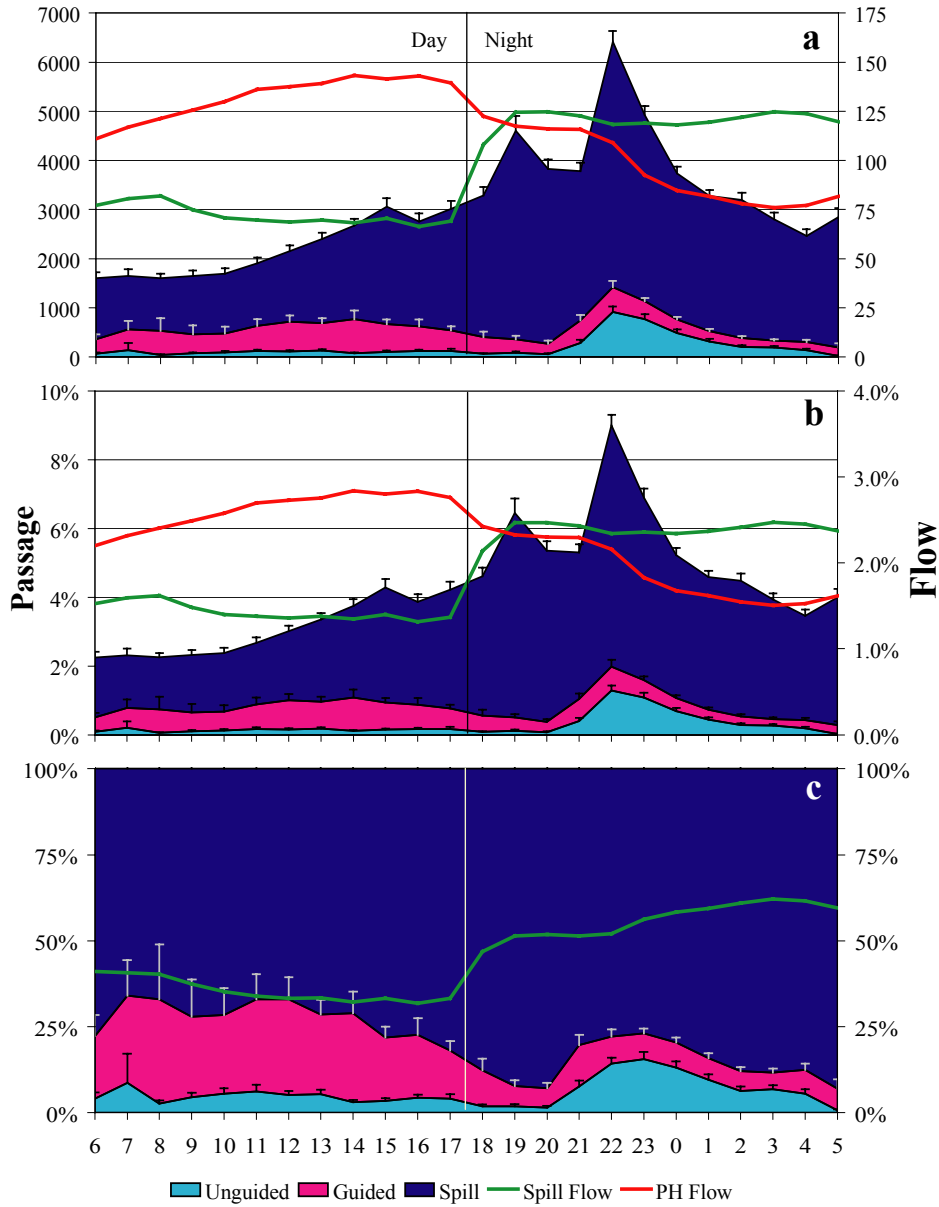


Figure 3.16. Diel Passage during the Summer. All spill treatments were pooled. Passage is expressed as fish/h and flow as kcfs (a), proportion of total (b), and proportion within the hour (c). Error bars are 95% confidence intervals based on measurement uncertainty (Equation A29, Appendix A).

3.2.4 Seasonal Horizontal Distributions

On the following graphs the column chart portion is the fish passage by unit across the entire dam, and the line chart portion is the flow of water by unit. At both the powerhouse and spillway, fish tended to pass in greatest number nearer the shore (Figure 3.17 and Figure 3.18). FGE at individual turbine intakes were highly variable, but unit performance was consistent from spring to summer. FGE was consistently lower at night than during the day. This trend was uniform across the powerhouse (Figure 3.19 and Figure 3.20).

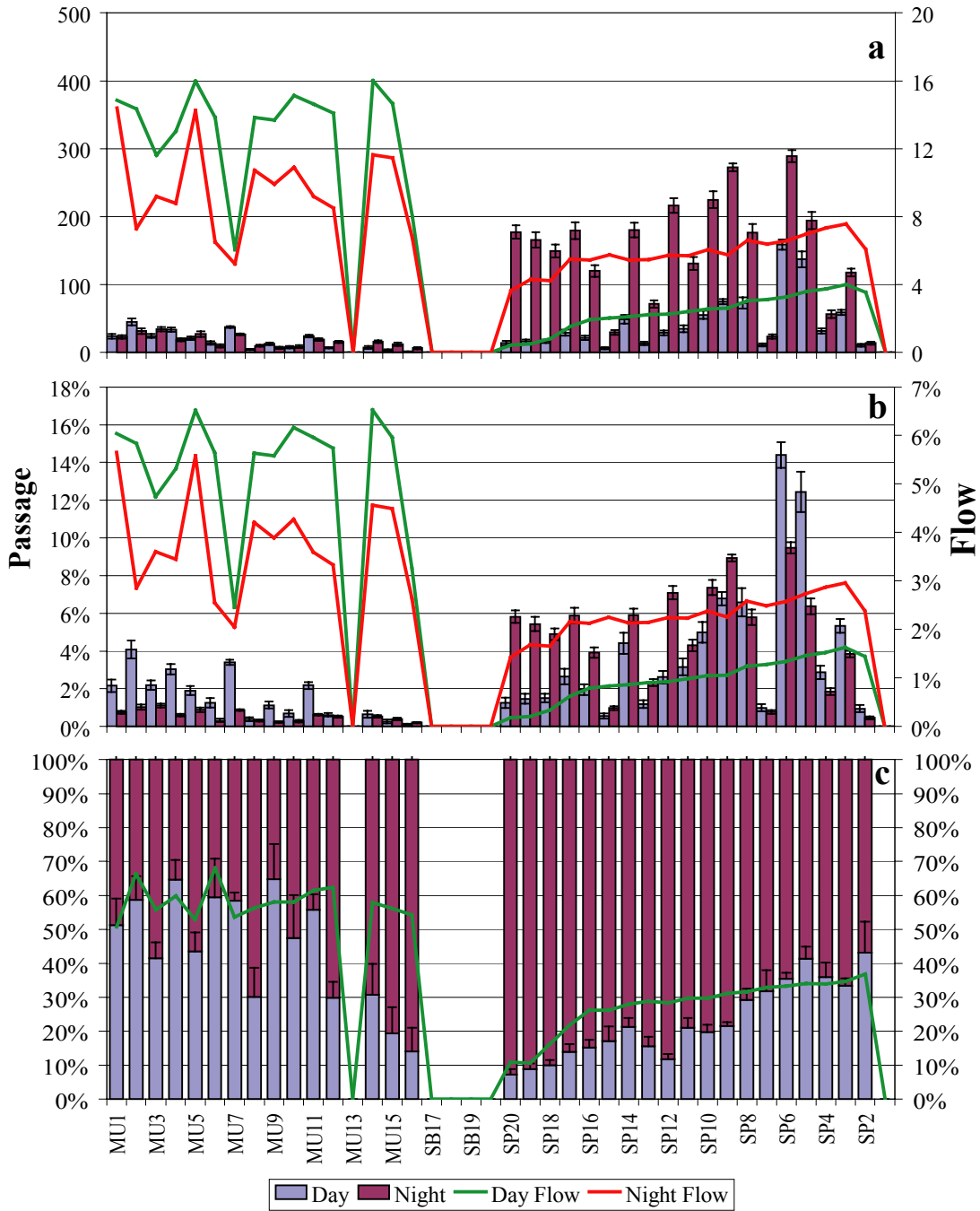


Figure 3.17. Horizontal Distribution of Fish Passage and Flow during the Spring. Passage is expressed as fish/h and flow as kcfs (a), proportion of total (b), and proportion per diel period by route (c). Error bars are 95% confidence intervals based on measurement uncertainty (Equation A29, Appendix A) (MU = main turbine unit, SB = skeleton bay, SP = spill bay).

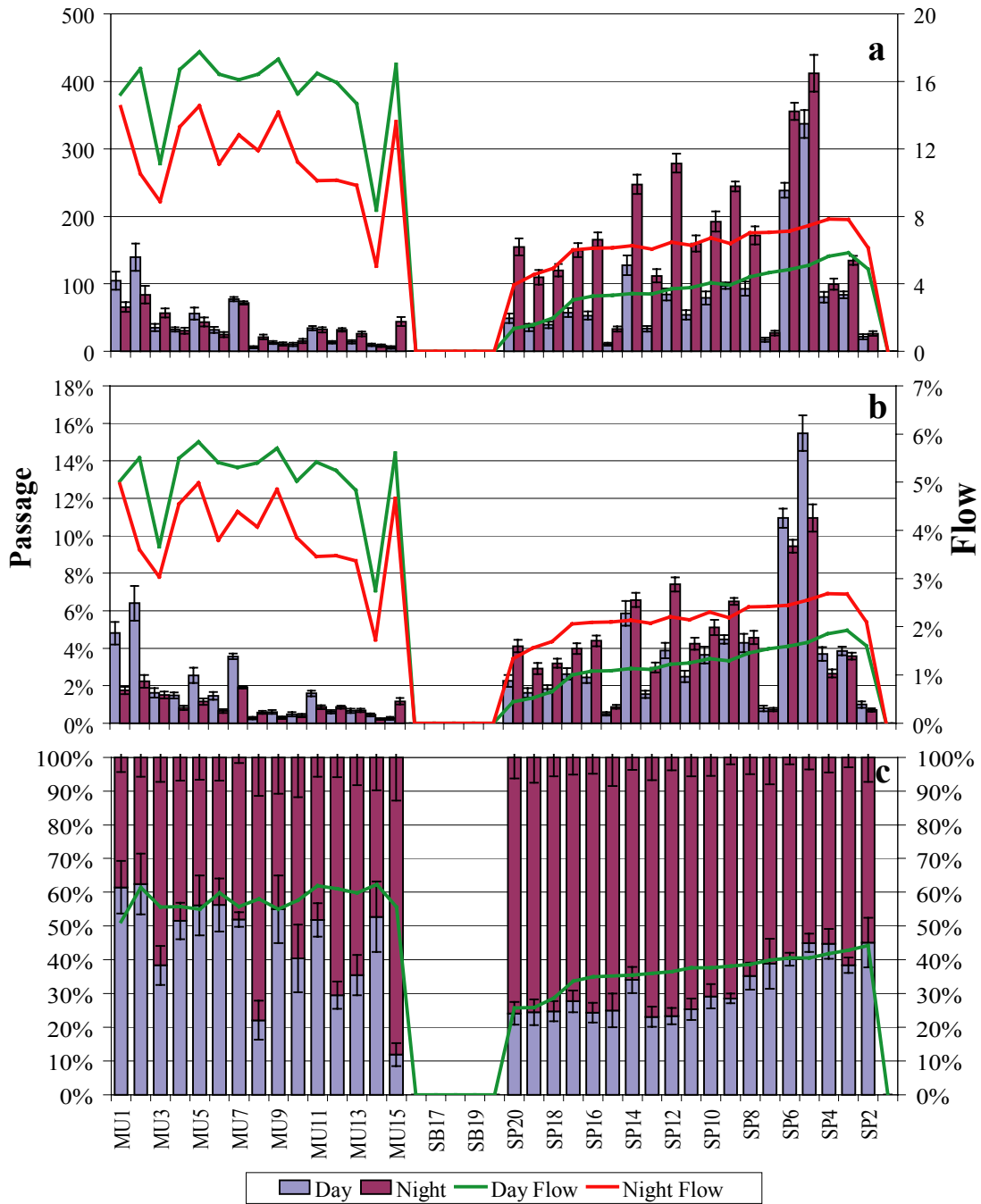


Figure 3.18. Horizontal Distribution of Fish Passage and Flow during the Summer. Passage is expressed as fish/h and flow as kcfs (a), proportion of total (b), and proportion per diel period by route (c). Error bars are 95% confidence intervals based on measurement uncertainty (Equation A29, Appendix A).

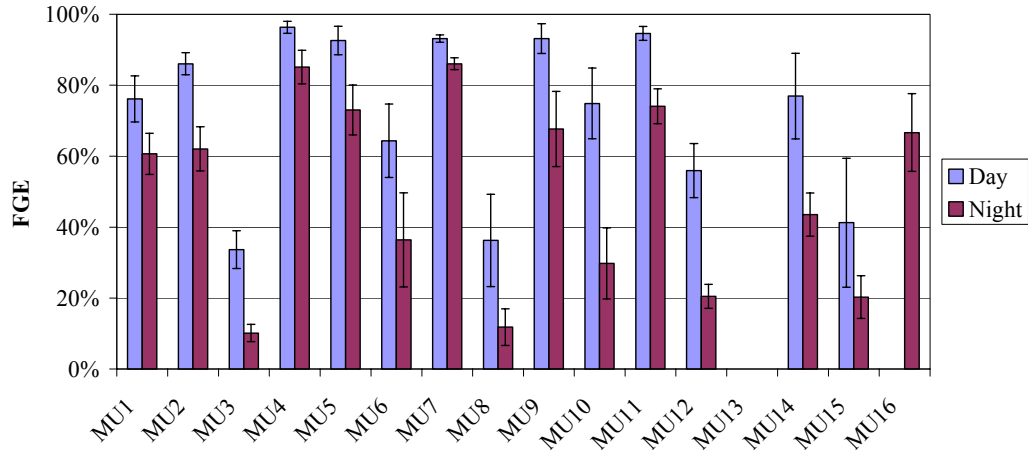


Figure 3.19. Spring Fish Guidance Efficiency (FGE) by Powerhouse Unit. Error bars are 95% confidence intervals based on measurement uncertainty (Equation A29, Appendix A).

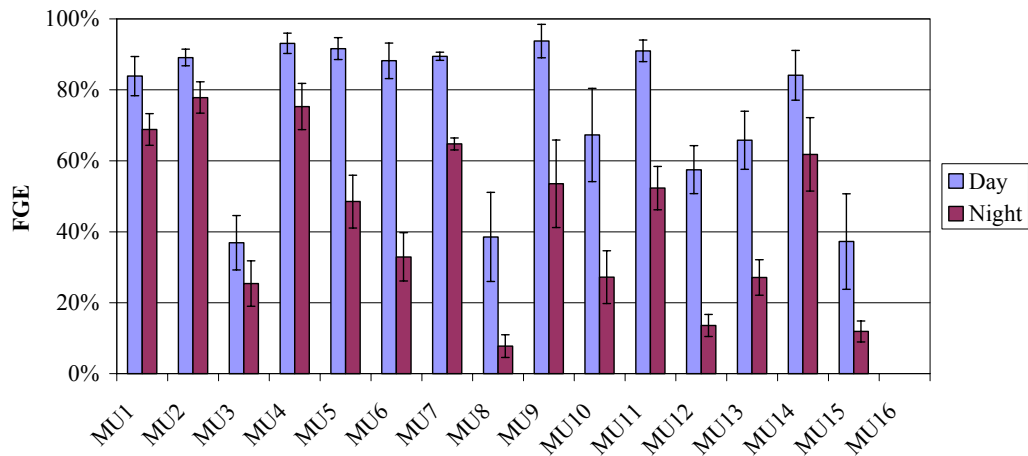


Figure 3.20. Summer Fish Guidance Efficiency (FGE) by Powerhouse Unit. Error bars are 95% confidence intervals based on measurement uncertainty (Equation A29, Appendix A).

3.2.5 Continuous Spill Curves

The failure to meet spill treatment conditions during some periods provided results for spill proportions outside the planned treatments. As a result, it was possible to more fully evaluate the relationship between spill proportion and the passage performance metrics. The additional information is useful, with the caveat that it cannot substitute for a more direct study of spill proportion. Actual proportions are mostly clumped near the planned treatment spill proportions. The amount of time that spill differed widely from the planned treatments was insufficient to account for the influence of factors such as diel period and temporal trends in passage across the sampling season. The data, given these limitations, still provide a basic understanding of the trend of passage performance metrics across spill proportions.

Fish passage efficiency (FPE) generally increased with the proportion of spill, as expected, with more fish proportionately passing via the spillway. Fish passage efficiency was also generally higher during the day than at night for similar percent spill (Figure 3.21). Even in the absence of spill, FPE cannot drop

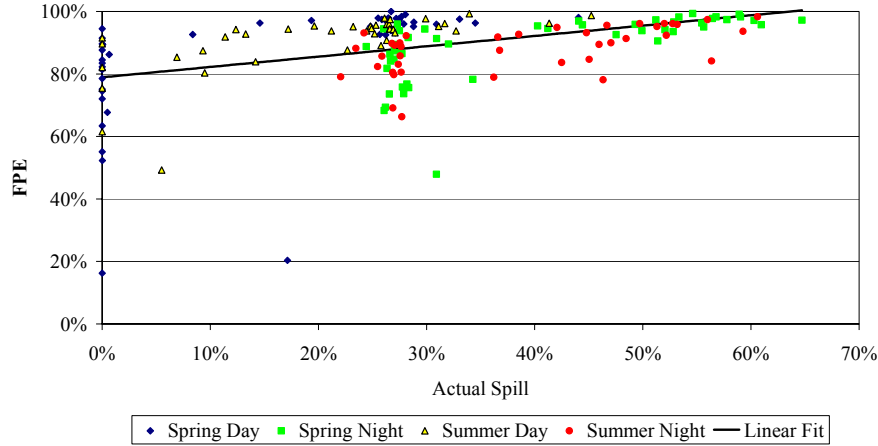


Figure 3.21. Fish Passage Efficiency vs. Percent Spill by Season and Diel Period. The curve fit is linear.

below FGE, so the trend does not approach zero. Spill passage efficiency (SPE) increased with the proportion of spill, and spill passage effectiveness (SPS) decreased rapidly toward 1 with increasing spill proportion (Figure 3.22 and Figure 3.23, respectively). Fish guidance efficiency (FGE) was consistently lower at night and also more variable and lower in the summer (Figure 3.24). The overall trend is partially the result of spill treatment effects, but day and night differences remain when looking only at 30% spill, indicating that fish behavior is influencing FGE.

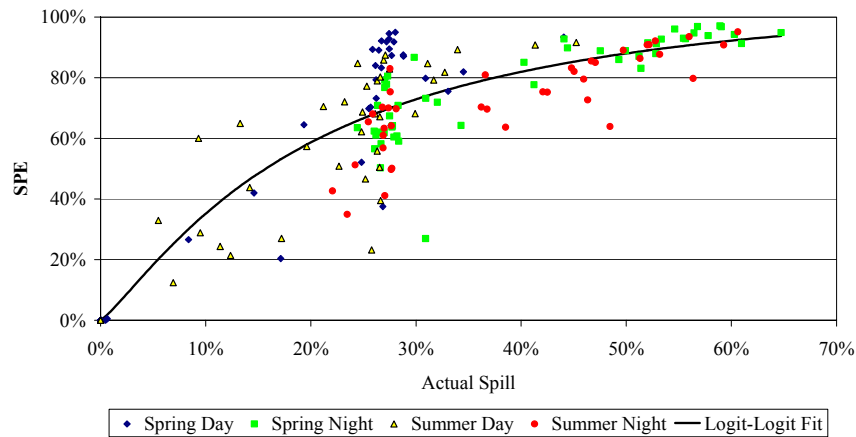


Figure 3.22. Spill Passage Efficiency vs. Percent Spill by Season and Diel Period. The curve fit is logit-logit, which forces the line through both 0,0 and 100,100.

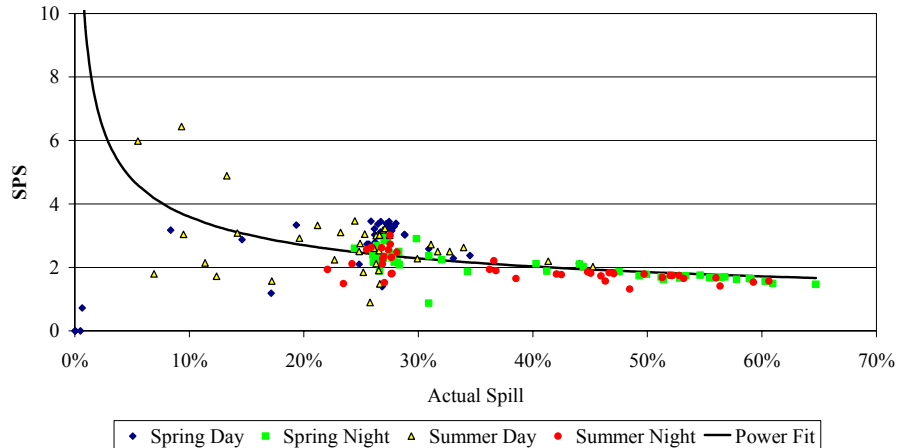


Figure 3.23. Spill Passage Effectiveness vs. Percent Spill by Season and Diel Period. The power curve fit is based on the premise that spill effectiveness should approach infinity where fish pass via an amount of water that approaches 0, and asymptote to 1 where all of the fish pass when all of the water is spilled.

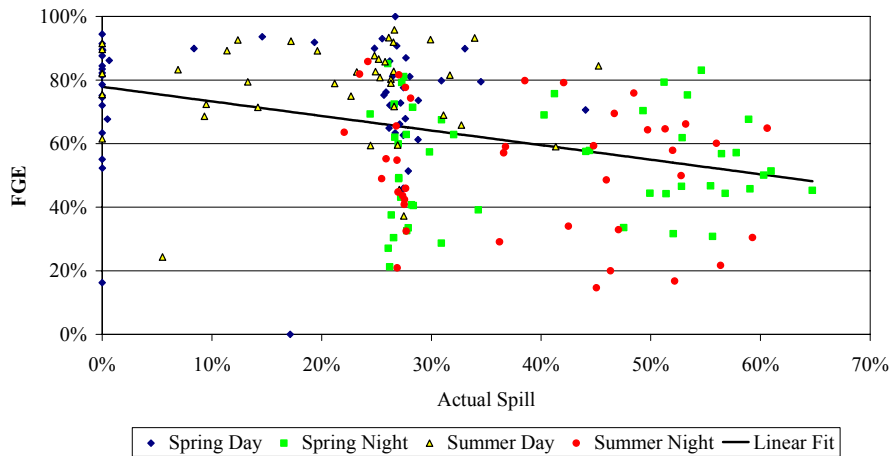


Figure 3.24. Fish Guidance Efficiency vs. Continuous Percent Spill by Season and Diel Period. The curve fit is linear.

3.2.6 FGE by Screen Type

This section compares the performance of the STS intakes with the ESBS intake at unit 7 over the season and includes only the time period following 22 May--when the ESBS unit was operational. The ESBS was operational and available for comparison for the latter third of the spring portion and the entire summer portion of the sampling season. For these comparisons, STS estimates were pooled across the remainder of the powerhouse. Fish guidance efficiency (FGE) at the ESBS was higher than for the STS during spring and summer, day and night. The ESBS made the largest improvement in FGE at night when compared with STS performance, but the difference between screen types was relatively small during daytime hours (Figure 3.25).

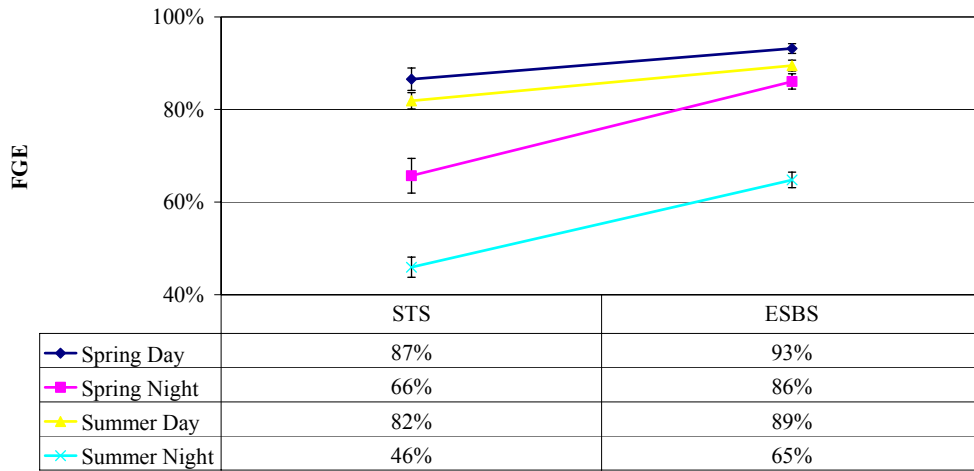


Figure 3.25. Comparison of FGE for STS Intakes vs. the ESBS Intake. Error bars are 95% confidence intervals based on measurement uncertainty (Equation A29, Appendix A).

Variability between blocks of the planned treatment schedule was high, but the ESBS performed consistently better with respect to FGE than the STS (Figure 3.26). STS performance during the period before the ESBS was operational was relatively poor. If the two screen types could have been sampled through the entire spring portion of the season, we could have determined whether ESBS performance was also poor in early spring. The diel trends show that while the ESBS consistently performed better than the STS intakes overall, the greatest differences were at night (Figure 3.27 and Figure 3.28).

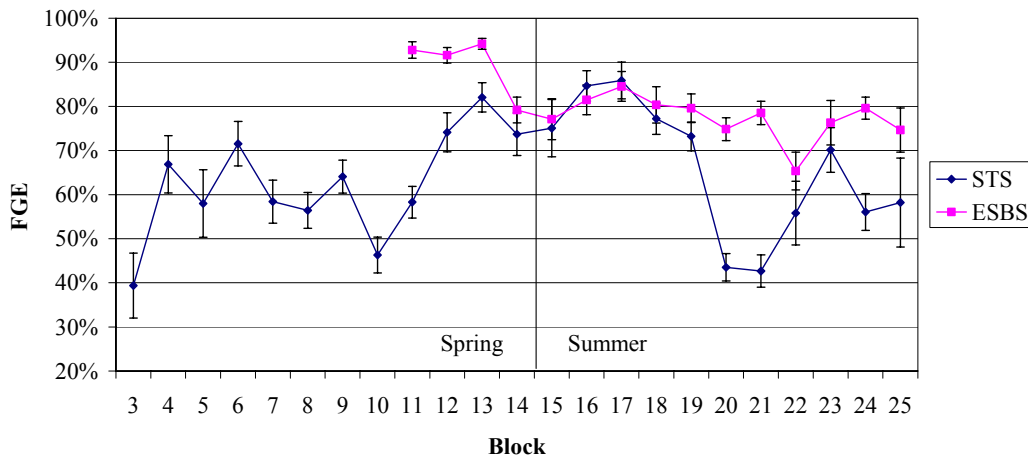


Figure 3.26. FGE by Screen Type by Block. Error bars are 95% confidence intervals (Equation A29, Appendix A).

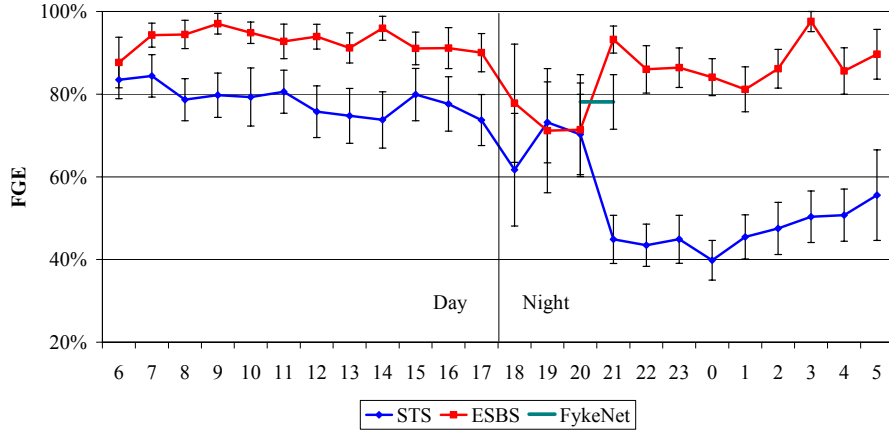


Figure 3.27. Diel Trends of the ESBS and STS in Spring. The time and duration of fyke net testing is also shown with the level illustrating the mean FGE for all species. Error bars are 95% confidence intervals based on measurement uncertainty (Equation A29, Appendix A). Fyke net error bars are based on variation among sample days.

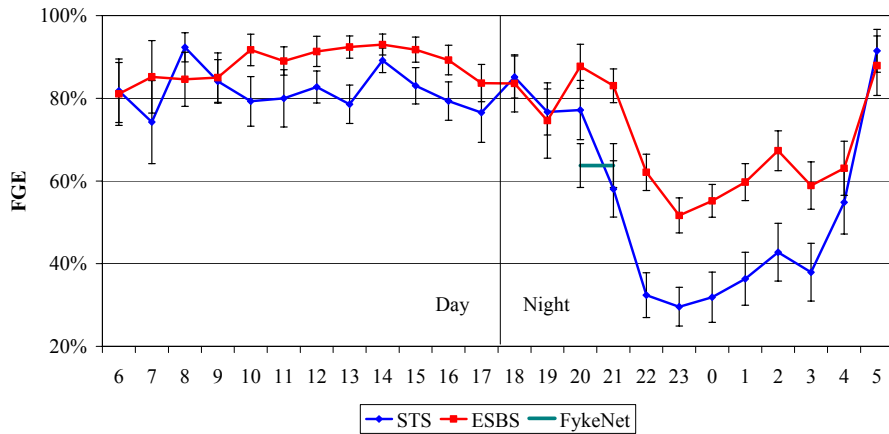


Figure 3.28. Diel Trends of the ESBS and STS in Summer. The time and duration of fyke net testing is also shown with the level illustrating the mean FGE for all species. Error bars are 95% confidence intervals based on measurement uncertainty (Equation A29, Appendix A). Fyke net error bars are based on variation among sample days.

3.2.7 Fish Trajectories

The acoustic screen model assumes that fish pass through the beam once and only once. It is critical that this assumption is not violated for estimates to be unbiased. The following fish trajectory information is shown for verification that fish are entrained and committed to passage within the sampling volumes. This data is derived from split-beam transducers only. Since the deployment at an STS and an ESBS intake were different, both deployment types are shown. The high percentage of fish moving downstream at all ranges of interest indicates that the assumptions of the acoustic screen model were met. (Figure 3.29 and Figure 3.30). Low percentages moving downstream behind the ESBS screen are based on a very

small number of tracks. In addition, the trajectories suggest that flows there are not strongly directed across the beam, but fish are moving rapidly and are unlikely to be counted multiple times.

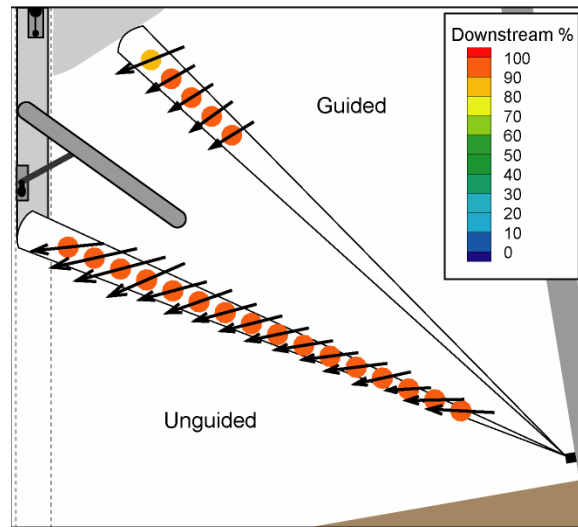


Figure 3.29. Fish Trajectories at an STS Deployment. The arrows are fish velocity vectors (both magnitude and direction). Circle color indicates percentage of fish moving downstream in the azimuth plane (in and out of the page).

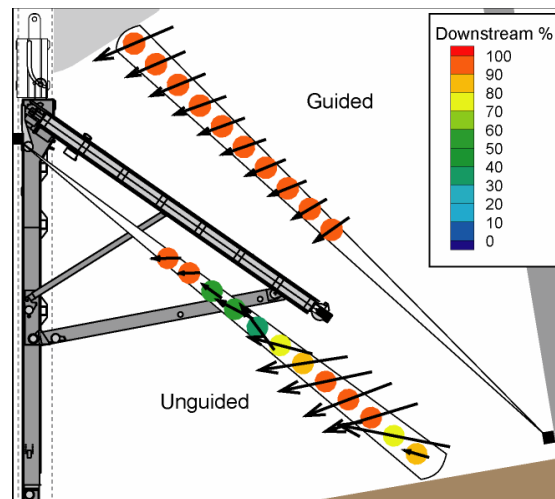


Figure 3.30. Fish Trajectories at the ESBS Deployment. The arrows are fish velocity vectors (both magnitude and direction). Circle color indicated percentage of fish moving downstream in the azimuth plane (in and out of the page).

The spillway represented a special opportunity to compare both fish and flow trajectories, since flow trajectories were available from a computational fluid dynamics (CFD) model of the spillway. No comparable hydraulic information was available for the powerhouse. Fish were neither entrained nor counted as such above a 6-m range from the transducer (239 ft MSL elevation) for gate openings greater than 6 ft or above a 9-m range (230 ft MSL elevation) from the transducer at gate openings less than or equal to 6 ft. Support for these range limits is found in the comparison of fish trajectories and flows. Fish

speeds were the same as or slightly less than flow speeds estimated by the CFD model except near the surface where water velocities were very low. At these low velocities, fish were observed as free swimming—that is, swimming faster than the relatively still waters near the surface (Figure 3.31).

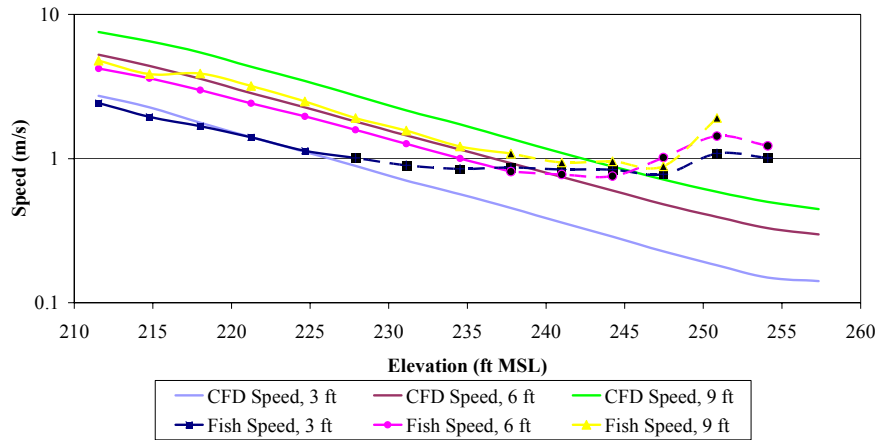


Figure 3.31. Speeds of Fish and CFD Flow for a 3-, 6-, and 9-ft Gate Opening at the Spillway. Elevations where fish were not considered entrained are illustrated by dotted lines and markers with black fill.

Plunge is defined as the angle in degrees below horizontal. Fish plunge was the same as or slightly less than CFD plunge (Figure 3.32). Near the surface where water velocities were very low, fish were swimming nearly horizontally (Figure 3.31). Fish trajectory and flow information both indicate areas where fish would not be committed to passage (Figure 3.33-36). This supports the need to carefully select the sample volume used to estimate fish passage. This need was addressed in the current study by setting range limits specific to each deployment type and by accounting for the range of spill gate openings.

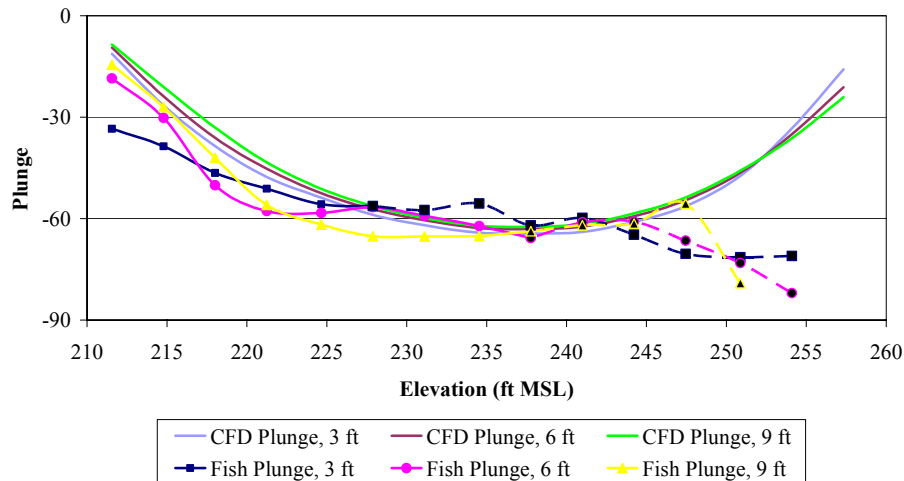


Figure 3.32. Plunge (the angle in degrees below horizontal) of Fish and CFD Flow for a 3-, 6-, and 9-ft Gate Opening at the Spillway. Elevations where fish were not considered entrained are illustrated by dotted lines and markers with black fill.

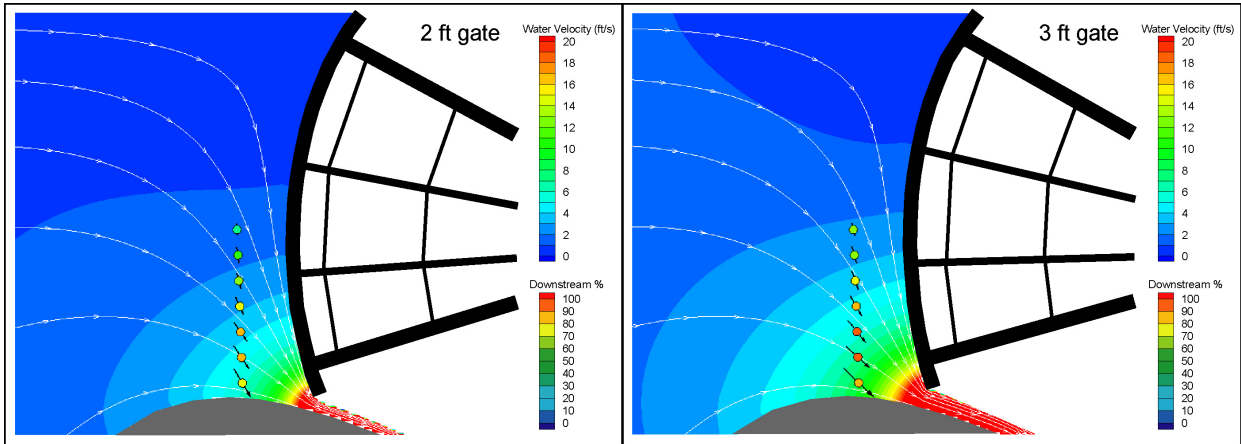


Figure 3.33. Fish and Flow at the Spillway with a 2-ft (left) and 3-ft (right) Gate Opening. The white streamtraces show the water's path and the field contours show the water's velocity magnitude. The black arrows show the fish velocity with circles contouring the percentage of fish that were headed downstream based on azimuth direction.

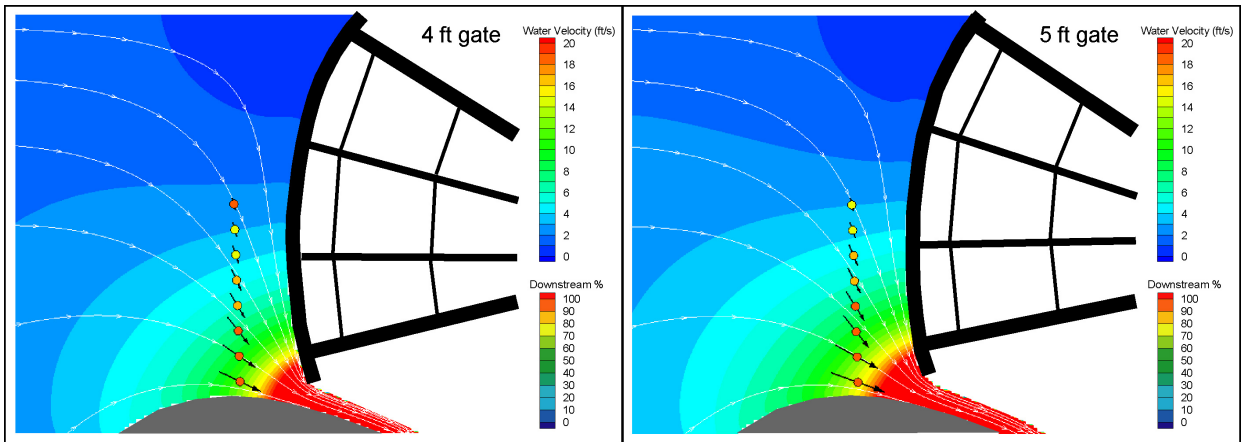


Figure 3.34. Fish and Flow at the Spillway with a 4-ft (left) and 5-ft (right) Gate Opening. The white streamtraces show the water's path and the field contours show the water's velocity magnitude. The black arrows show the fish velocity with circles contouring the percentage of fish that were headed downstream based on azimuth direction.

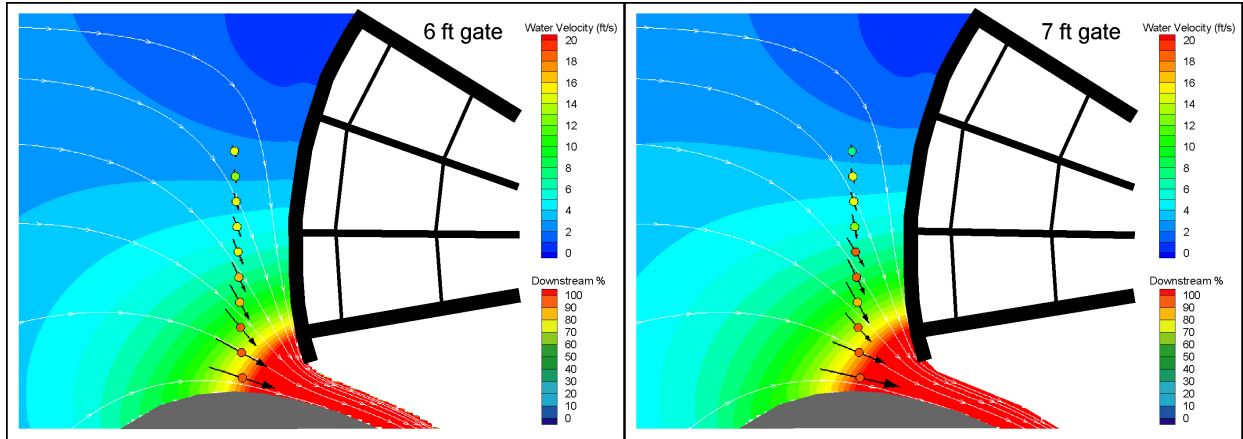


Figure 3.35. Fish and Flow at the Spillway with a 6-ft (left) and 7-ft (right) Gate Opening. The white streamtraces show the water’s path and the field contours show the water’s velocity magnitude. The black arrows show the fish velocity with circles contouring the percentage of fish that were headed downstream based on azimuth direction.

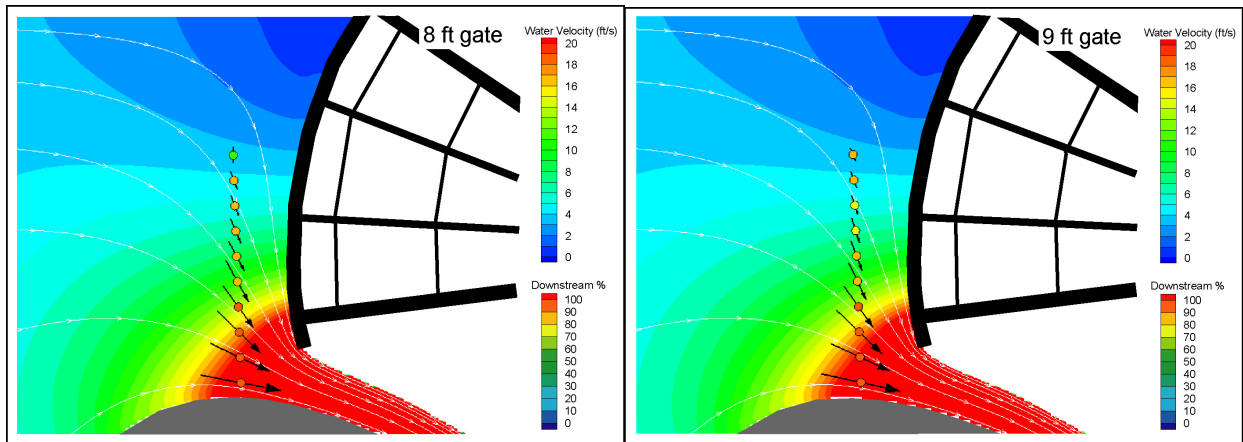


Figure 3.36. Fish and Flow at the Spillway with an 8-ft (left) and 9-ft (right) Gate Opening. The white streamtraces show the water’s path and the field contours show the water’s velocity magnitude. The black arrows show the fish velocity with circles contouring the percentage of fish that were headed downstream based on azimuth direction.

3.3 Treatment Effects

The fish passage metric responses to the spill treatments are described in this section. Recall that spill treatments were either 12-h spill (0% daytime with 60% nighttime) or 24-h spill (constant 30%). In spring, the nine selected blocks were 5-13. In summer, five blocks were selected: 17-19 and 23-24. Trends within season did not show any bias over time (Figure 3.37 through Figure 3.40). The statistical inferences from the data presented in this section are for the treatment effects only. The ANOVA methods are specified in detail in Appendix A. The results refute the null hypothesis that project passage during

24-h spill treatment does not differ from that during 12-h spill treatment, at least for fish passage efficiency (FPE). We can, therefore, accept the alternate hypothesis that project passage during 24-h spill treatment differs from that during 12-h spill treatment.

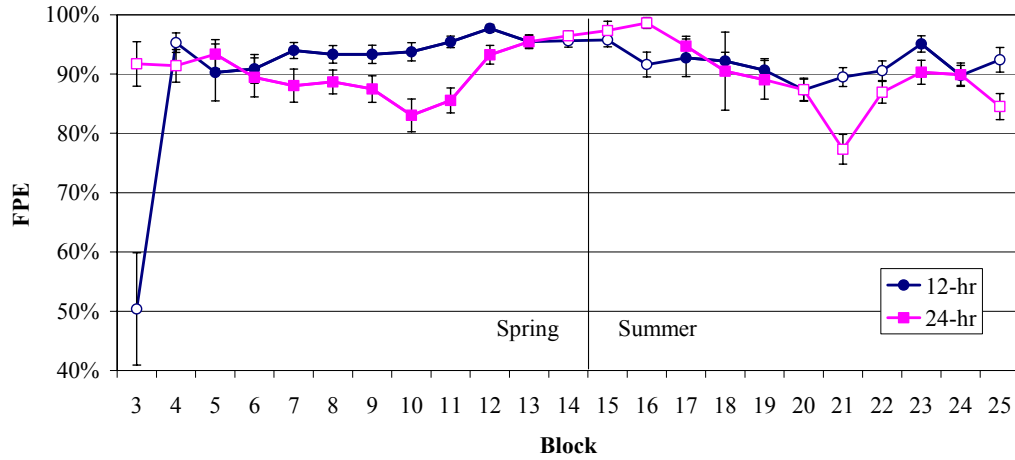


Figure 3.37. Fish Passage Efficiency (FPE) by Block. Open symbols indicate blocks censored from the statistical analysis. Error bars are 95% confidence intervals based on measurement uncertainty (Equation A29, Appendix A).

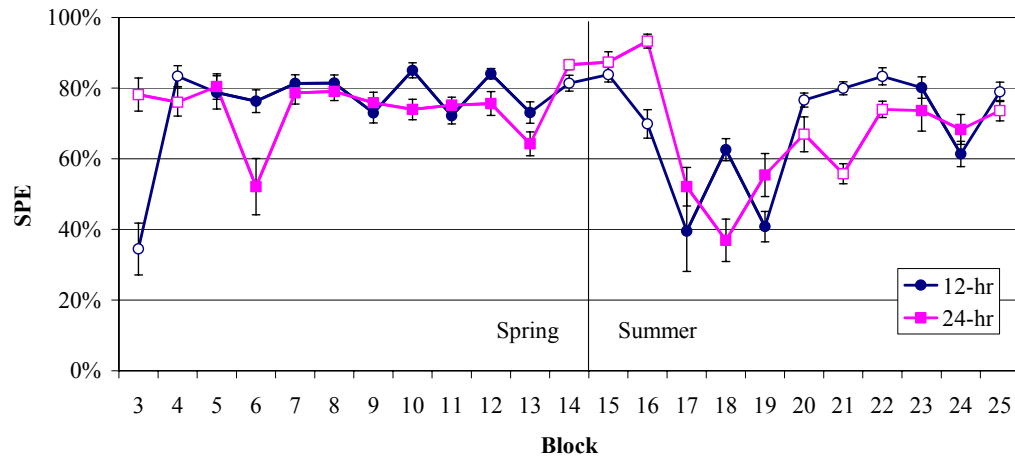


Figure 3.38. Spill Passage Efficiency (SPE) by Block. Open symbols indicate blocks censored from the statistical analysis. Error bars are 95% confidence intervals based on measurement uncertainty (Equation A29, Appendix A).

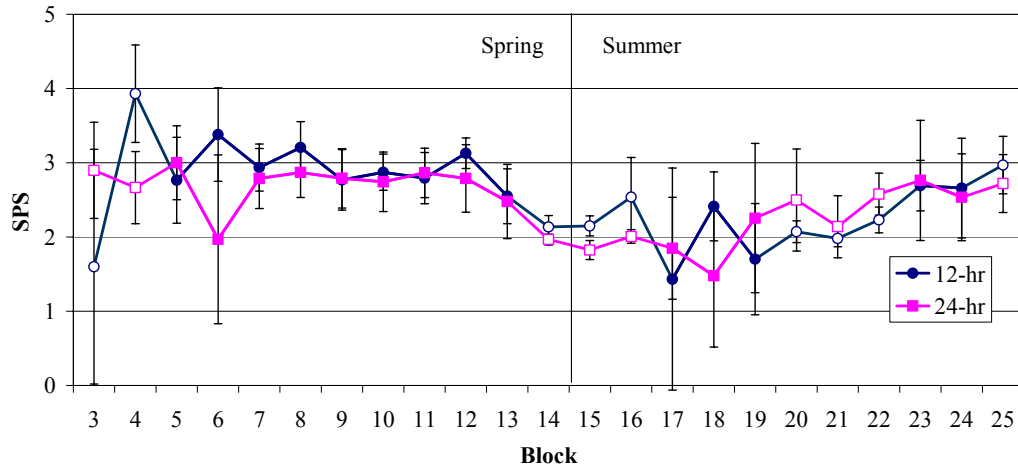


Figure 3.39. Spill Passage Effectiveness (SPS) by Block. Open symbols indicate blocks censored from the statistical analysis. Error bars are 95% confidence intervals based on measurement uncertainty (Equation A29, Appendix A).

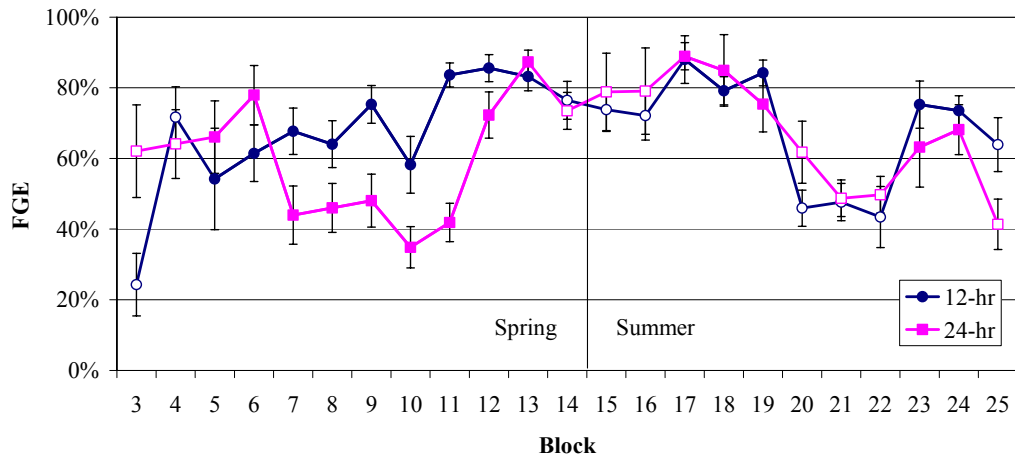


Figure 3.40. Fish Guidance Efficiency (FGE) by Block. Open symbols indicate blocks censored from the statistical analysis. Error bars are 95% confidence intervals based on measurement uncertainty (Equation A29, Appendix A).

3.3.1 Analysis of Variance

A two-way analysis of variance was performed on all the fish passage performance measures for both spring and summer. The data was ln-transformed prior to analysis to stabilize the variance (Appendix A). The selected blocks for analysis refer to those blocks with treatment trends in the correct direction, even though they may not have met the planned operational goals. Fish passage efficiency (FPE) was significantly different between treatments in both spring and summer ($\alpha = 0.05$). In summer the block effect was also significant. A significant block effect would normally be interpreted as the influence of

non-treatment factors, but in this case it could also be related to how spill conditions varied among blocks. None of the other fish passage performance metrics were significantly different among spill treatments (Table 3.2 through Table 3.9). ANOVA results for FPE in spring and summer are illustrated in Figures 3.41a- 3.41d.

Table 3.2. ANOVA Results for Fish Passage Efficiency (FPE) in Spring for the Nine Selected Blocks

Effect	Df	SS	MS	F	P
Intercept	1	0.142	0.142	115.349	0.000
Block	8	0.011	0.001	1.121	0.438
Treatment	1	0.011	0.011	8.755	0.018
Error	8	0.010	0.001		
Total	17	0.032			

Table 3.3. ANOVA Results for Spill Passage Efficiency (SPE) in Spring for the Nine Selected Blocks

Effect	Df	SS	MS	F	P
Intercept	1	1.469	1.469	166.853	0.000
Block	8	0.115	0.014	1.639	0.250
Treatment	1	0.029	0.029	3.255	0.109
Error	8	0.070	0.009		
Total	17	0.215			

Table 3.4. ANOVA Results for Spill Passage Effectiveness (SPS) in Spring for the Nine Selected Blocks

Effect	df	SS	MS	F	P
Intercept	1	19.076	19.076	1160.412	0.000
Block	8	0.058	0.007	0.441	0.866
Treatment	1	0.034	0.034	2.038	0.191
Error	8	0.132	0.016		
Total	17	0.223			

Table 3.5. ANOVA Results for Fish Guidance Efficiency (FGE) in Spring for the Nine Selected Blocks

Effect	df	SS	MS	F	P
Intercept	1	4.166	4.166	76.196	0.000
Block	8	0.621	0.078	1.419	0.316
Treatment	1	0.245	0.245	4.483	0.067
Error	8	0.437	0.055		
Total	17	1.303			

Table 3.6. ANOVA Results for Fish Passage Efficiency (FPE) in Summer for the Five Selected Blocks

Effect	df	SS	MS	F	P
Intercept	1	0.108	0.108	958.333	0.000
Block	4	0.005	0.001	10.034	0.023
Treatment	1	0.005	0.005	40.330	0.003
Error	4	0.000	0.000		
Total	9	0.010			

Table 3.7. ANOVA Results for Spill Passage Efficiency (SPE) in Summer for the Five Selected Blocks

Effect	df	SS	MS	F	P
Intercept	1	3.227	3.227	85.445	0.001
Block	4	0.528	0.132	3.493	0.127
Treatment	1	0.011	0.011	0.281	0.624
Error	4	0.151	0.038		
Total	9	0.689			

Table 3.8. ANOVA Results for Spill Passage Effectiveness (SPS) in Summer for the Five Selected Blocks

Effect	df	SS	MS	F	P
Intercept	1	6.067	6.067	352.120	0.000
Block	4	0.497	0.124	7.205	0.041
Treatment	1	0.010	0.010	0.561	0.495
Error	4	0.069	0.017		
Total	9	0.575			

Table 3.9. ANOVA Results for Fish Guidance Efficiency (FGE) in Summer for the Five Selected Blocks

Effect	df	SS	MS	F	P
Intercept	1	1.102	1.102	41.553	0.003
Block	4	0.219	0.055	2.064	0.250
Treatment	1	0.114	0.114	4.310	0.106
Error	4	0.106	0.027		
Total	9	0.439			

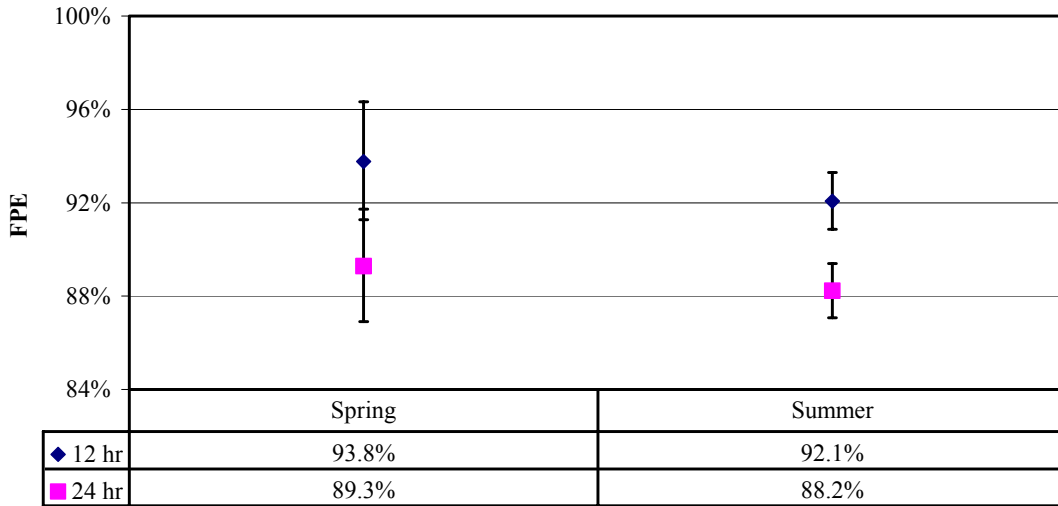


Figure 3.41a. FPE ANOVA Results. Error bars are 95% confidence intervals based on ANOVA MSE (Appendix A: Equation A30).

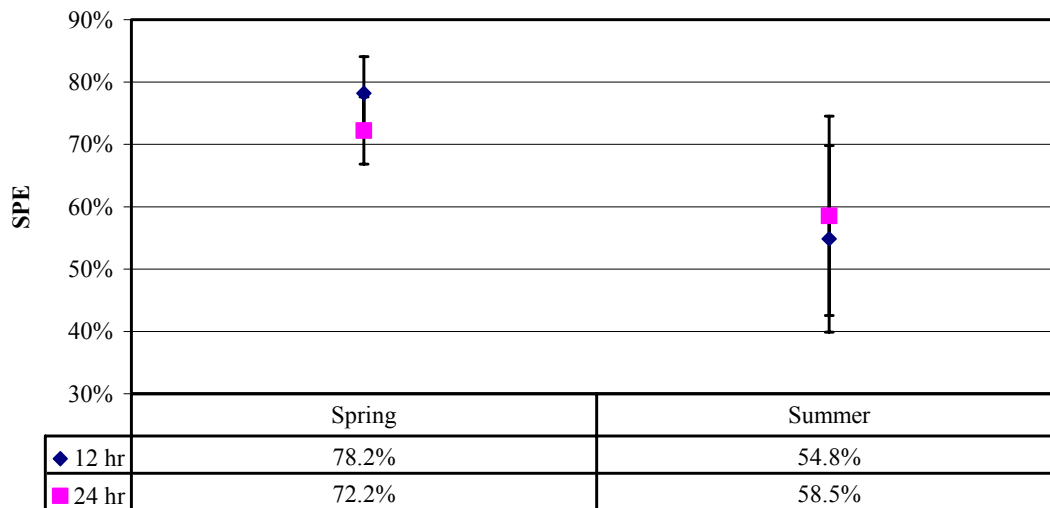


Figure 3.41b. SPE ANOVA Results. Error bars are 95% confidence intervals based on ANOVA MSE (Appendix A: Equation A30).

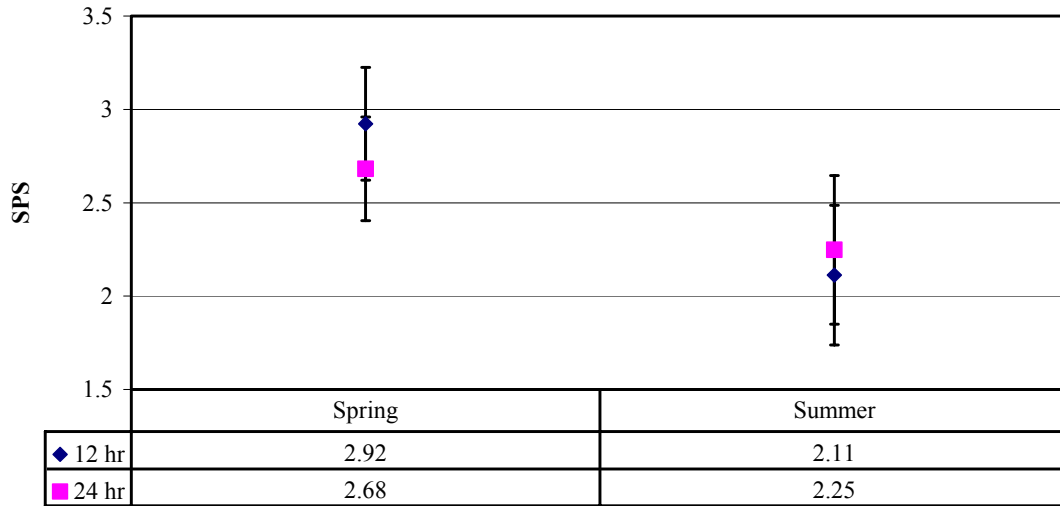


Figure 3.41c. SPS ANOVA Results. Error bars are 95% confidence intervals based on ANOVA MSE (Appendix A: Equation A30).

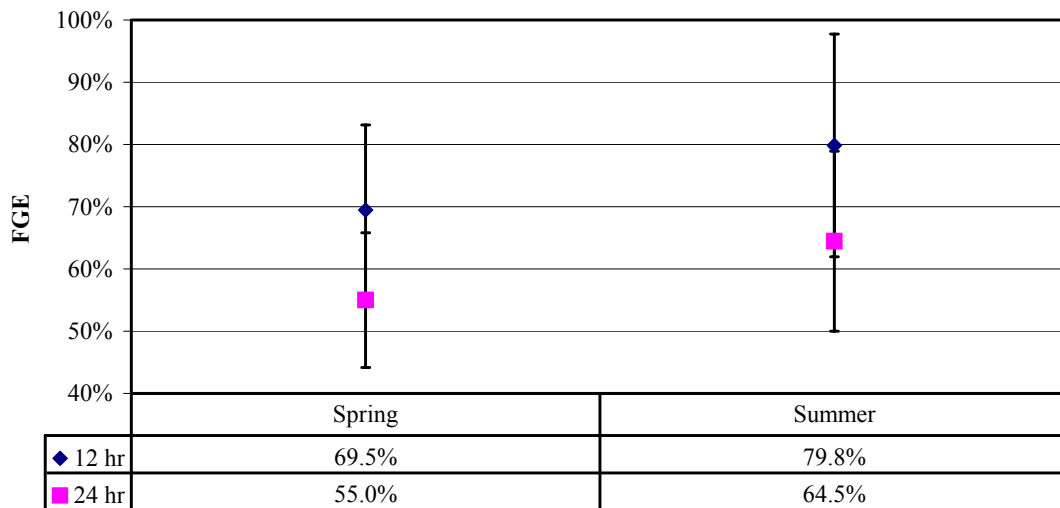


Figure 3.41d. FGE ANOVA Results. Error bars are 95% confidence intervals based on ANOVA MSE (Appendix A: Equation A30).

3.3.2 Fish Passage Metrics by Treatment

The following series of charts show the trends of the fish passage metrics during spring and summer and by diel period. By differentiating seasons, treatments, and diel periods, these charts provide information useful for interpreting how seasonal changes in species composition, diel trends, and spill treatments affected passage performance. Fish passage efficiency trends generally showed the influence of nominal spill treatments. FPE was higher during 60% spill at night than during 30% spill at night for both spring and summer. Conversely, FPE was higher during 30% day spill than during 0% day spill

(Figure 3.42). Spill passage efficiency showed the expected trend, which was that more fish passed via the spillway when more water was spilled (Figure 3.43). The estimates of spill passage effectiveness during the day of the 12-h treatment are not really meaningful because of the few periods when spill occurred during the planned 0% spill. Spill passage effectiveness at night was lower during planned 60% spill simply because of the increased volume of water (Figure 3.44). FGE showed little change between treatments, but was clearly lower during the night (Figure 3.45).

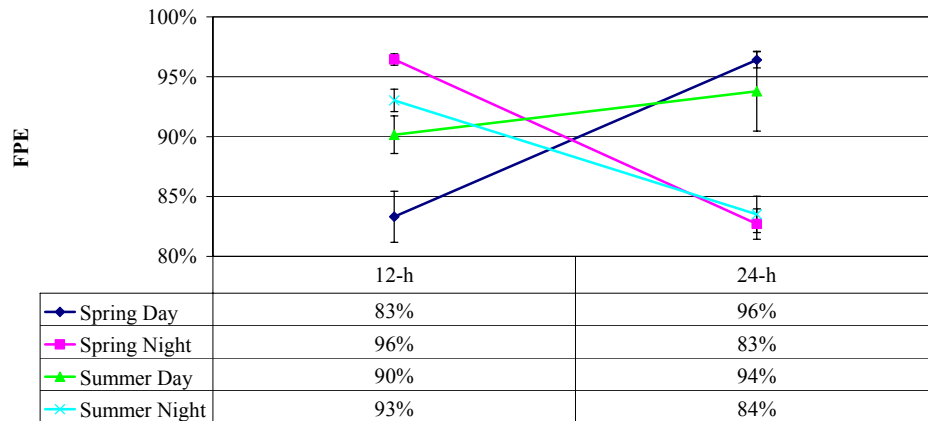


Figure 3.42. Fish Passage Efficiency (FPE) by Treatment for the Selected Blocks. Error bars are 95% confidence intervals based on measurement uncertainty (Equation A29, Appendix A).

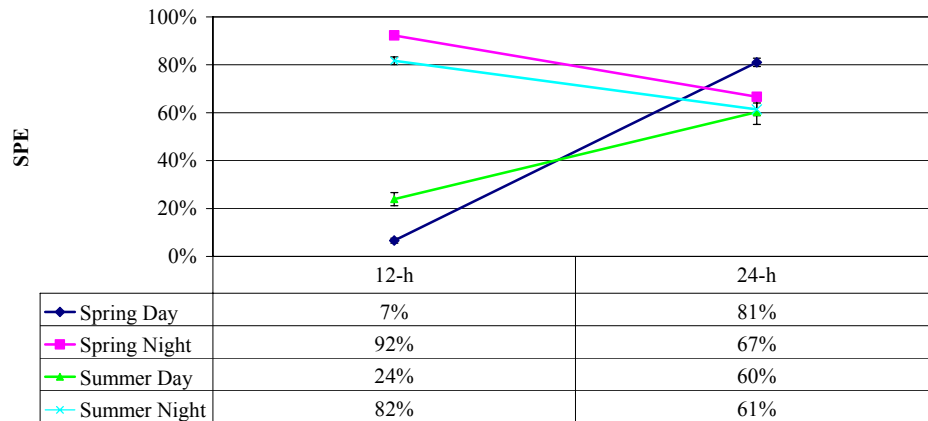


Figure 3.43. Spill Passage Efficiency (SPE) by Treatment for the Selected Blocks. Error bars are 95% confidence intervals based on measurement uncertainty (Equation A29, Appendix A).

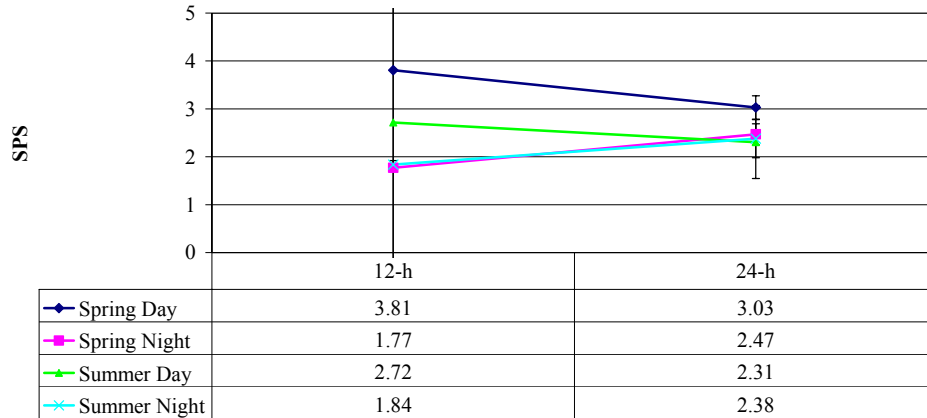


Figure 3.44. Spill Passage Effectiveness (SPS) by Treatment for the Selected Blocks. Error bars are 95% confidence intervals based on measurement uncertainty (Equation A29, Appendix A).

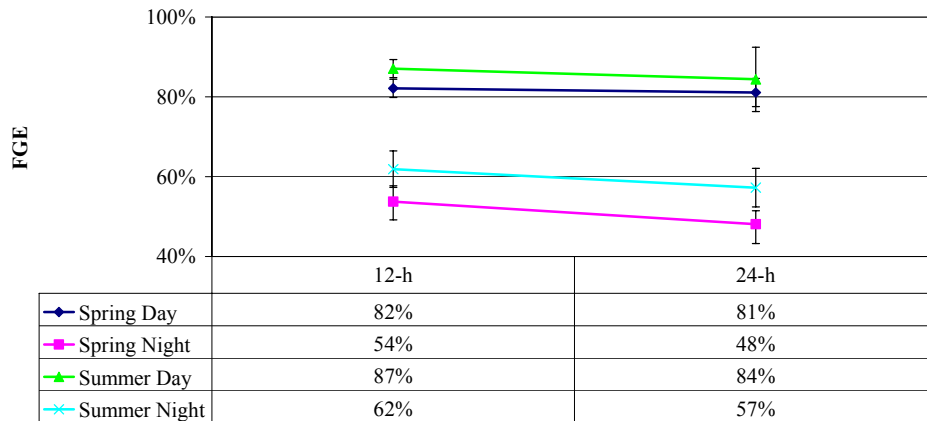


Figure 3.45. Fish Guidance Efficiency (FGE) by Treatment for the Selected Blocks. Error bars are 95% confidence intervals based on measurement uncertainty (Equation A29, Appendix A).

3.3.3 Diel Trends by Treatment

Because of the diel nature of the spill treatments, the presentation of fish passage performance by hour of the day is particularly informative. On the following graphs, flow through the powerhouse and spillway are also shown. The plots of flow show that overall discharge was relatively consistent across treatments, and that treatments differed principally in the distribution of overall discharge among the spillway and powerhouse. To facilitate interpretation of passage trends relative to trends in spill, multiple plots of each season by treatment combination are presented with both absolute and relative scaling.

During the spring 12-h spill treatment, the effect of spill proportion on spillway passage was clear. Of interest is the first peak of spillway passage at 1800 h. This peak suggests that fish were holding in the forebay during the day until the spillway opened. Immediately after the spillway transitioned from 0% to 60% of the flow, a large number of fish passed via the spillway. Passage then declined rapidly as fish in the immediate forebay became less abundant. At 2100h an additional peak in passage was observed at the

spillway and the powerhouse (Figure 3.46). During the spring 24-h spill treatment, the number of fish utilizing the spillway as a passage route throughout a 24-h period exceeds the proportion of flow over that route. What is noteworthy is the increase in unguided fish in the evening, from 2000 to 0500 h (Figure 3.47), in the absence of a concurrent change in flow.

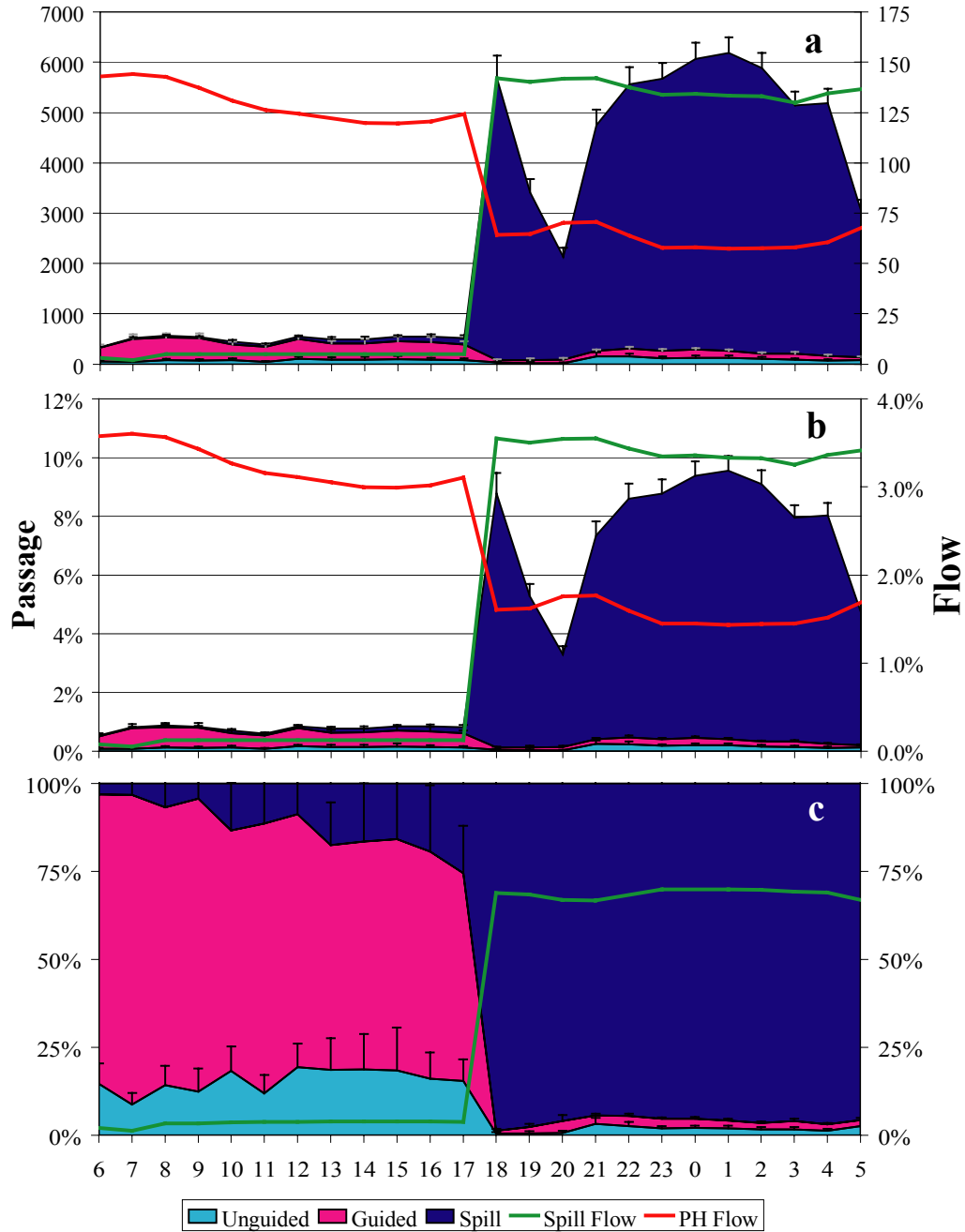


Figure 3.46. Diel Passage during the Spring 12-h Spill Treatment for the Nine Selected Blocks. Passage is expressed as fish/h and flow as kcfs (a), proportion of total (b), and proportion within the hour (c). Error bars are 95% confidence intervals based on measurement uncertainty (Equation A29, Appendix A).

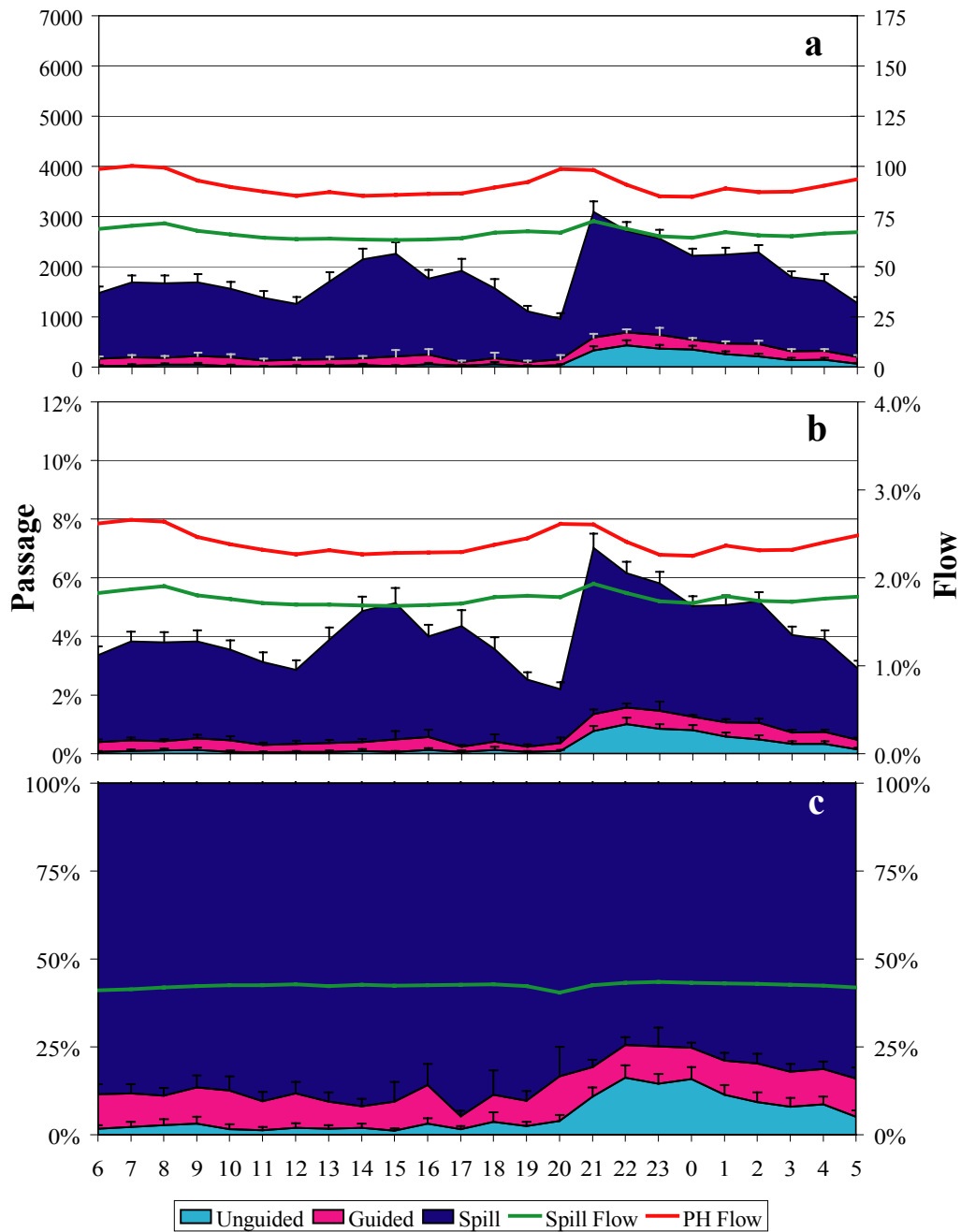


Figure 3.47. Diel Passage during the Spring 24-h Spill Treatment for the Nine Selected Blocks. Passage is expressed as fish/h and flow as kcfs (a), proportion of total (b), and proportion within the hour (c). Error bars are 95% confidence intervals based on measurement uncertainty (Equation A29, Appendix A).

For the summer 12-h spill treatment, the effect of opening the spillway is less pronounced than in spring because the spill treatment condition of 0% day spill was rarely met. Also of interest is the fact that while powerhouse passage increased during the day, the screens were effective at guiding fish in the daytime (Figure 3.48). In the summer 24-h spill treatment, passage was relatively uniform over the 24-h period

with a peak in unguided passage at 2200 to 2300 h, coincident with peak passage over the spillway (Figure 3.49). In both spring and summer, the increase in unguided passage at night during the 24-h treatment is the basis of lower FPE relative to the 12-h treatment. Daytime guidance is relatively high in both seasons, keeping FPE high during daytime. As nighttime guidance drops, the 60% spill of the 12-h treatment minimizes powerhouse passage and FPE remains high.

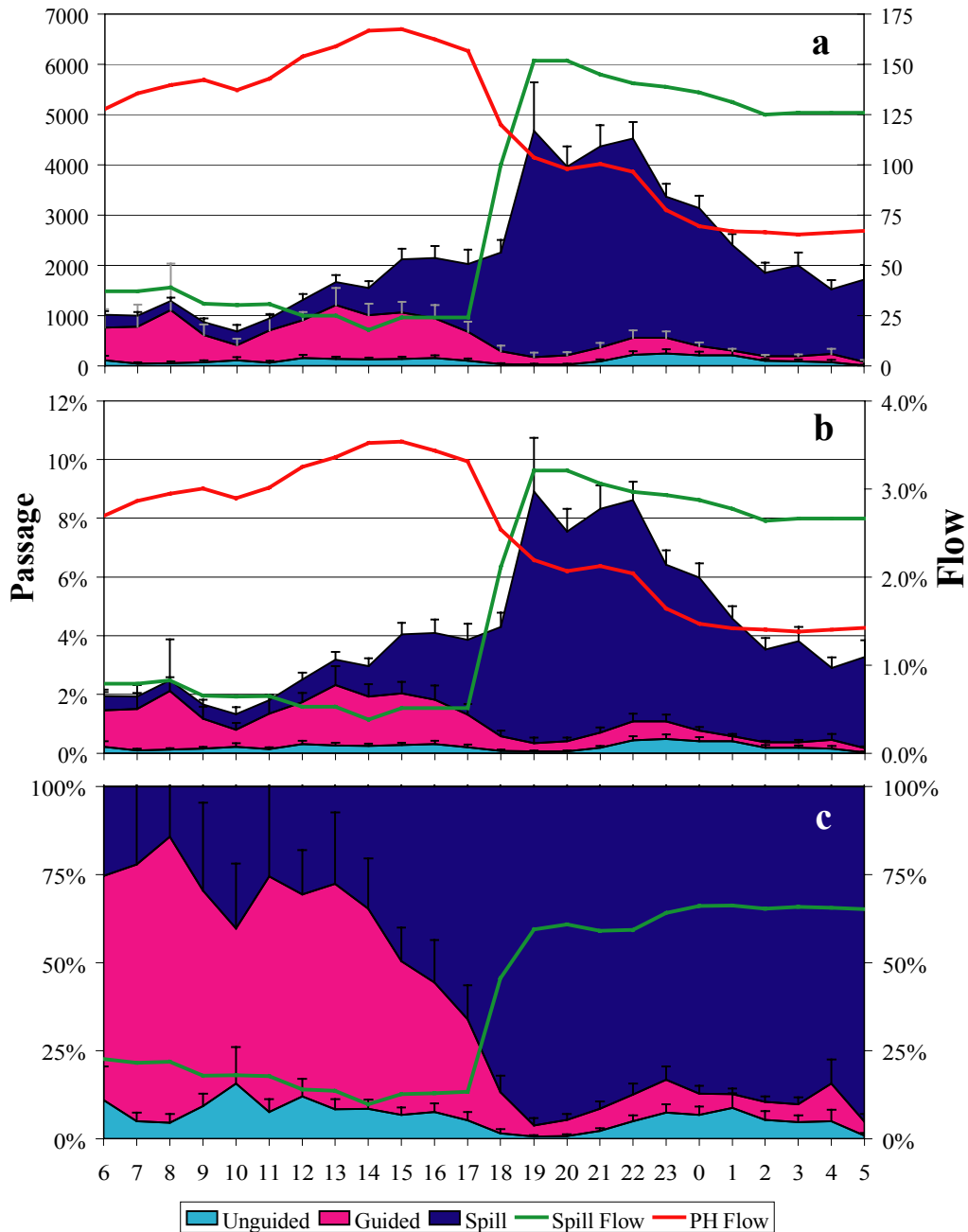


Figure 3.48. Diel Passage during the Summer 12-h Spill Treatment for Five Selected Blocks. Passage is expressed as fish/h and flow as kcfs (a), proportion of total (b), and proportion within the hour (c). Error bars are 95% confidence intervals based on measurement uncertainty (Equation A29, Appendix A).

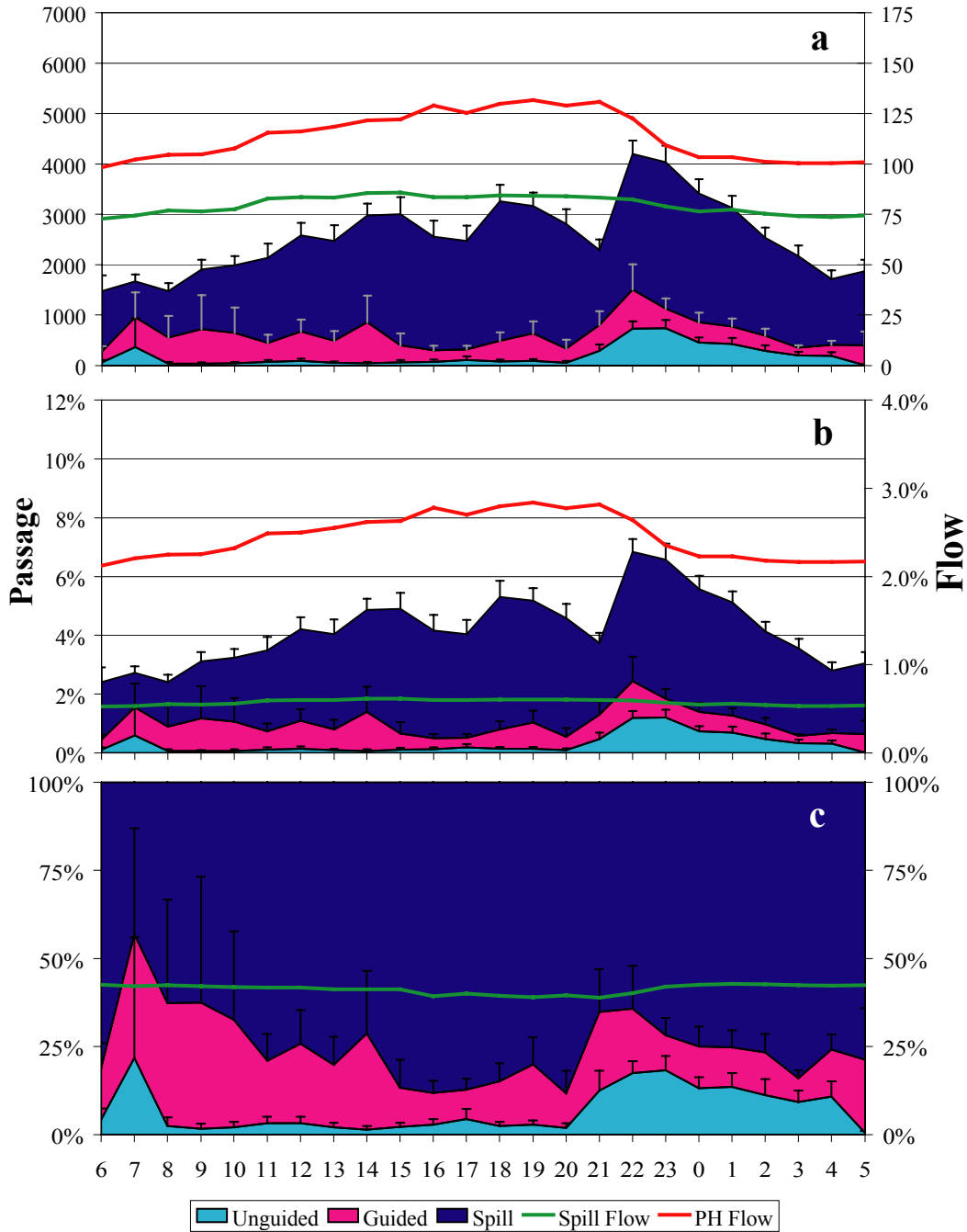


Figure 3.49. Diel Passage during the Summer 24-h Spill Treatment for Five Selected Blocks. Passage is expressed as fish/h and flow as kcfs (a), proportion of total (b), and proportion within the hour (c). Error bars are 95% confidence intervals based on measurement uncertainty (Equation A29, Appendix A).

3.3.4 Horizontal Distribution by Treatment

In the following series of charts, the column elements represent fish passage through each unit. The line elements are the water flow through each unit by treatment. Plots are again presented with both absolute and relative scaling to facilitate interpretation of passage and spill trends. In general, more fish passed through units along either shoreline at both the powerhouse and spillway during either treatment. At the powerhouse, this occurred with fairly uniform loading across the structure. At the spillway, however, the spill pattern opened the northern (Washington shore) bays first. This is reflected in more water going through the northern bays. During the higher 60% flows the spill pattern was uniform across the structure, which resulted in a more uniform passage pattern during the 60% nighttime spill periods (Figure 3.50 through Figure 3.53).

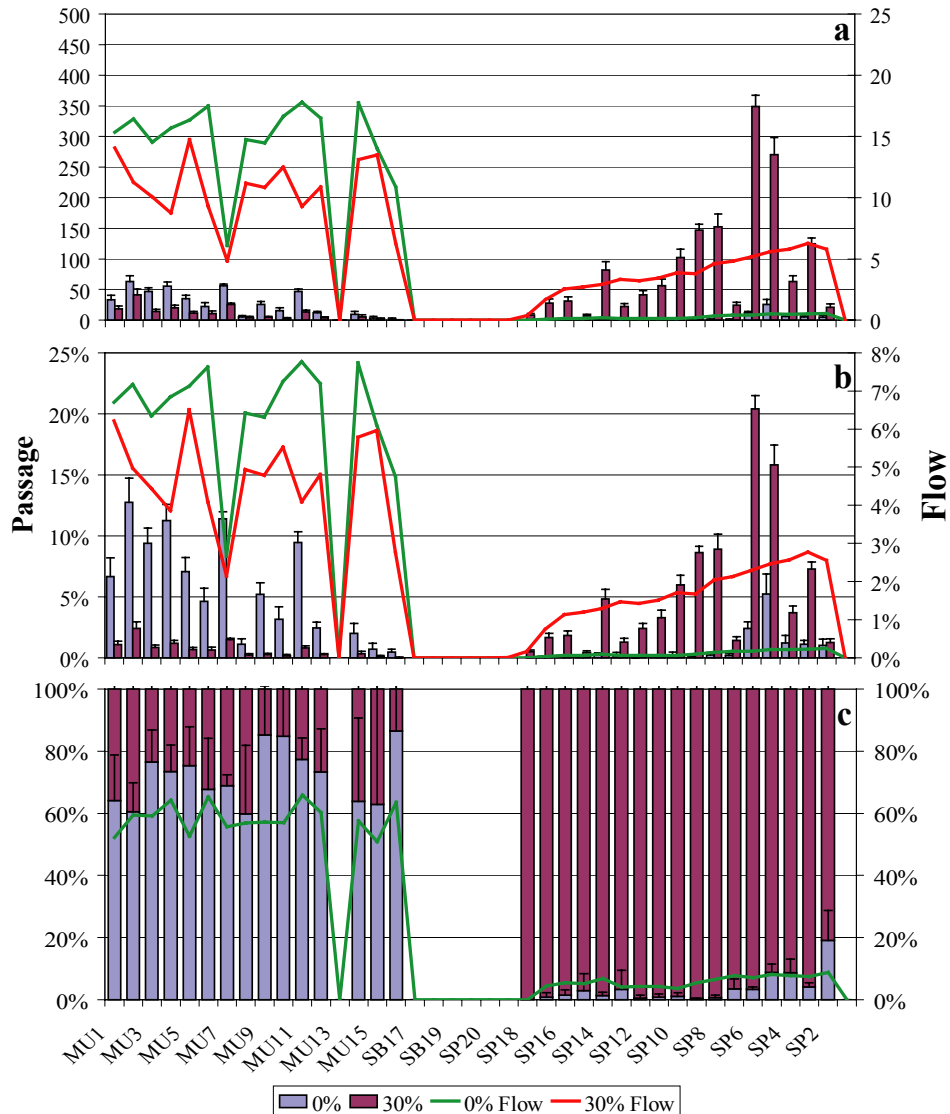


Figure 3.50. Horizontal Passage and Flow Distribution in Spring during the Day and by Treatment for the Nine Selected Blocks included in the Statistical Comparison of Treatments. Passage is expressed as fish/h and flow as kfs (a), proportion of total (b), and proportion by treatment within each route (c). Error bars are 95% confidence intervals based on measurement uncertainty (Equation A29, Appendix A).

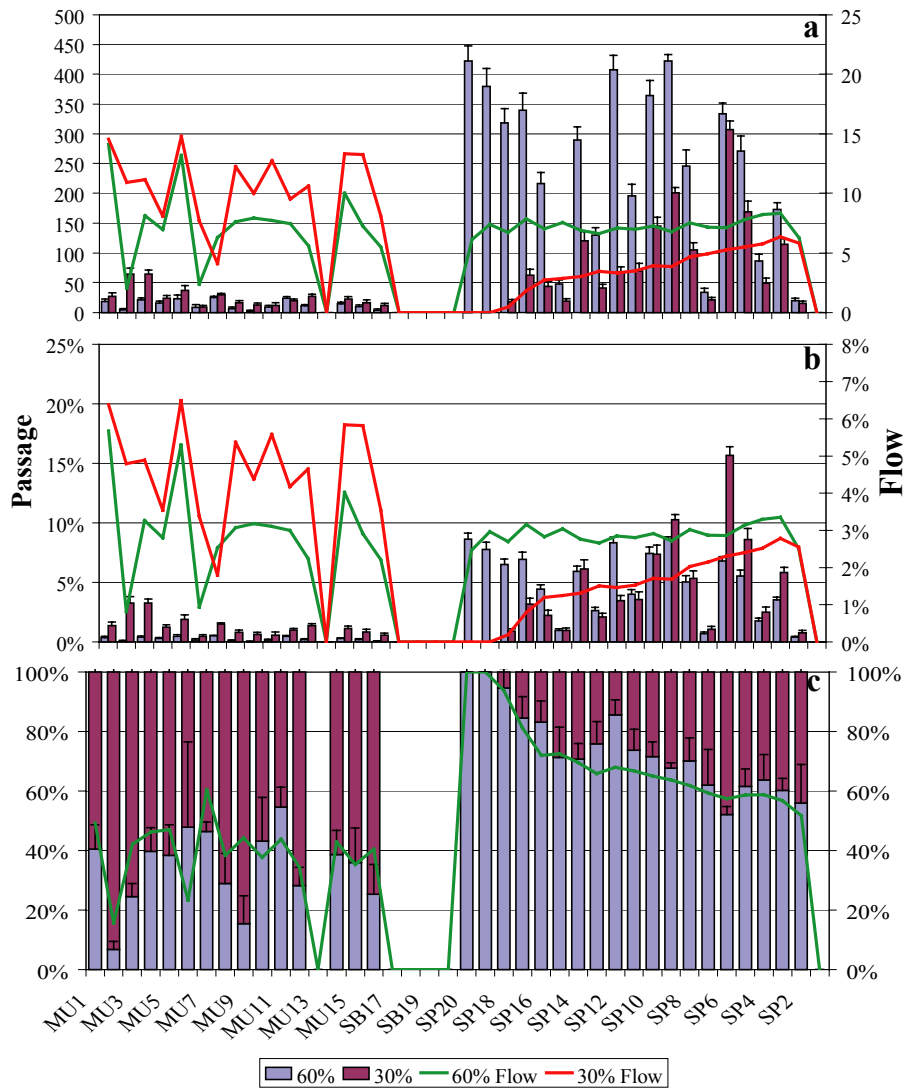


Figure 3.51. Horizontal Passage and Flow Distribution in Spring during the Night and by Treatment for the Nine Selected Blocks included in the Statistical Comparison of Treatments. Passage is expressed as fish/h and flow as kcfs (a), proportion of total (b), and proportion by treatment within each route (c). Error bars are 95% confidence intervals based on measurement uncertainty (Equation A29, Appendix A).

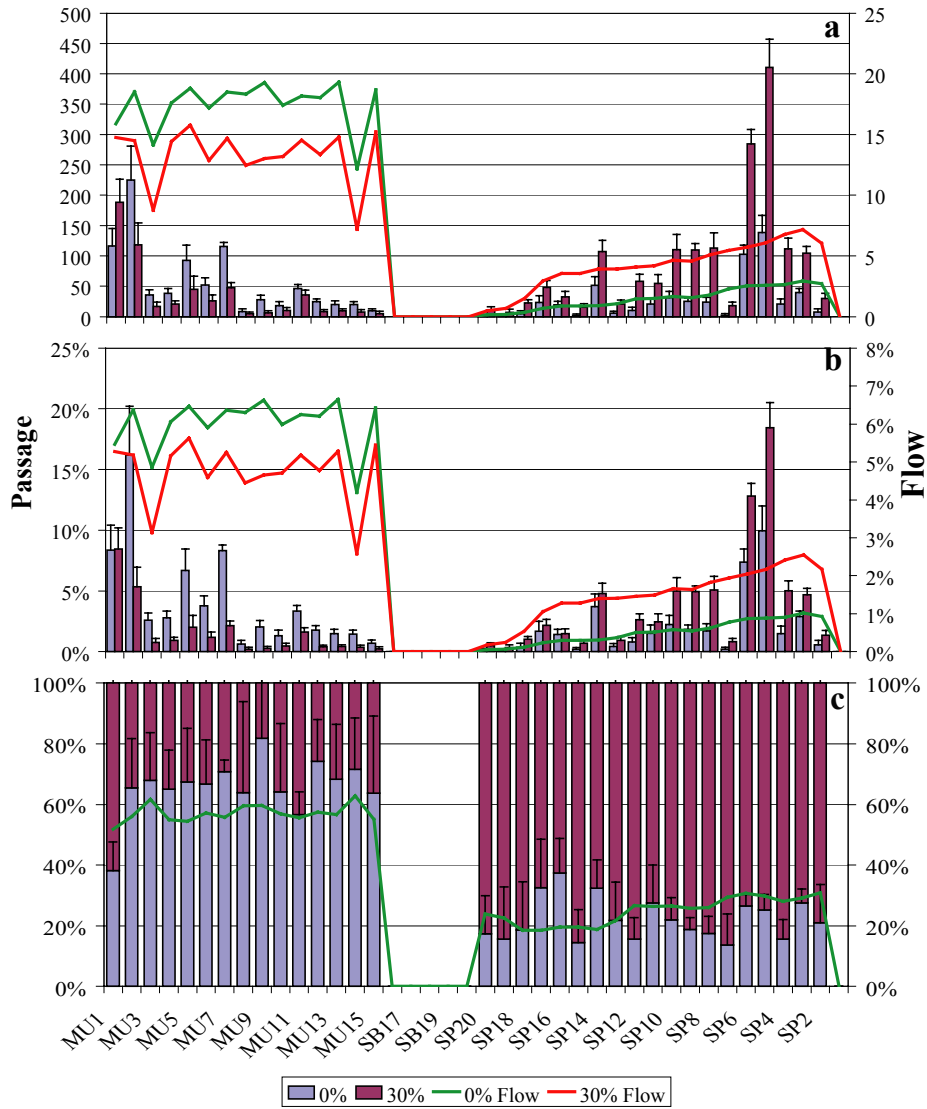


Figure 3.52. Horizontal Passage and Flow Distribution in Summer during the Day and by Treatment for the Five Selected Blocks included in the Statistical Comparison of Treatments. Passage is expressed as fish/h and flow as kcfs (a), proportion of total (b), and proportion by treatment within each route (c). Error bars are 95% confidence intervals based on measurement uncertainty (Equation A29, Appendix A).

3.3.5 Vertical Distributions by Treatment

Vertical distribution of fish differed among day and night periods, but not among spill treatments. Data are presented by season, spill proportion, and diel period for the two screen types at the powerhouse and the most common spill gate openings. For both STS and ESBS, vertical distributions shifted deeper during the night. This agrees with observations of greater unguided passage during the night at the powerhouse (Figure 3.54 through Figure 3.57). At the spillway, fish were observed higher in the water column at night in the spring, regardless of spill gate opening (Figure 3.58 through Figure 3.66). This difference was not as clear in the summer, but the night 60% spill condition was also the shallowest.

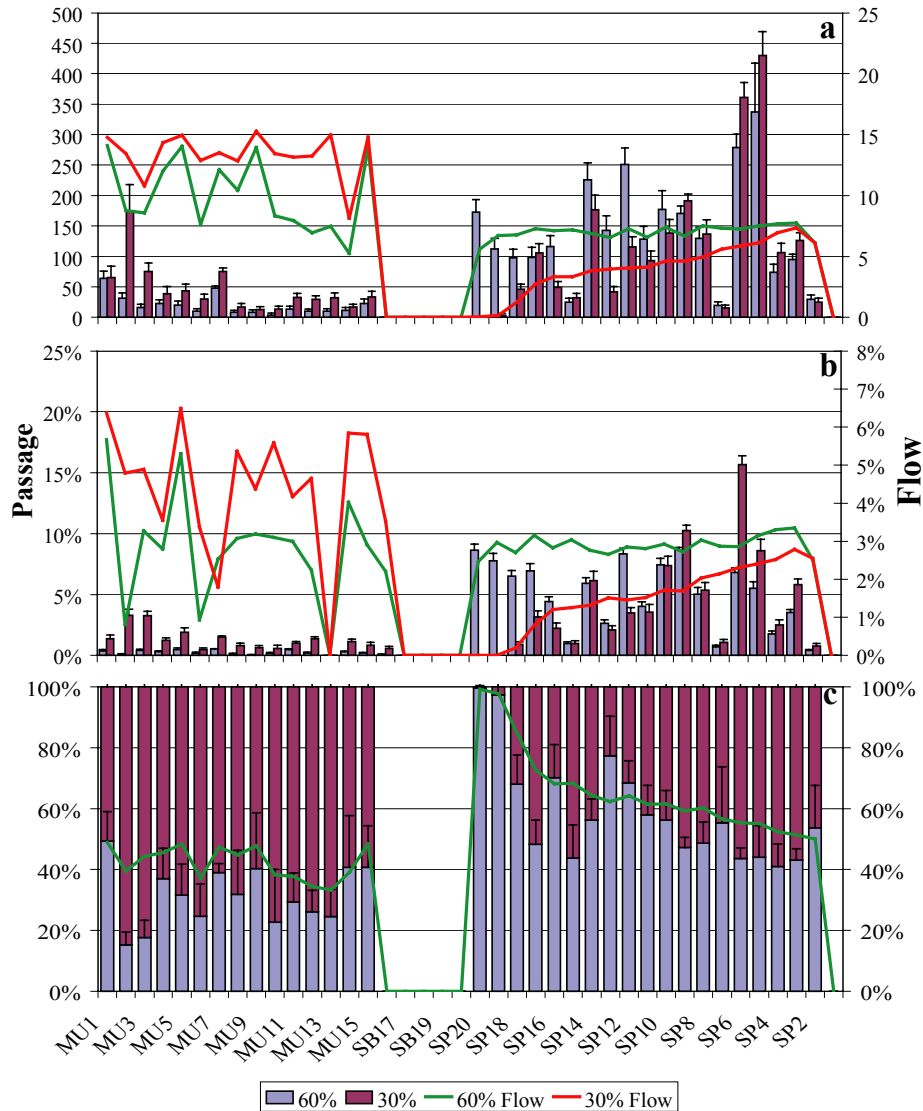


Figure 3.53. Horizontal Passage and Flow Distribution in Summer during the Night and by Treatment for the Nine Selected Blocks. Passage is expressed as fish/h and flow as kcfs (a), proportion of total (b), and proportion by treatment within each route (c). Error bars are 95% confidence intervals based on measurement uncertainty (Equation A29, Appendix A).

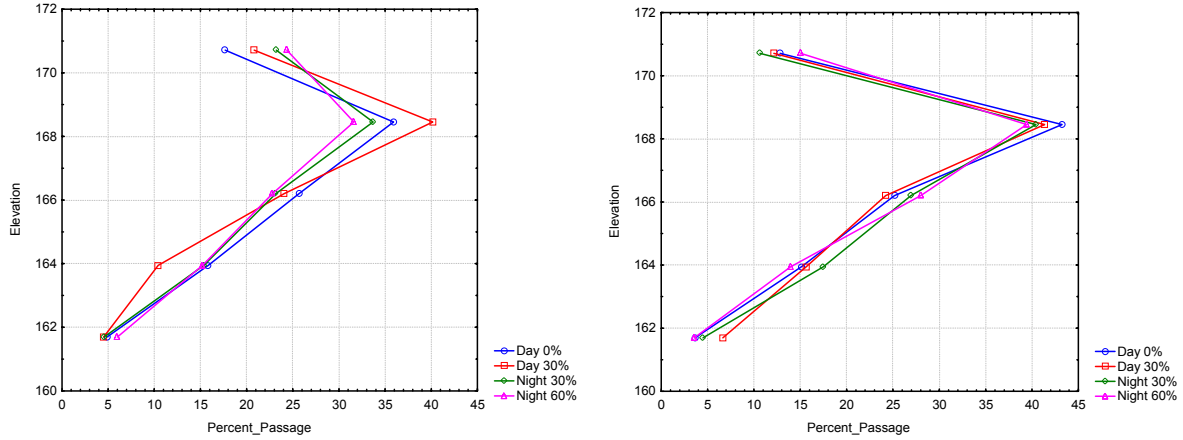


Figure 3.54. Vertical Distribution of Guided Fish at STS Units in Spring (left) and Summer (right)

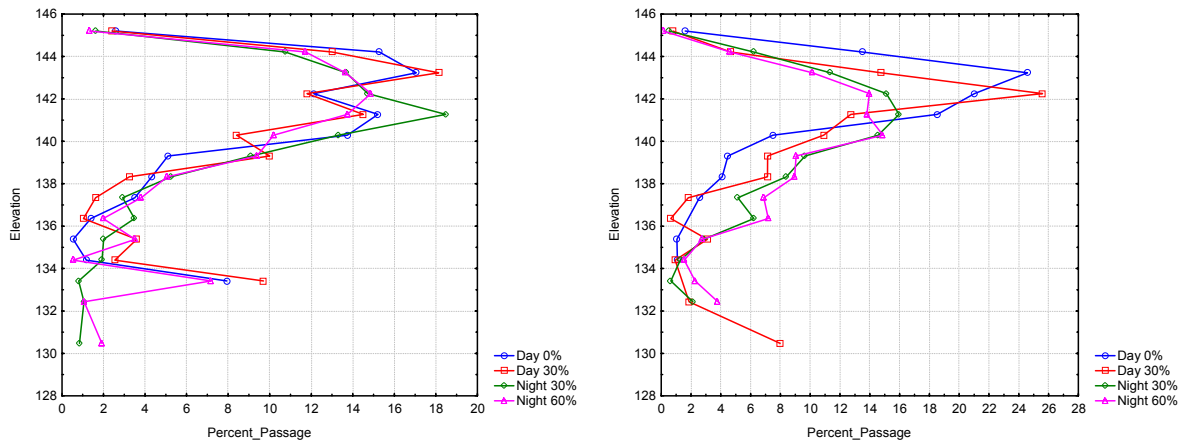


Figure 3.55. Vertical Distribution of Unguided Fish at STS Units in Spring (left) and Summer (right)

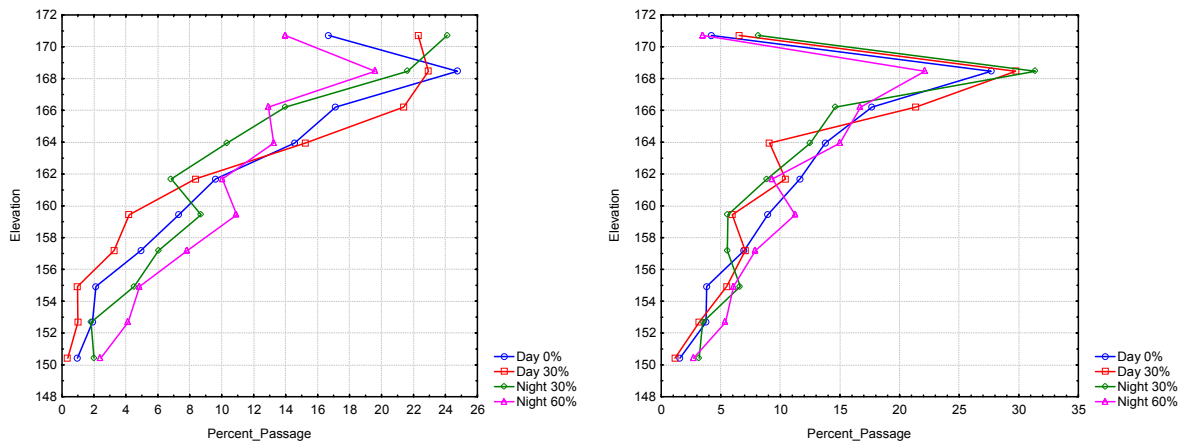


Figure 3.56. Vertical Distribution of Guided Fish at the ESBS Unit in Spring (left) and Summer (right)

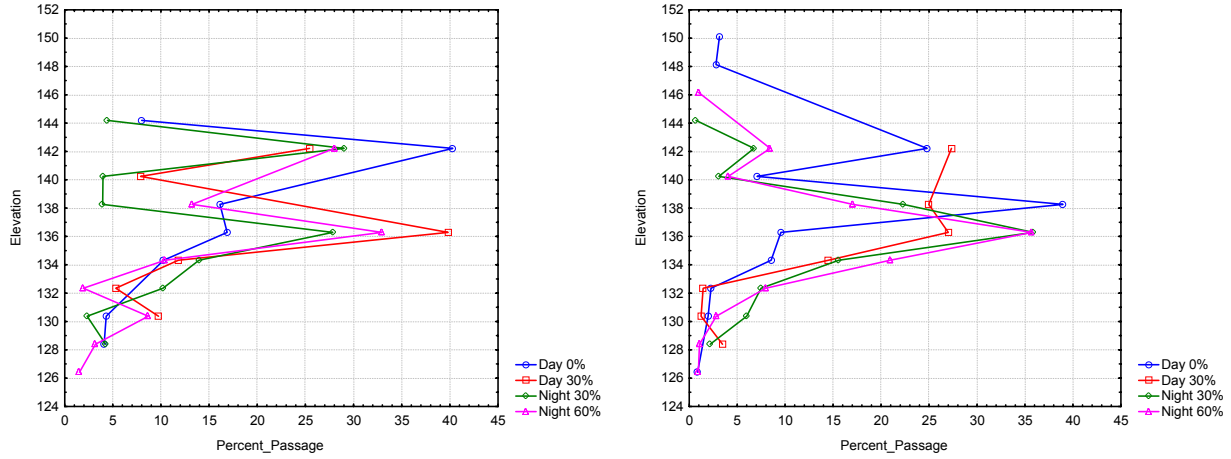


Figure 3.57. Vertical Distribution of Unguided Fish at the ESBS Unit in Spring (left) and Summer (right)

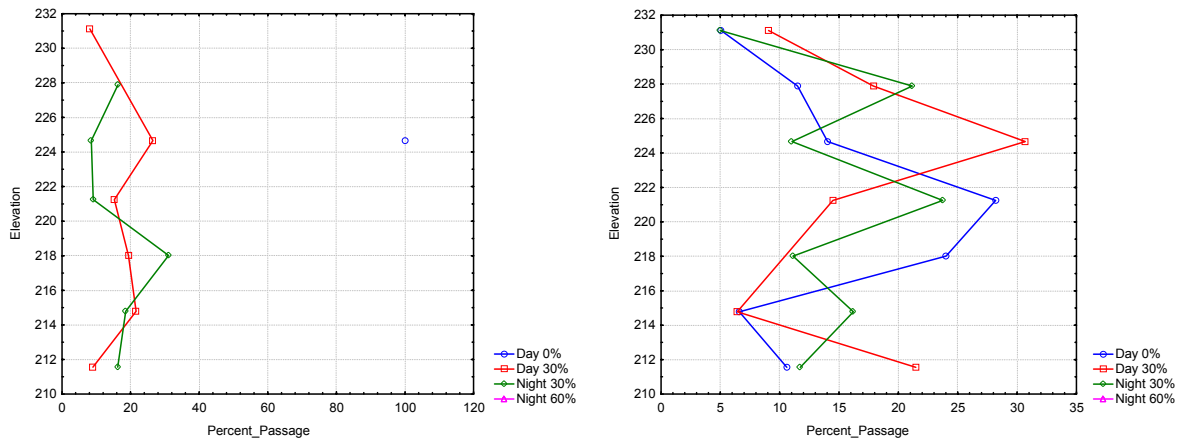


Figure 3.58. Vertical Distribution of Fish Passing in Spill at a 1-ft Spill Gate Opening in Spring (left) and Summer (right)

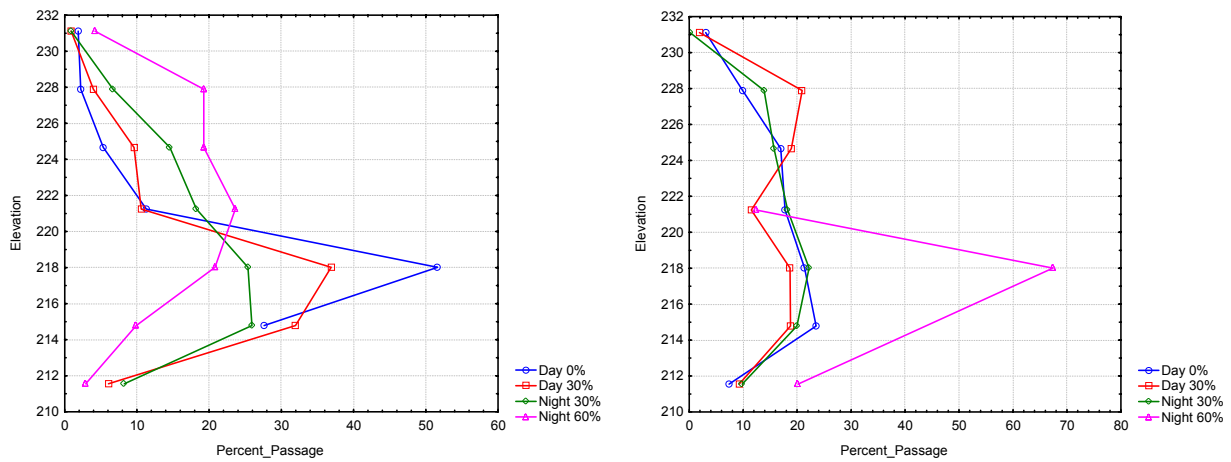


Figure 3.59. Vertical Distribution of Fish Passing in Spill at a 2-ft Spill Gate Opening in Spring (left) and Summer (right)

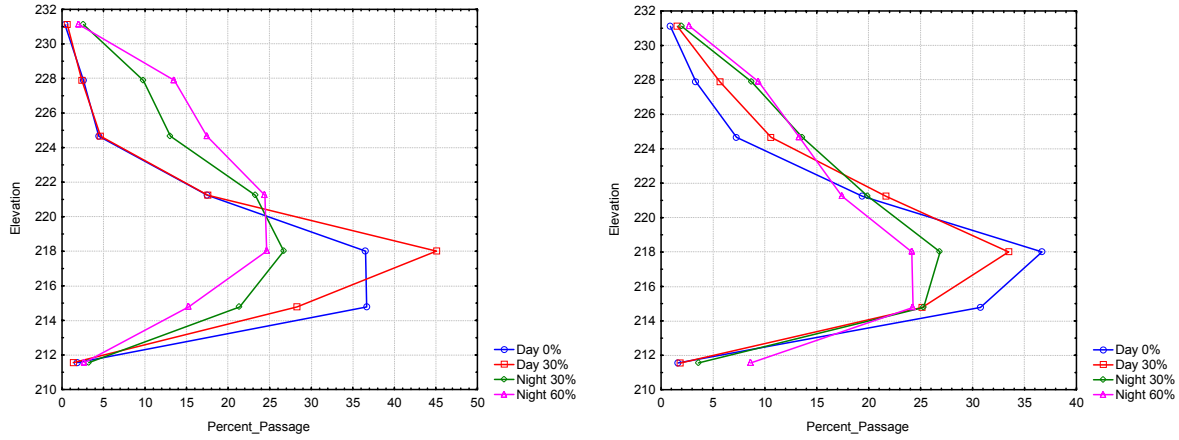


Figure 3.60. Vertical Distribution of Fish Passing in Spill at a 3-ft Spill Gate Opening in Spring (left) and Summer (right)

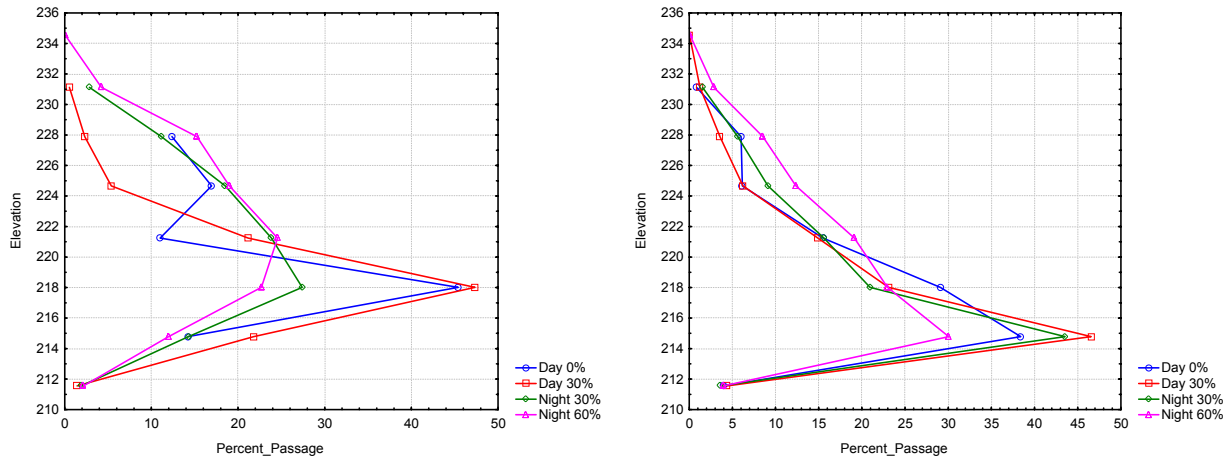


Figure 3.61. Vertical Distribution of Fish Passing in Spill at a 4-ft Spill Gate Opening in Spring (left) and Summer (right)

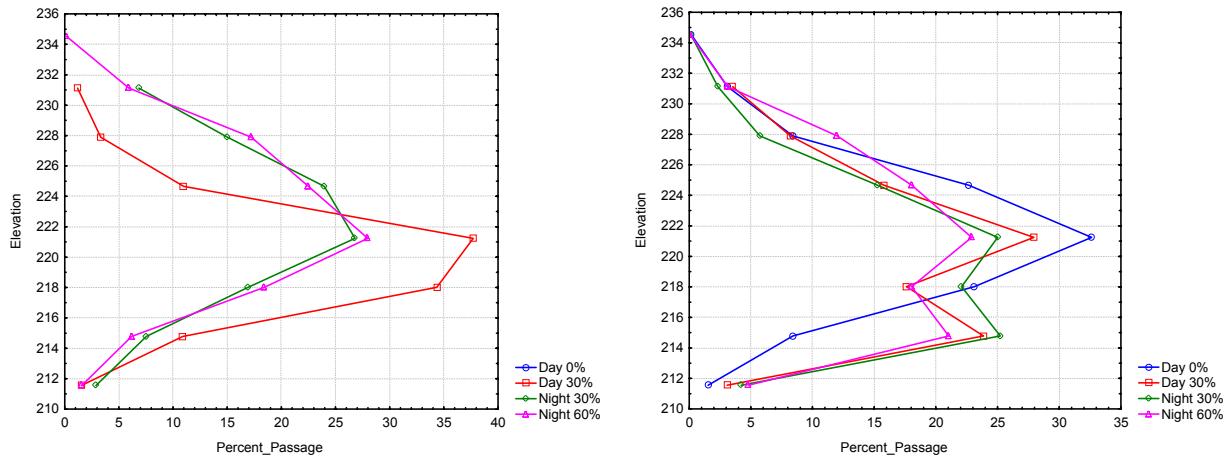


Figure 3.62. Vertical Distribution of Fish Passing in Spill at a 5-ft Spill Gate Opening in Spring (left) and Summer (right)

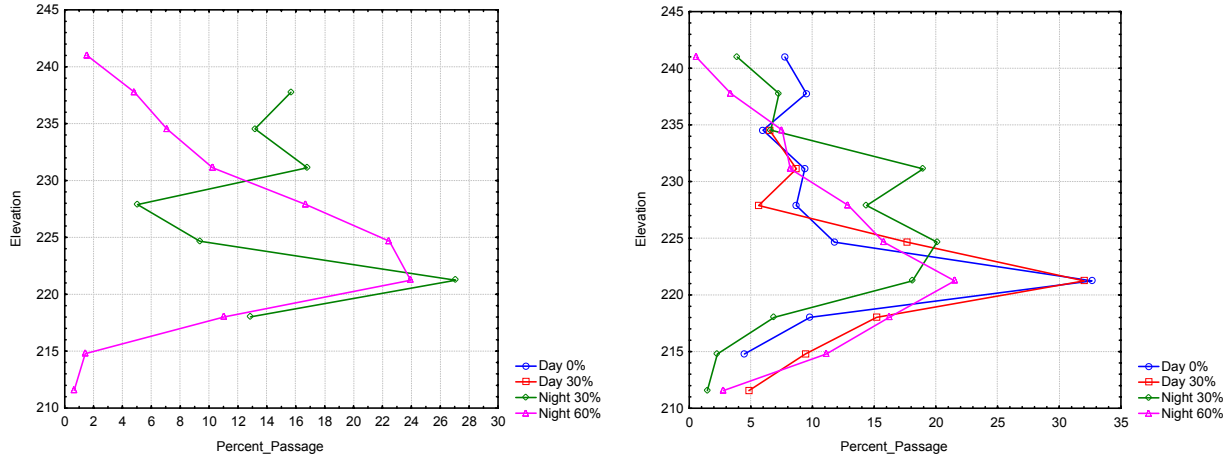


Figure 3.63. Vertical Distribution of Fish Passing in Spill at a 6-ft Spill Gate Opening in Spring (left) and Summer (right)

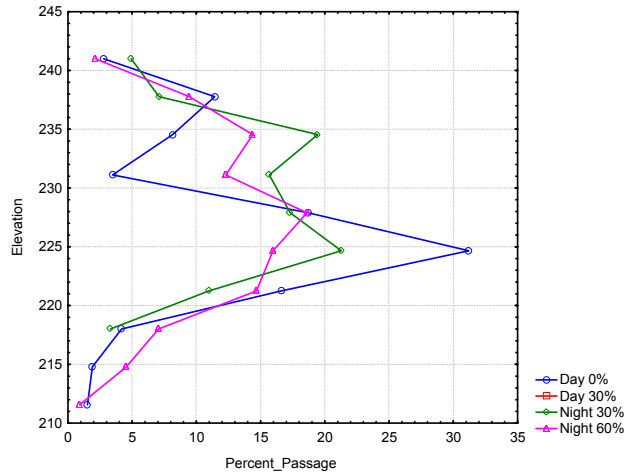


Figure 3.64. Vertical Distribution of Fish Passing in Spill at a 7-ft Spill Gate Opening in Summer Only

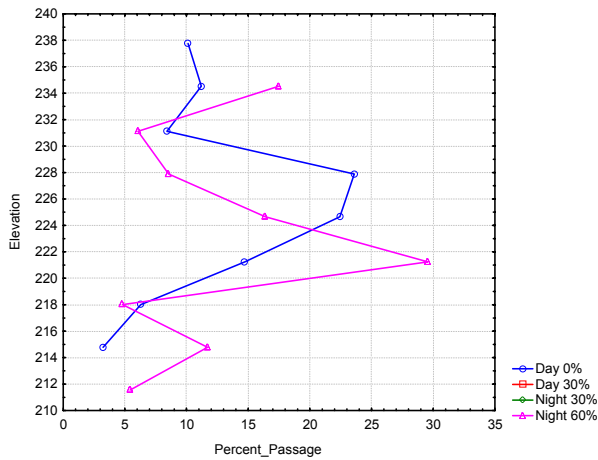


Figure 3.65. Vertical Distribution of Fish Passing in Spill at an 8-ft Spill Gate Opening in Summer Only

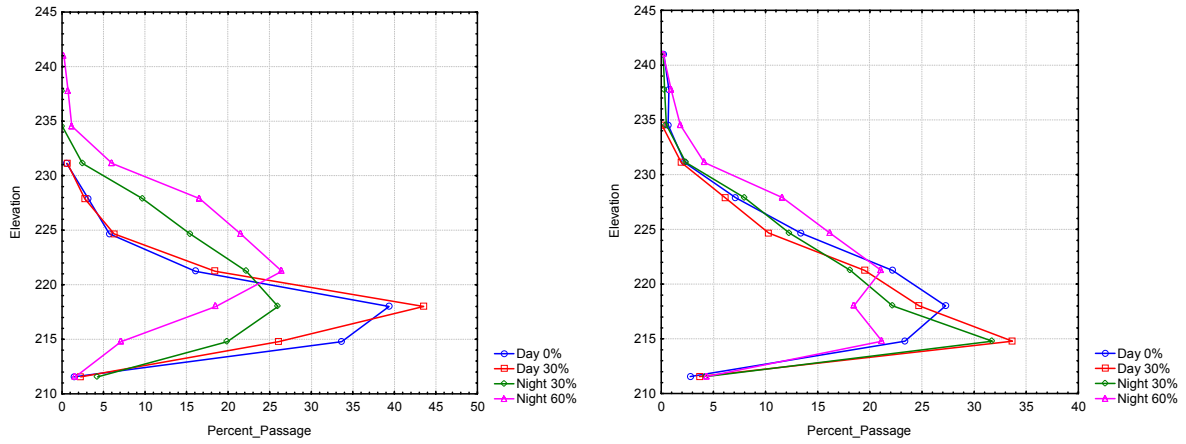


Figure 3.66. Vertical Distribution of Fish Passing in Spill at All Spill Gate Openings Combined in Spring (left) and Summer (right)

4.0 Discussion

This section begins with the study conditions, which provide the river environment context for the study. Then the general fish passage results are discussed. These results contain where and when fish passed the dam regardless of dam operations, and are based on the inclusive data set. Finally, the influences of the spill treatments on fish passage are discussed. These results were based on censored data that best fit the planned spill conditions.

4.1 Study Conditions

River flows during this sample period were near the 10-year average, but with peak flows delayed until summer. The spring migratory fish composition was a bit unusual in that one-quarter of the migrants were sockeye, which is higher than recent years. Yearling chinook salmon were the most abundant spring migrants. During summer, nearly all of the downstream migrants were subyearling chinook. Spill treatments altered day and night spill proportion and their influence is evident in some of the seasonal comparisons.

4.2 General Fish Passage

The general fish passage performance metrics are estimated by season, spring and summer, in response to changes in species composition during the salmonid outmigration. The following three sections discuss the performance metrics related to the major structures of the dam. Dam operations, including spill treatments, are not considered. Inferences of these general passage results do not go beyond the observation year.

4.2.1 Fish Passage Efficiency

Project passage estimates have been made previously with both hydroacoustic and radio telemetry methodologies. These were summarized recently in a synthesis report of studies from 1980 to 2000 (Anglea et al. 2001). Project FPE was computed for the first time at John Day Dam with hydroacoustic methods. Daily trends showed the influence of spill treatments, yet the tendency of fish to pass in greater numbers at night was evident during all treatments. Horizontal distributions were consistent with proportion of flow through a route, except that fish pass in greater proportion than flow at the spillway, relative to the powerhouse. FPE increased slightly with increasing proportion of spill.

Both spring and summer fish passage metrics fell within the range of previous hydroacoustic (Table 4.1) and radio telemetry (Table 4.2) studies (Anglea et al. 2001). These tables have been updated and modified for this report. The major metrics are labeled consistently between the tables and for this report.

Table 4.1. Summary of Fixed Location Hydroacoustic Fish Passage Studies from 1988 to 2002. The fish passage performance metrics were altered from Anglea et al. (2001) to be defined consistently with those used in this report.

Sampling Metric	Study Year													This Study	
	1980	1981	1983	1984	1985	1986	1987	1988	1989	1996	1997	1998	1999		2000
Performance/Passage Metrics															
Fish passage efficiency (spring/summer)	NA	NA	NA	NA	NA	NA	NA	NA	NA	NA	NA	NA	NA	NA	0.93 spr./0.89 sum.
Spill passage efficiency (spring/summer)	NA	NA	0.39 spr. 0.40 sum	0.38 sum.	0.21 spr.	0.32 sum.	0.23 sum.	0.19 sum.	0.28 sum.	NA	0.53 spr./0.85 sum.	0.63 spr./0.49 sum.	0.82 spr./0.93 sum.	0.79 sum.	0.78 spr./0.67 sum.
Powerhouse fraction (spring/summer)	NA	NA	0.63	0.58	0.67	NA	0.89	0.9	0.86	NA	0.49 spr./0.19 sum.	0.34	0.18 spr./0.07 sum.	0.21	0.22 spr./0.33 sum.
Fish guidance efficiency (spring/summer)	NA	NA	NA	NA	NA	NA	NA	NA	NA	NA	NA	NA	NA	NA	0.66 spr./0.66 sum
Spill effectiveness (spring/summer)	NA	NA	0.79 spr. 1.04 sum.	0.76 sum.	0.75 spr.	1.04 sum.	1.3 sum.	1.1 sum.	1.4 sum.	NA	2.32 spr./3.92 sum.	2.92 spr./1.89 sum.	2.74 spr./3.76 sum.	2.79 sum.	2.71 spr./2.27 sum.
Sampling dates	4/22-6/11	4/20-8/13	4/23-8/26	6/5-8/26	4/21-7/28	7/17-8/14	6/7-8/15	5/13-8/15	6/11-8/23	5/8-7/23	5/5-7/24	4/19-7/18	5/1-7/8	6/6-7/9	4/18-7/15
Sampling duration	0000-2300	1700-0500	2000-0600	2100-0500	2100-0500	2000-0500	2100-0500	2100-0500	2000-0600	0000-2300	0000-2300	0000-2300	0000-2300	0000-2300	0600-0559
Mean discharge (ft/s)	259,188	263,447	257,501	233,233	186,423	150,238	118,793	142,086	119,249	335,947	486,676	283,387	313,225	195,324	274,000
Spill discharge fraction	0.08	0.19	0.33	0.3	0.38	0.3	0.18	0.18	0.21	0.21	0.35	0.32	0.27	0.36	0.31
Turbines sampled	2 of 16	3 of 16	7 of 16	6 of 16	6 of 16	7 of 16	6 of 16	6 of 16	6 of 16	1 of 16	8 of 16	8 of 16	15 of 16	16 of 16	16 of 16
Spill bays sampled	1 of 20	2 of 20	6 of 20	6 of 20	6 of 20	6 of 20	5 of 20	4 of 20	6 of 20	0 of 20	10 of 20	11 of 20	11 of 20	11 of 20	18 of 20
Run timing		Yes	Yes	Yes	Yes	Yes	Yes	Yes	Yes	NA	Yes	Yes	Yes	Yes	Yes
Powerhouse Metrics															
Horizontal distributions	Yes	Yes	Yes	NA	NA	Yes	Yes	Yes	Yes	NA	Yes	Yes	Yes	Yes	Yes
Vertical distributions	Yes	Yes	Yes	NA	NA	Yes	Yes	Yes	Yes	NA	Yes	Yes	Yes	Yes	Yes
Spillway Metrics															
Horizontal distributions	NA	NA	Yes	NA	NA	Yes	NA	NA	Yes	NA	Yes	Yes	Yes	Yes	Yes
Vertical distributions	NA	NA	NA	NA	NA	NA	NA	NA	Yes	NA	Yes	Yes	Yes	Yes	Yes
Detection modeling	?	?	?	?	?	Yes	Yes	Yes	Yes	?	Yes	Yes	Yes	Yes	Yes
Detectability corrected?	No	No	No	No	No	No	No	No	No	No	No	No	No	No	Yes

Table 4.2. Summary of Radio Telemetry Studies from 1984 to 2000. The 1999 and 2000 results are preliminary updates from Anglea et al. (2001), and the fish passage performance metrics were altered to be defined consistently with those used in this report.

Species and Study Year	Sample Size	Sample Dates	SPE = % Fish Passing Spill	% Spill (ave) of Total Discharge	Spill Effectiveness	FPE = Fish Passage Efficiency	Spill Range (kcfs)	River Discharge Range (kcfs)
1984								
CHIN 1	95	5/1-5/25	74	42	1.8:1	NA		260-370
1995								
CHIN 1	100	5/2-6/8	24.5	3.9	6.3:1	NA	8-13	250-296
1996								
CHIN 1	138	4/25-6/5	43.1	20.7	2.1:1	NA	47-125	298-450
CHIN 0	75	6/12-7/19	39.5	18.4	2.1:1	NA	55-56	225-359
1997								
STH 1	122	4/28-6/9	54.6	33	1.7:1	NA	92-215	397-540
CHIN 1	115	4/28-6/9	64.2	33	1.9:1	NA	92-215	397-540
CHIN 0	95	7/2-7/22	49.6	19.9	2.5:1	NA	58-62	291-308
1998								
STH 1	119	5/1-5/22	52.3	43.3	1.2:1	NA	150-223	292-468
CHIN 1	120	5/1-5/22	74.7	43.3	1.7:1	NA	150-223	292-468
CHIN 0	119	6/22-7/17	76.5	53.2	1.4:1	NA	116-141	208-302
1999								
STH 1 (12-h)	138	5/7-5/30	44.9	00/45	1.6:1	94.2	0-123	250-367
STH 1 (24-h)	156	5/7-5/30	52.6	30/45	1.1:1	90.4	76-130	254-366
CHIN 1 (12-h)	154	5/7-5/30	52.6	00/45	3.0:1	82.5	0-123	250-367
CHIN 1 (24-h)	160	5/7-5/30	65.6	30/45	1.4:1	87.5	76-130	254-366
Pooled (12-h)	292	5/7-5/30	49.0	00/45		88.0	0-123	250-367
Pooled (24-h)	316	5/7-5/30	59.2	30/45		88.9	76-130	254-366
2000								
STH 1 (12-h)	202	5/1-5/26		00/53	2.3:1	93.0	0-143	217-312
STH 1 (24-h)	229	5/1-5/26		30/53	1.4:1	91.3	74-150	247-299
CHIN 1 (12-h)	214	5/1-5/26	75.1	00/53	2.4:1	89.7	0-143	217-312
CHIN 1 (24-h)	241	5/1-5/26	85.8	30/53	1.4:1	91.8	74-150	247-299
Pooled (12-h)	416	5/1-5/26		00/53			0-143	217-312
Pooled (24-h)	470	5/1-5/26		30/53			74-150	247-299
CHIN1 = yearling chinook salmon.				STH1 = yearling steelhead.				
CHIN0 = subyearling chinook salmon.				Pooled = yearling steelhead and yearling chinook salmon combined.				

4.2.2 Spill Passage

Estimates of spill passage effectiveness from both hydroacoustic and radio telemetry studies have ranged from about 1 in the 1980s to over 3 in the 1990s. The spillway continues to be an effective passage route in the 2000s as fisheries managers have actively manipulated the spill pattern to optimize fish passage. For all seasons and diel periods in 2002, a greater proportion of fish passed via the spillway than proportion of flow. Project fish passage rates decreased when the spillway was closed during the day period of the 12-h treatment, suggesting that fish were reluctant to pass via the turbines during the day, relative to the spillway.

At the spillway, fish passed in greatest numbers near the Washington shore. This trend was confounded somewhat with the spill pattern which opened bays from the Washington shore, starting with bay 2. (Spill bay 1 was not opened due to downstream egress concerns.) As an interim smolt protection measure, spill contributed considerably to FPE by passing about 2/3 of the fish and was an effective passage route by using only 1/3 of project discharge during the study.

4.2.3 Screens

Five fyke net studies were completed at John Day Dam by NOAA Fisheries in 1985, 1986, 1996, 1999, and concurrent to this study in 2002 (see Figure 4.1) (Brege et al. 1987, 1997, 2001, and 2002; Krcoma et al. 1986). Fyke net estimates of FGE were less variable and in the lower part of the range of hydroacoustic estimates. The earlier two studies tested STS and the latter three tested ESBS. Data from the 2002 ESBS study are preliminary. Overall estimates of fish guidance efficiency at an STS were 21% in 1985 and 35% in 1986. In the later studies, fish guidance efficiency was broken down by species. Overall, the estimates of FGE at the ESBS were much higher than for the STS (Table 4.3).

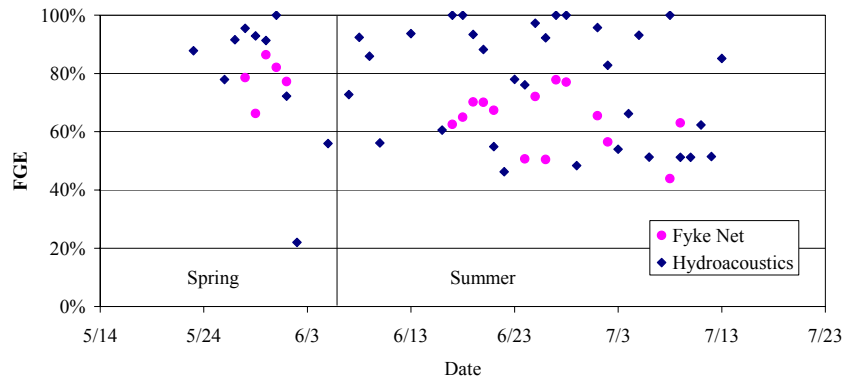


Figure 4.1. Hydroacoustic and Fyke Net Daily Estimates of Fish Guidance Efficiency at Unit 7B. Fyke net data courtesy of NOAA Fisheries (Brege et al. 2002).

In 2002, hydroacoustic estimates of overall FGE were 66% for both spring and summer, but a strong diel trend was evident at both STS and ESBS. Fish guidance was lower at night, regardless of screen type. FGE showed a decreasing trend with increasing spill proportion, but the influence of day versus night is confounded with spill proportion due to the nature of the spill treatments. ESBS guided a greater proportion of fish than did STS during all seasons and diel periods. In addition, FGE at the ESBS declined less at night during the summer, when FGE at STS was lowest.

Table 4.3. Fyke Net Study Results of Fish Guidance Efficiency at an ESBS at John Day Dam. The 2002 results are preliminary.

Species	1996	1999	2002 Spring	2002 Summer
Yearling Chinook	84.0 ± 1.6%	80.2 ± 4.4%	80 ± 9.4%	
Steelhead	94.1 ± 1.8%	94.0 ± 3.8%		
Coho	94.8 ± 2.6%	99.5 ± 1.2%		
Sockeye	78.9 ± 3.8%	25.4 ± 4.1%		
Subyearling Chinook	60.2 ± 6.3%	No data	72 ± 13.2%	63.8 ± 5.8%

A simple paired t-test was used to compare daily hydroacoustic and fyke net estimates of FGE (all species combined) for the same time period. Differences were not significant in spring ($p=0.29$) but they were in summer ($p=0.001$). Hydroacoustic estimates of FGE in summer were generally higher than fyke net estimates, and may have been biased because few fish passed the sample volume within the two-hour period or because hourly dam operations data is not sufficient to account for the operational changes required to conduct fyke net tests. If we do not restrict ourselves to the times when netting was conducted, the average summer FGE is within 4% of the mean fyke net value.

Though we do not expect perfect agreement between any two methods of estimating passage, there may be room for improvement. Hydroacoustic estimates of FGE at John Day Dam could be made with greater certainty if better flow information were available. If a turbine intake flow model were available, cut-off points for guided fish could be estimated with greater certainty. Flow information would also indicate whether unguided fish at the ESBS may be moving more rapidly than we can detect. If fish velocity is higher than we have been able to measure, detectability models could be run with updated velocities to correct for the potential bias. To reduce the uncertainty in future hydroacoustic estimates of fish passage, we recommend that a turbine intake flow model be constructed for both STS and ESBS.

In spring, the ESBS guided more fish than STS, especially at night. ESBS performance remained high during the night when STS guidance efficiency dropped considerably. The ESBS was operated only during the latter third of the spring period, so uncertainty remains about ESBS performance in early spring. STS guidance during early spring was relatively low, so we speculate that ESBS would also be lower, but would likely remain higher than STS. In summer, ESBS guided more fish than STS, but performance of both screen types declined at night. Nighttime FGE for ESBS remained higher than for STS. The manipulation of spill proportion for the spill treatment comparison had little effect on FGE of either screen type.

4.3 Spill Treatment Effects

Recall that a randomized block design was used to compare treatments. Treatments were either 12-h spill (0% daytime with 60% nighttime) or 24-h spill (constant 30%). Each treatment day began at 0600 h and ended at 0559 h. The following section discusses how the spill treatments affected the various fish passage performance metrics. Beyond that, a synthesis section extrapolates the data for a look at how an all-ESBS powerhouse might perform under the same spill treatments. The statistical inferences in this section are applicable beyond the study year.

The spill treatments were generally met in the spring until the beginning of summer. Blocks in both spring and summer were included only if they met or nearly met the planned treatment conditions. In summer, the spill proportion of selected blocks was less different among treatments than planned. The expected effect would be a reduced difference among treatments, making the test a more conservative evaluation of whether there is a treatment effect than the planned test. The inclusion of blocks that did not exactly meet the target spill levels may reduce the statistical power to differentiate among treatments, but it makes inferences from statistical tests more broadly applicable to realistic dam operations. In the summer period, the performance of the treatments should be judged relative to actual, rather than nominal spill proportion.

4.3.1 Performance Metrics

The synthesis report concluded that a lack of statistical rigor precluded the use of much of the radio telemetry and hydroacoustic data collected over past years at John Day Dam. In spite of operational challenges, this year was different: The experimental test achieved adequate statistical power to detect differences among spill treatments.

Fish passage efficiency during the 12-h (0% daytime and 60% nighttime) spill treatment condition was significantly higher than during 24-h (constant 30%) spill treatment condition. The tendency of smolts to pass at night maximized the benefit of increased spill passage efficiency with 60% spill. Lower nighttime FGE also suggests that any improvement in SPE at night would have greater than proportional effect on FPE across the entire treatment day. Differences among spill treatments in fish guidance efficiency (FGE), spill passage efficiency (SPE), and spill passage effectiveness (SPS) were not significant in either spring or summer. These results comport with the concurrent radio telemetry study results (Beeman et al. 2002). Our results suggest that passage through non-turbine routes will be maximized by spilling a greater proportion of total flow during hours of darkness to compensate for low FGE during that time.

4.3.2 Synthesis of Spill Treatment and Screen Results

It is pertinent to ask how the powerhouse would perform with an all-ESBS deployment. What would treatment effects be if the powerhouse were fully fitted with extended screens? We attempted to answer that question with the data collected in 2002 by creating a hypothetical all-ESBS powerhouse scenario. We based that scenario on several assumptions, which may or may not be met in an actual installation. We assumed that the measured performance of the single ESBS could be applied throughout each season and across the powerhouse. The FGE for the ESBS for each hour of a 24-h cycle (Figure 3.27 and Figure 3.28) was then applied to the total count for passage at the powerhouse for each treatment by season. The resulting values were combined into FPE values and compared with those of the measured values in the same way we used in the ANOVA of this year's results. The all-ESBS scenario performed much better than the current deployment in spring (Figure 4.2), but about the same in summer (Figure 4.3).

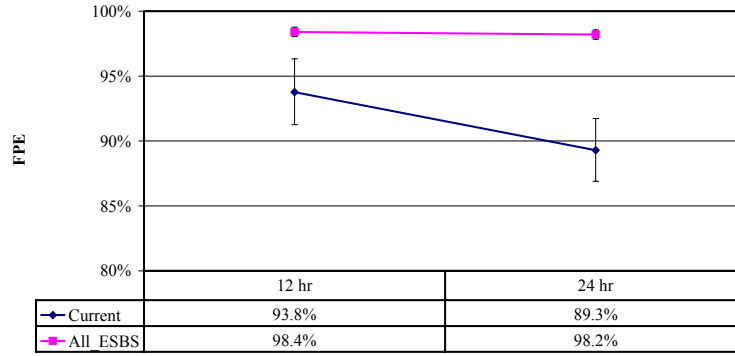


Figure 4.2. Hypothetical Diagram of FPE for an All-ESBS Powerhouse Scenario in Spring. This assumes that the fish passage at unit 7, while it was operational, is representative of a full powerhouse. Error bars are 95% confidence intervals based on ANOVA MSE (Appendix A: Equation A30).

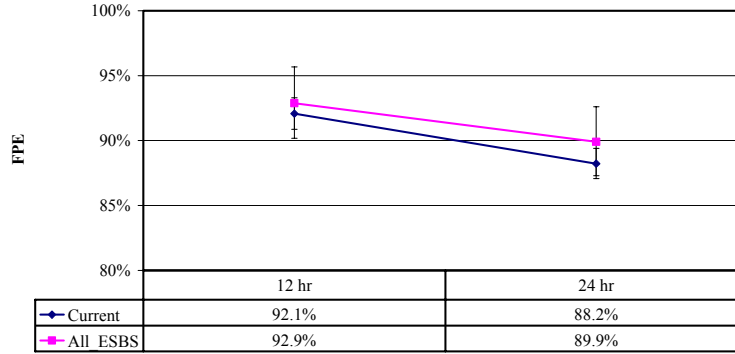


Figure 4.3. Hypothetical Diagram of FPE for an All-ESBS Powerhouse Scenario in Summer. This assumes that the fish passage at unit 7, while it was operational, is representative of a full powerhouse. Error bars are 95% confidence intervals based on ANOVA MSE (Appendix A: Equation A30).

5.0 Conclusions

The results from this study provide new insights into how fish passage at John Day Dam can be optimized, particularly through project operations. Some of the stated goals are to maximize downstream passage while minimizing turbine passage, reducing voluntary spill and dissolved gas levels, and providing safe egress.

The treatment comparisons indicated that 12-h spill outperformed 24-h spill by resulting in reduced turbine passage. The diel differences in spill treatments were critical to their overall performance. The benefit of daytime spill was minimal because daytime fish guidance was high in all treatments, meaning FPE would be high even in the absence of spill. As long as juvenile bypass system survival is high, daytime spill will not have a large impact on project survival. In contrast, nighttime fish guidance was relatively poor, and the higher spill provided in the 12-h treatment had the effect of reducing powerhouse passage and improving FPE, relative to the lower nighttime spill of the 24-h treatment.

These results suggest that night spill proportion should be relatively high and that daytime spill is not critical for minimizing turbine passage. Minimizing turbine passage is just one aspect in maximizing project survival. The benefits of minimizing turbine passage depend on relative survival among available routes, which are being estimated in concurrent studies. The idea that minimizing non-turbine passage results in the greatest project survival relies on the assumption that JBS and spill survival are high and turbine survival is lower. If relative route-specific survivals reverse with spill proportion or time of day, optimizing project survival would have to consider route-, time-, and spill proportion-specific survival estimates.

When we combined spill and screen results into a hypothetical all-ESBS condition, the relative benefits of spill versus screens were potentially biased or confounded with failure to achieve spill treatments. The hypothetical scenario suggested a large positive effect of changing to ESBS in the spring. In summer, the hypothetical ESBS screens do not provide benefits of a similar magnitude. Unfortunately, the portion of the scenario showing strong benefits is based on FGE from a limited time period when the ESBS was operational in spring. Spill treatment proportions were not met in the summer period, even for the selected blocks. Future studies should endeavor to monitor the ESBS throughout the spring period and more strictly apply spill treatments during the summer season.

6.0 References

- Anglea, S., T. Poe, and A. Giorgi. 2001. Synthesis of radio telemetry, hydroacoustic, and survival studies of juvenile salmon at John Day Dam (1980-2000). Prepared for the U.S. Army Corps of Engineers, Portland District, Portland, Oregon.
- Beeman, J.W., H.C. Hansel, P.V. Haner. 2002. FPE of radio-tagged smolts at John Day Dam in 2002. Preliminary data.
- Brege, D.A., R.F. Absolon, J.W. Ferguson, and B.P. Sandford. 2002. Evaluation of the extended-length bypass screens at John Day Dam, 2002. Preliminary results.
- Brege, D.A., D.R. Miller, and R.D. Ledgerwood. 1987. Evaluation of the rehabilitated juvenile salmonid collection and passage system at John Day Dam – 1986. Report to U.S. Army Corps of Engineers, Contact DACW57-86-0245, 30 p. plus Appendices. (Available from Northwest Fisheries Science Center, 2725 Montlake Boulevard East, Seattle, WA 98112-2097.)
- Brege, D.A., J.W. Ferguson, R.F. Absolon, and B.P. Sandford. 2001. Evaluation of the extended-length bypass screens at John Day Dam, 1999. Report to U.S. Army Corps of Engineers, Portland District Delivery Order W66QKZ90392273, 21 p. plus Appendices. (Available from Northwest Fisheries Science Center, 2725 Montlake Boulevard East, Seattle, WA 98112-2097.)
- Brege, D.A., R.F. Absolon, B.P. Sandford, and D.B. Dey. 1997. Studies to evaluate the effectiveness of extended-length screens at John Day Dam, 1996. Report to U.S. Army Corps of Engineers, Portland District Delivery Order E96960028, 22 p. plus Appendices. (Available from Northwest Fisheries Science Center, 2725 Montlake Boulevard East, Seattle, WA 98112-2097.)
- DART. 2001. Columbia River Data Access in Real Time <http://www.cqs.washington.edu/dart/dart.html>. School and Aquatic & Fishery Sciences, University of Washington, Seattle, Washington.
- Krcma, R.F., D.A. Brege, and R.D. Ledgerwood. 1986. Evaluation of the rehabilitated juvenile salmonid collection and passage system at John Day Dam – 1985. Report to U.S. Army Corps of Engineers, Contact DACW57-85-H -0001, 25 p. plus Appendices. (Available from Northwest Fisheries Science Center, 2725 Montlake Boulevard East, Seattle, WA 98112-2097.)
- National Marine Fisheries Service. 2000. Biological Opinion: Reinitiation of consultation on operation of the Federal Columbia River Power System, including the juvenile fish transportation program, and 19 Bureau of Reclamation projects in the Columbia Basin. Date issued: December 21, 2000. National Marine Fisheries Service, Northwest Region: Seattle, Washington.
- Ploskey, G.R., C.B. Cook, P.S. Titzler, and R.A. Moursund. 2002. Optimization of hydroacoustic deployments at John Day Dam. PNNL-14062. Prepared for the U.S. Army Corps of Engineers, Portland District, Portland, Oregon.

Appendix A

Statistical Methods for Hydroacoustic Data Analysis

at John Day Dam 2002

Appendix A - Statistical Methods for Hydroacoustic Data Analysis at John Day Dam 2002

1.0 Introduction

The purpose of this synopsis is to describe the statistical methods used in the analysis of the 2002 hydroacoustic study at John Day Dam. The study will estimate fish passage through the powerhouse (i.e., turbines) and spillway during the spring and summer smolt outmigration. These estimates of fish passage will be used to estimate various measures of fish passage performance including the following:

- a. Fish passage efficiency (FPE)
- b. Spill passage efficiency (SPE)
- c. Spill passage effectiveness (SPS)
- d. Fish guidance efficiency (FGE).

These performance measures will be compared under two different spill treatments conducted during the course of this study.

2.0 Transducer Deployment and Sampling Scheme

This section describes the hydroacoustic sampling schemes that were used to estimate smolt passage at the powerhouse and spillway at John Day Dam in 2002.

2.1 Sampling at Powerhouse

The John Day powerhouse is comprised of 16 turbine units, each with 3 turbine intake slots (i.e., A, B, and C). At all units except unit 7, there are standard-length submerged traveling screens (STS). At unit 7, there are extended-length submerged bar screens (ESBS). One of the 3 intake slots was randomly selected for hydroacoustic sampling at each turbine unit. A pair of transducers (Figure A1) was used within an intake slot to monitor guided and unguided fish passage. Single-beam transducers were used at turbine units 1-6, 8-10, 13-16 sampling 59- or 74-second intervals, 6 times per hour (interval is a function of the number of

transducers per system). Split-beam transducers were deployed at turbine units 11 and 12 sampling 89-second intervals, 10 times per hour. At unit 7, a split-beam system sampled 177-second intervals, 10 times per hour.

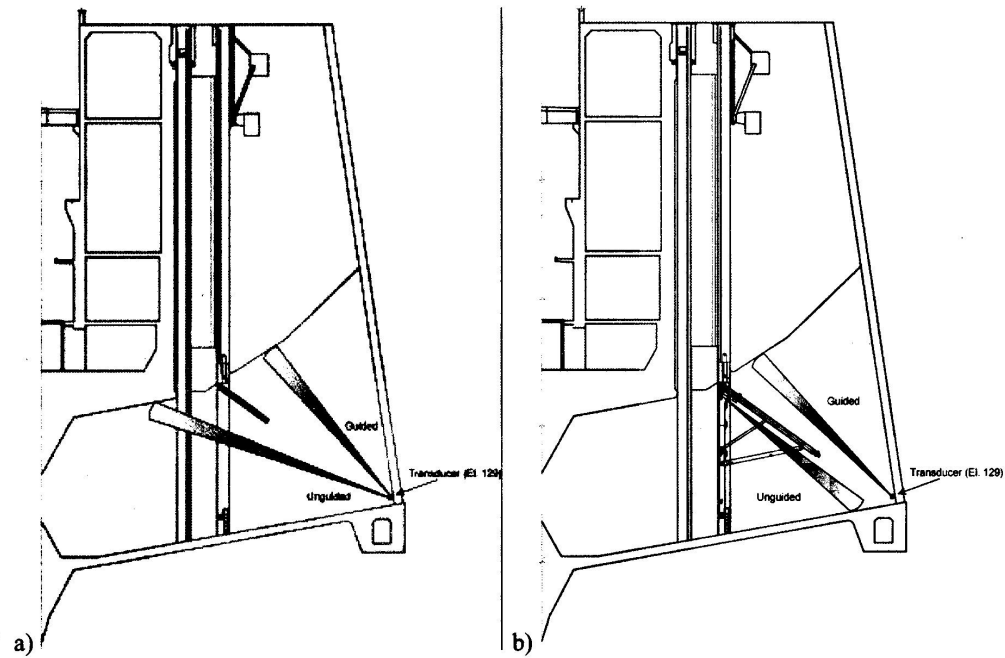


Figure A1. Deployment of Hydroacoustic Transducers at a) STS Intakes and b) ESBS Intakes

2.2 Sampling at Spillway

There are 20 spillbays at John Day Dam. In 2002, spillbays 1 and 19 were not used at anytime during the study. One downlooking-transducer monitored fish passage at each of the remaining 18 spillbays. Spillbays 2, 4, 5, 7, 8, and 10-20 were monitored using single-beam transducers at a rate of six 74- or 85-second intervals per hour (interval is a function of the number of transducers per system). Split-beam transducers were deployed at spillbays 3, 6, and 9 and sampled at a rate of ten 118-second intervals per hour.

3.0 Estimating Fish Passage

The following sections describe how the estimates of smolt passage will be calculated at the various locations at John Day Dam.

3.1 Powerhouse Passage – Unguided Fish

3.1.1 Total Powerhouse

The sampling at the powerhouse can be viewed as a two-stage sampling scheme. The first stage is the sampling of intake slots within a stratum composed of neighboring turbine units that were operating simultaneously. Typically, three consecutive turbine units would be grouped together to form a stratum, and it would be assumed that 3 of 9 intake slots were randomly selected for monitoring. Neighboring turbine units would be grouped into strata while still retaining the ability to calculate spatial sampling variances. The resulting variance estimates can generally be considered conservative for they often include more between-intake variance than expected under the original sampling design.

The unguided fish passage at the powerhouse (U) will be estimated by the quantity

$$\hat{U} = \sum_{i=1}^D \sum_{j=1}^{24} \sum_{k=1}^{K_{ij}} \left[\frac{A_{ijk}}{a_{ijk}} \left[\sum_{l=1}^{a_{ijk}} \hat{U}_{ijkl} \right] \right] \quad (\text{A1})$$

where

\hat{U}_{ijkl} = estimated fish passage in the l th intake slot ($l = 1, \dots, a_{ijk}$) within the k th turbine stratum ($k = 1, \dots, K_{ij}$) during the j th hour ($j = 1, \dots, 24$) on the i th day ($i = 1, \dots, D$);

a_{ijk} = number of intake slots actually sampled in the k th turbine stratum ($k = 1, \dots, K_{ij}$) during the j th hour ($j = 1, \dots, 24$) on the i th day ($i = 1, \dots, D$);

K_{ij} = number of turbine strata created during the j th hour ($j = 1, \dots, 24$) on the i th day
($i = 1, \dots, D$).

Because of the varying power loads over time, the number of spatial strata (i.e., K_{ij}) formed by post-stratification of adjacent turbine units may vary between hours ($j = 1, \dots, 24$) and days ($i = 1, \dots, D$).

The estimate of \hat{U}_{ijkl} is based on the assumption of simple random sampling within a slot-hour, in which case

$$\hat{U}_{ijkl} = \frac{B_{ijkl}}{b_{ijkl}} \sum_{b=1}^{b_{ijkl}} z_{ijklg} . \quad (\text{A2})$$

Combining Equations (A1) and (A2), the overall estimate of unguided fish passage during D days can be expressed as

$$\hat{U}_{ijkl} = \sum_{i=1}^D \sum_{j=1}^{24} \sum_{k=1}^{K_{ij}} \left[\frac{A_{ijk}}{a_{ijk}} \left[\frac{B_{ijkl}}{b_{ijkl}} \sum_{b=1}^{b_{ijkl}} z_{ijklg} \right] \right] \quad (\text{A3})$$

where

z_{ijklg} = expanded fish count in the g th sampling unit ($g = 1, \dots, b_{ijkl}$) in the l th intake slot
($l = 1, \dots, a_{ijk}$) within the k th turbine stratum ($k = 1, \dots, K_{ij}$) during the j th hour
($j = 1, \dots, 24$) on the i th day ($i = 1, \dots, D$);

b_{ijkl} = number of sampling units actually observed in the l th intake slot ($l = 1, \dots, a_{ijk}$)
within the k th turbine stratum ($k = 1, \dots, K_{ij}$) during the j th hour ($j = 1, \dots, 24$) on
the i th day ($i = 1, \dots, D$);

B_{ijkl} = total number of sampling units within the l th intake slot ($l = 1, \dots, a_{ijk}$) within the k th turbine stratum ($k = 1, \dots, K_{ij}$) during the j th hour ($j = 1, \dots, 24$) on the i th day ($i = 1, \dots, D$).

Nominally, $B_{ijkl} = 20, 40, 48$ or $60 \forall ijkl$ and $b_{ijkl} = 6$ or 10 , depending on location. Based on the assumption of simple random sampling

$$\widehat{Var}(\hat{U}_{ijkl}) = \frac{B_{ijkl}^2 \left(1 - \frac{b_{ijkl}}{B_{ijkl}}\right) s_{z_{ijkl}}^2}{b_{ijkl}} \quad (\text{A4})$$

where

$$s_{z_{ijkl}}^2 = \frac{\sum_{g=1}^{b_{ijkl}} (z_{ijklg} - \bar{z}_{ijkl})^2}{(b_{ijkl} - 1)}$$

and where

$$\bar{z}_{ijkl} = \frac{1}{b_{ijkl}} \sum_{g=1}^{b_{ijkl}} z_{ijklg} .$$

The variance of \hat{U} can then be estimated by the formula

$$\widehat{Var}(\hat{U}) = \sum_{i=1}^D \sum_{j=1}^{24} \sum_{k=1}^{K_{ij}} \left[\frac{A_{ijk}^2 \left(1 - \frac{a_{ijk}}{A_{ijk}}\right) s_{\hat{U}_{ijk}}^2}{a_{ijk}} + \frac{A_{ijk} \sum_{l=1}^{a_{ijk}} \widehat{Var}(\hat{U}_{ijkl})}{a_{ijk}} \right] \quad (\text{A5})$$

where

$$s_{\hat{U}_{ijk}}^2 = \frac{\sum_{l=1}^{a_{ijk}} (\hat{U}_{ijkl} - \hat{U}_{ijk})^2}{(a_{ijk} - 1)},$$

$$\hat{U}_{ijk} = \frac{1}{a_{ijk}} \sum_{l=1}^{a_{ijk}} \hat{U}_{ijkl}.$$

3.1.2 Single Turbine Unit

The estimator of unguided passage at a single turbine is as follows:

$$\hat{U}_k = \frac{3}{1} \sum_{i=1}^D \sum_{j=1}^{24} \left[\frac{B_{ijk}}{b_{ijk}} \sum_{g=1}^{b_{ijk}} z_{ijk} \right] \quad (\text{A6})$$

where

z_{ijk} = expanded fish passage in the g th sampling unit ($g = 1, \dots, b_{ijk}$) at the k th turbine unit during the j th hour ($j = 1, \dots, 24$) on the i th day ($i = 1, \dots, D$);

b_{ijk} = number of sampling intervals monitored at the k th turbine unit during the j th hour ($j = 1, \dots, 24$) on the i th day ($i = 1, \dots, D$);

B_{ijk} = total number of possible sampling intervals at the k th turbine unit during the j th hour ($j = 1, \dots, 24$) on the i th day ($i = 1, \dots, D$).

The variance of \hat{U}_k can be estimated by

$$\widehat{Var}(\hat{U}_k) = \sum_{i=1}^D \sum_{j=1}^{24} \left[\frac{B_{ijk}^2 \left(1 - \frac{b_{ijk}}{B_{ijk}} \right) s_{z_{ijk}}^2}{b_{ijk}} \right] \quad (\text{A7})$$

where

$$s_{z_{ijk}}^2 = \frac{\sum_{g=1}^{b_{ijk}} (z_{ijkg} - \bar{z}_{ijk})^2}{(b_{ijk} - 1)},$$

$$\bar{z}_{ijk} = \frac{\sum_{g=1}^{b_{ijk}} z_{ijkg}}{b_{ijk}}.$$

It should be noted that the variance estimator (A7) will underestimate the true sampling variance at a specific turbine unit.

3.2 Powerhouse Passage – Guided Fish

3.2.1 Total Powerhouse

The post-stratification used in estimating unguided passage should be the same as used to estimate guided passage at the powerhouse. Hence, the estimator for guided fish passage can be written as

$$\hat{G} = \sum_{i=1}^D \sum_{j=1}^{24} \sum_{k=1}^{K_{ij}} \left[\frac{A_{ijk}}{a_{ijk}} \left[\frac{B_{ijkl}}{b_{ijkl}} \sum_{g=1}^{b_{ijkl}} y_{ijklg} \right] \right] \quad (\text{A8})$$

where

y_{ijklg} = expanded fish passage in the g th sampling unit ($g = 1, \dots, b_{ijkl}$) in the l th intake slot ($l = 1, \dots, a_{ijk}$) within the k th turbine stratum ($k = 1, \dots, K_{ij}$) during the j th hour ($j = 1, \dots, 24$) on the i th day ($i = 1, \dots, D$).

The estimated variance of \hat{G} can then be expressed as

$$\widehat{Var}(\hat{G}) = \sum_{i=1}^D \sum_{j=1}^{24} \sum_{k=1}^{K_{ij}} \left[\frac{A_{ijk}^2 \left(1 - \frac{a_{ijk}}{A_{ijk}} \right) s_{G_{ijk}}^2}{a_{ijk}} + \frac{A_{ijk} \sum_{l=1}^{a_{ijk}} \widehat{Var}(\hat{G}_{ijkl})}{a_{ijk}} \right] \quad (\text{A9})$$

where

$$\widehat{Var}(\hat{G}_{ijkl}) = \frac{B_{ijkl}^2 \left(1 - \frac{b_{ijkl}}{B_{ijkl}}\right) s_{y_{ijkl}}^2}{b_{ijkl}},$$

$$s_{y_{ijkl}}^2 = \frac{\sum_{g=1}^{b_{ijkl}} (y_{ijklg} - \bar{y}_{ijkl})^2}{(b_{ijkl} - 1)},$$

$$\bar{y}_{ijkl} = \frac{1}{b_{ijkl}} \sum_{g=1}^{b_{ijkl}} y_{ijklg},$$

and where

$$s_{\hat{G}_{ijk}}^2 = \frac{\sum_{l=1}^{a_{ijk}} (\hat{G}_{ijkl} - \hat{G}_{ijk})^2}{(a_{ijk} - 1)},$$

$$\hat{G}_{ijk} = \frac{1}{a_{ijk}} \sum_{l=1}^{a_{ijk}} \hat{G}_{ijkl}.$$

3.2.2 Single Turbine Unit

The estimator of guided passage at a single turbine is as follows:

$$\hat{G}_k = \frac{3}{1} \sum_{i=1}^D \sum_{j=1}^{24} \left[\frac{B_{ijk}}{b_{ijk}} \sum_{g=1}^{b_{ijk}} y_{ijkg} \right] \quad (\text{A10})$$

where

y_{ijkg} = expanded fish passage in the g th sampling unit ($g = 1, \dots, b_{ijk}$) at the k th turbine unit during the j th hour ($j = 1, \dots, 24$) on the i th day ($i = 1, \dots, D$);

b_{ijk} = number of sampling intervals monitored at the k th turbine unit during the j th hour ($j = 1, \dots, 24$) on the i th day ($i = 1, \dots, D$);

B_{ijk} = total number of possible sampling intervals at the k th turbine unit during the j th hour ($j = 1, \dots, 24$) on the i th day ($i = 1, \dots, D$).

The variance of \hat{G}_k can be estimated by

$$\widehat{Var}(\hat{G}_k) = 9 \sum_{i=1}^D \sum_{j=1}^{24} \left[\frac{B_{ijk}^2 \left(1 - \frac{b_{ijk}}{B_{ijk}} \right) s_{y_{ijk}}^2}{b_{ijk}} \right] \quad (\text{A11})$$

where

$$s_{y_{ijk}}^2 = \frac{\sum_{g=1}^{b_{ijk}} (y_{ijk} - \bar{y}_{ijk})^2}{(b_{ijk} - 1)},$$

$$\bar{y}_{ijk} = \frac{\sum_{g=1}^{b_{ijk}} z_{ijk}}{b_{ijk}}.$$

It should be noted that the variance estimator (A11) will underestimate the true sampling variance at a specific turbine unit.

3.3 Spillway Passage

The sampling at the John Day spillway can be envisioned as stratified random sampling within spillbay-hours. In which case, total spillway passage over D days can be estimated by the formula

$$\widehat{SP} = \sum_{i=1}^D \sum_{j=1}^{24} \sum_{k=1}^{18} \left[\frac{T_{ijk}}{t_{ijk}} \sum_{l=1}^{t_{ijk}} x_{ijkl} \right] \quad (\text{A12})$$

where

x_{ijkl} = expanded fish passage in the l th sampling interval ($l = 1, \dots, t_{ijk}$) during the j th hour ($j = 1, \dots, 24$) at the k th spillbay ($k = 1, \dots, 18$) on the i th day ($i = 1, \dots, D$);

T_{ijk} = total number of possible sampling units within the j th hour ($j = 1, \dots, 24$) at the k th spillbay ($k = 1, \dots, 18$) on the i th day ($i = 1, \dots, D$);

t_{ijk} = number of sampling units actually observed within the j th hour ($j = 1, \dots, 24$) at the k th spillbay ($k = 1, \dots, 18$) on the i th day ($i = 1, \dots, D$).

Nominally, $T_{ijk} = 30, 42$ or $48 \forall ijk$ and $t_{ijk} = 6$ or 10 depending on location.

The variance of \widehat{SP} can be estimated by the quantity

$$\widehat{var}(\widehat{SP}) = \sum_{i=1}^D \sum_{j=1}^{24} \sum_{k=1}^{18} \left[\frac{T_{ijk}^2 \left(1 - \frac{t_{ijk}}{T_{ijk}}\right) s_{x_{ijk}}^2}{t_{ijk}} \right] \quad (\text{A13})$$

where

$$s_{x_{ijk}}^2 = \frac{\sum_{l=1}^{t_{ijk}} (x_{ijkl} - \bar{x}_{ijk})^2}{(t_{ijk} - 1)}$$

and where

$$\bar{x}_{ijk} = \frac{1}{t_{ijk}} \sum_{l=1}^{t_{ijk}} x_{ijkl} .$$

3.4 Estimating Missing Values

Occasionally throughout the sampling season, sample observations were missed when hydroacoustic equipment failed, log debris damaged equipment, or other unexpected events occurred. This loss of information typically occurred at only one or a few locations at a time. The majority of the data from many of these sites is still available when these lapses occurred.

Two specific missing-value scenarios make up a majority of the occurrences; these scenarios were:

1. In a turbine, the unguided turbine fish counts were missing, while the guided turbine fish counts were present.
2. Some spillbays were missing values, while concurrently, other spillbays were monitored.

Both approaches apply to the discussion.

Ratio or regression estimators can be used to estimate missing values on an hourly basis with associated variances (Snedecor and Cochran 1989: 165-167).

3.4.1 Regression Estimator

Figure A.2 illustrates the typical scenario for missing values. Let

x_i = hourly passage estimate for the i th interval at a location with complete data,

y_i = hourly passage estimate for the i th interval at a location with missing values.

From hourly time intervals with complete data, a regression model of the form

$$y_i = \hat{\alpha} + \hat{\beta}x_i \quad (\text{A14})$$

is fitted using ordinary least squares. A missing y -value is then predicted by substituting into Equation (A14) the corresponding x -value where

$$\hat{y}_m = \hat{\alpha} + \hat{\beta}x_m . \quad (\text{A15})$$

The estimated variance for the predicted \hat{y}_m is computed according to the formula

$$\widehat{Var}(\hat{y}_m) = \text{MSE} \left(1 + \frac{1}{n} + \frac{(x_m - \bar{x})^2}{\sum_{i=1}^n (x_i - \bar{x})^2} \right) \quad (\text{A16})$$

where

n = number of observations used in estimating the regression line,

MSE = mean square for error resulting from the regression,

\bar{x} = mean value of x_i from the location with complete data,

x_m = value of x corresponding to the observation with a missing y -value,

\hat{y}_m = estimated missing value.

These results can be found in Snedecor and Cochran (1989: 165-167). The regression approach is most appropriate if the relationship is a straight-line not through the origin.

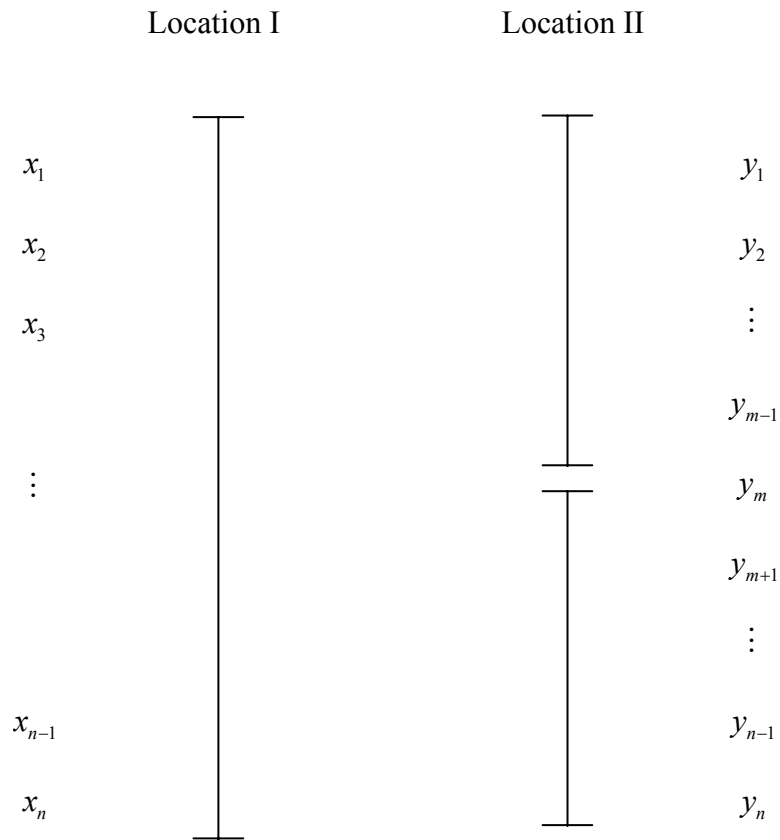


Figure A2. Schematic of Missing Value Scenarios, where at one Location (I) all values are completed and at another location (II) values are missing for an interval of time

3.4.2 Ratio Estimator

Alternatively, if the relationship is a straight line through the origin of the form

$$y_i = \beta x_i$$

then a ratio estimator can be used to estimate missing values. The ratio estimator can be written as

$$\hat{y}_m = \frac{\sum_{i=1}^n y_i}{\sum_{i=1}^n x_i} x_m \quad (\text{A17})$$

where the summations are over all paired observations where both the x and y values are present (i.e., n paired values). The variance of \hat{y}_m can be estimated by

$$\widehat{Var}(\hat{y}_m) = \frac{x_m^2 \sum_{i=1}^n (y_i - \hat{R}x_i)^2}{\bar{x}^2 n(n-1)}. \quad (\text{A18})$$

The method can be found in Cochran 1977 (pp. 153-156).

3.4.3 Interpolation Method

An estimate of a missing value can also be calculated by interpolating between neighboring values. Let y_m be a missing value for the m th hour, then it can be estimated by

$$\hat{y}_m = \frac{y_{m-1} + y_{m+1}}{2} \quad (\text{A19})$$

with interpolated variance

$$\widehat{Var}(\hat{y}_m) = \frac{\widehat{Var}(\hat{y}_{m-1}) + \widehat{Var}(\hat{y}_{m+1})}{2^2} \quad (\text{A20})$$

where

$\hat{y}_{m\pm 1}$ = passage one hour on either side of the m th hour with a missing value.

4.0 Estimating Passage Performance

4.1 Fish Passage Efficiency (FPE)

The fish passage efficiency (FPE) at John Day Dam will be estimated by the quotient

$$\widehat{FPE} = \frac{\widehat{SP} + \hat{G}}{\widehat{SP} + \hat{G} + \hat{U}} \quad (\text{A21})$$

where

\widehat{SP} = estimated fish passage through the spillway,

\hat{G} = estimated guided fish passage through the turbine routes,

\hat{U} = estimated unguided fish passage through the turbine routes.

The denominator of Equation (A21) is an estimate of total project passage. The variance of \widehat{FPE} can be estimated by the quantity

$$\widehat{Var}(\widehat{FPE}) = \widehat{FPE}^2 (1 - \widehat{FPE})^2 \left[\frac{\widehat{Var}(\widehat{SP}) + \widehat{Var}(\hat{G})}{(\widehat{SP} + \hat{G})^2} + \frac{\widehat{Var}(\hat{U})}{\hat{U}^2} \right]. \quad (\text{A22})$$

4.2 Spill Efficiency (SPE)

Spill efficiency (SPE) at John Day Dam will be estimated by the quotient

$$\widehat{SPE} = \frac{\widehat{SP}}{\widehat{SP} + \hat{G} + \hat{U}}. \quad (\text{A23})$$

The variance of \widehat{SPE} can then be expressed as

$$\widehat{Var}(\widehat{SPE}) = \widehat{SPE}^2 (1 - \widehat{SPE})^2 \left[\frac{\widehat{Var}(\widehat{SP})}{\widehat{SP}^2} + \frac{\widehat{Var}(\hat{G}) + \widehat{Var}(\hat{U})}{(\hat{G} + \hat{U})^2} \right]. \quad (\text{A24})$$

4.3 Spill Effectiveness (SPS)

Spill effectiveness (SPS) at John Day Dam will be estimated by the function

$$\widehat{SPS} = \frac{\left(\frac{\widehat{SP}}{f_{SP}}\right)}{\left(\frac{\widehat{SP} + \widehat{G} + \widehat{U}}{f}\right)} = \left(\frac{f}{f_{SP}}\right) \widehat{SPE} \quad (\text{A25})$$

where

f = project-wide flow volume,

f_{SP} = spill flow volume.

The variance of \widehat{SPS} can be estimated by the quantity

$$\widehat{Var}(\widehat{SPS}) = \left(\frac{f}{f_{SP}}\right)^2 \cdot \widehat{Var}(\widehat{SPE}). \quad (\text{A26})$$

4.4 Fish Guidance Efficiency (FGE)

Fish guidance efficiency at John Day Dam will be estimated by the quotient

$$\widehat{FGE} = \frac{\widehat{G}}{\widehat{G} + \widehat{U}} \quad (\text{A27})$$

with an associated variance estimate of

$$\widehat{Var}(\widehat{FGE}) = \widehat{FGE}^2 (1 - \widehat{FGE})^2 \left[\frac{\widehat{Var}(\widehat{G})}{\widehat{G}^2} + \frac{\widehat{Var}(\widehat{U})}{\widehat{U}^2} \right], \quad (\text{A28})$$

The same formulas (A27) and (A28) can be used to estimate the FGE and its variance at a specific turbine unit or more specifically at a specific intake slot.

5.0 Confidence Interval Estimation

For all estimated passage and performance parameters (say, θ), confidence interval estimates were based on the assumption of asymptotic normality. Interval estimates were calculated according to the formula

$$\text{CI} \left(\hat{\theta} - Z_{1-\frac{\alpha}{2}} \sqrt{\widehat{\text{Var}}(\hat{\theta})} < \theta < \hat{\theta} + Z_{1-\frac{\alpha}{2}} \sqrt{\widehat{\text{Var}}(\hat{\theta})} \right) = 1 - \alpha \quad (\text{A29})$$

where

$$Z_{1-\frac{\alpha}{2}} = \text{standard normal deviate corresponding to the probability } P \left(|Z| < Z_{1-\frac{\alpha}{2}} \right) = 1 - \alpha .$$

For example, a Z-value of 1.96 is used to construct a 95% confidence interval. The interval estimate (A29) characterizes the statistical uncertainty associated with the measurement of a fish passage or performance parameter.

6.0 Test of Spill Regimes

During 2002, two different spill regimes were compared. These spill options were as follows: (a) 0% daytime and 60% nighttime spill, (b) 30% daytime and 30% nighttime spill. A randomized block experimental design was used over the season to compare treatments. Each block consisted of a four-day period, two consecutive days per treatment condition. A total of 22 blocks were planned between 18 April and 14 July 2002. Table A.1 has the planned schedule for the 2002 spill experiment.

Table A.1. Planned Treatment and Blocking Schedule for the 2002 John Day Experiment

Date	% Spill	Block	Date	% Spill	Block	Date	% Spill	Block
18 Apr	0 day/60 night	1	18 May	30 day/ 30 night	8	17 Jun	30 day/ 30 night	16
19 Apr	0 day/60 night	1	19 May	30 day/30 night	8	18 Jun	30 day/30 night	16
20 Apr	30 day/30 night	1	20 May	30 day/30 night	9	19 Jun	0 day/60 night	16
21 Apr	30 day/30 night	1	21 May	30 day/30 night	9	20 Jun	0 day/60 night	16
22 Apr	0 day/60 night	2	22 May	0 day/60 night	9	21 Jun	0 day/60 night	17
23 Apr	0 day/60 night	2	23 May	0 day/60 night	9	22 Jun	0 day/60 night	17
24 Apr	30 day/ 30 night	2	24 May	0 day/60 night	10	23 Jun	30 day/ 30 night	17
25 Apr	30 day/30 night	2	25 May	0 day/60 night	10	24 Jun	30 day/30 night	17
26 Apr	30 day/30 night	3	26 May	30 day/ 30 night	10	25 Jun	30 day/30 night	18
27 Apr	30 day/30 night	3	27 May	30 day/30 night	10	26 Jun	30 day/30 night	18
28 Apr	0 day/60 night	3	28 May	30 day/30 night	11	27 Jun	0 day/60 night	18
29 Apr	0 day/60 night	3	29 May	30 day/30 night	11	28 Jun	0 day/60 night	18
30 Apr	30 day/30 night	4	30 May	0 day/60 night	11	29 Jun	0 day/60 night	19
1 May	30 day/30 night	4	31 May	0 day/60 night	11	30 Jun	0 day/60 night	19
2 May	0 day/60 night	4	1 Jun	0 day/60 night	12	1 Jul	30 day/30 night	19
3 May	0 day/60 night	4	2 Jun	0 day/60 night	12	2 Jul	30 day/30 night	19
4 May	30 day/30night	5	3 Jun	30 day/ 30 night	12	3 Jul	0 day/60 night	20
5 May	30 day/30 night	5	4 Jun	30 day/30 night	12	4 Jul	0 day/60 night	20
6 May	0 day/60 night	5	5 Jun	30 day/30 night	13	5 Jul	30 day/ 30 night	20
7 May	0 day/60 night	5	6 Jun	30 day/30 night	13	6 Jul	30 day/30 night	20
8 May	0 day/60 night	6	7 Jun	0 day/60 night	13	7 Jul	30 day/30 night	21
9 May	0 day/60 night	6	8 Jun	0 day/60 night	13	8 Jul	30 day/30 night	21
10 May	30 day/30 night	6	9 Jun	0 day/60 night	14	9 Jul	0 day/60 night	21
11 May	30 day/30 night	6	10 Jun	0 day/60 night	14	10 Jul	0 day/60 night	21
12 May	30 day/30 night	7	11 Jun	30 day/ 30 night	14	11 Jul	0 day/60 night	22
13 May	30 day/30 night	7	12 Jun	30 day/30 night	14	12 Jul	0 day/60 night	22
14 May	0 day/60 night	7	13 Jun	30 day/30 night	15	13 Jul	30 day/30 night	22
15 May	0 day/60 night	7	14 Jun	30 day/30 night	15	14 Jul	30 day/30 night	22
16 May	0 day/60 night	8	15 Jun	0 day/60 night	15			
17 May	0 day/60 night	8	16 Jun	0 day/60 night	15			

A two-way analysis of variance will be used to analyze the fish passage performance measures (i.e., FPE, SPE, and SPS). The ANOVA table will be of the form:

Source	DF	SS	MS	F
Total _{Cor}	$2B-1$	SSTOT		
Blocks	$B-1$	SSB		
Treatments	1	SST	MST	$F_{1,B-1} = \frac{MST}{MSE}$
Error	$B-1$	SSE	MSE	

In the previous ANOVA table, B = number of blocks analyzed. Two-tailed tests of significance will be performed for each response variable. The fish passage measures will be ln-transformed prior to analysis to stabilize the variance and provide an additive model on the ln-scale.

Confidence interval estimates for the mean response for a treatment condition can be calculated from the ANOVA results as

$$CI \left(e^{\bar{x} \pm t_{B-1} \sqrt{\frac{MSE}{B}}} \right). \quad (A30)$$

In Equation (A30), \bar{x} is the sample mean based on the ln-transformed performance measures used in the ANOVA analysis. The confidence interval is based on assuming the ln-transformed values are normally distributed.

Appendix B
Equipment Diagrams

Appendix B

Equipment Diagrams

Complete schematics of the hydroacoustic equipment are shown below. The physical layout of each structure (powerhouse and spillway) is followed by wiring diagrams for each system. Cabling and connections are also shown for overall study reproducibility.

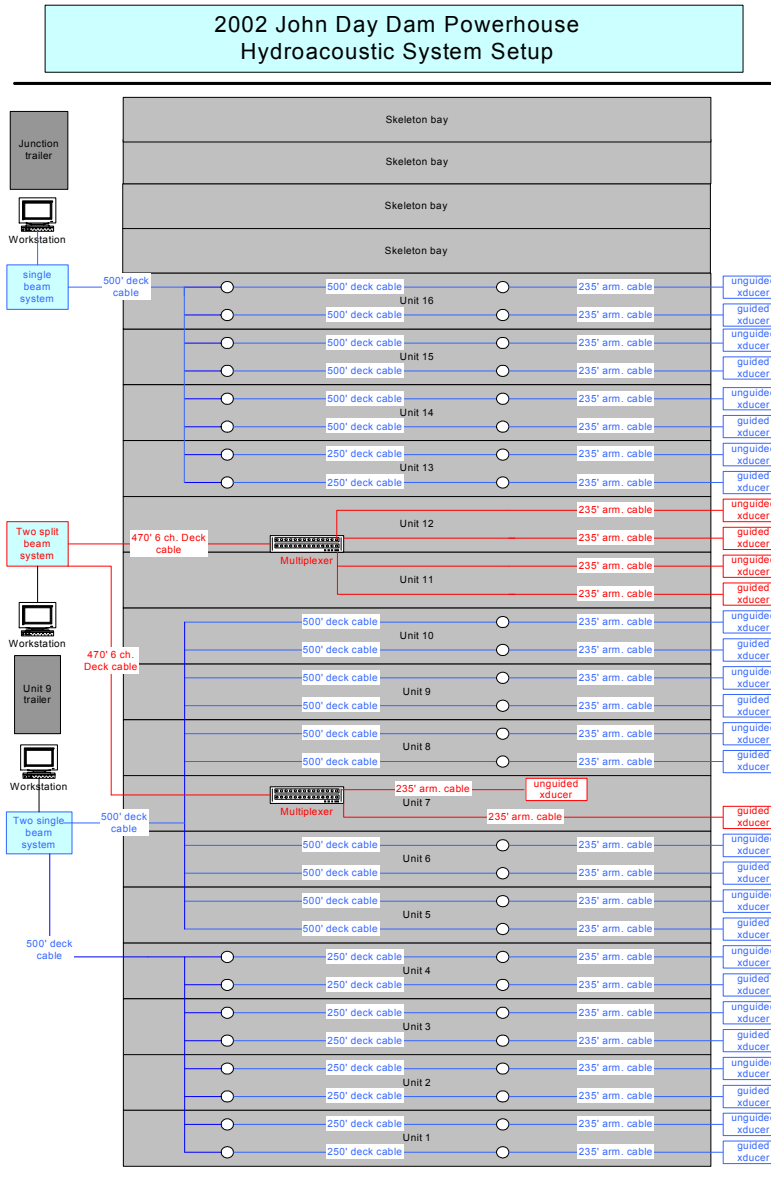


Figure 1. Physical layout of the hydroacoustic deployment at the powerhouse.

**John Day Dam Powerhouse
Singlebeam System "A" at Units 1-4**

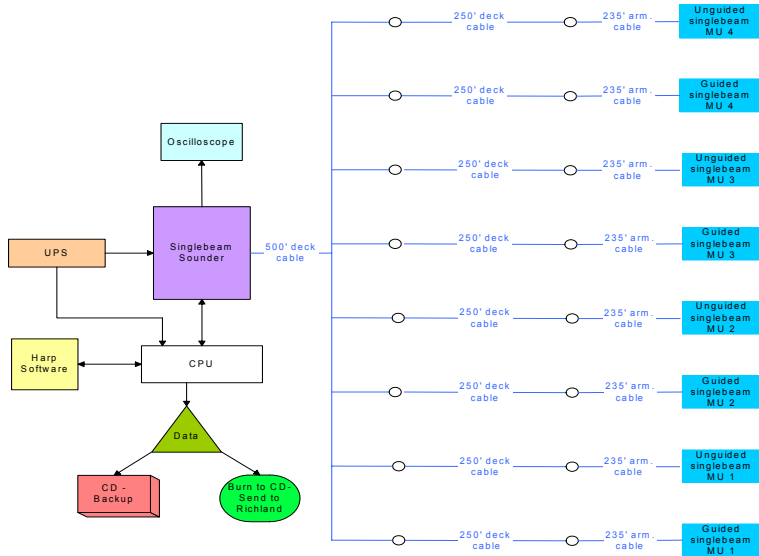


Figure 2. Wiring diagram of System A.

**John Day Dam Powerhouse
Singlebeam System "B" at Units 5-10**

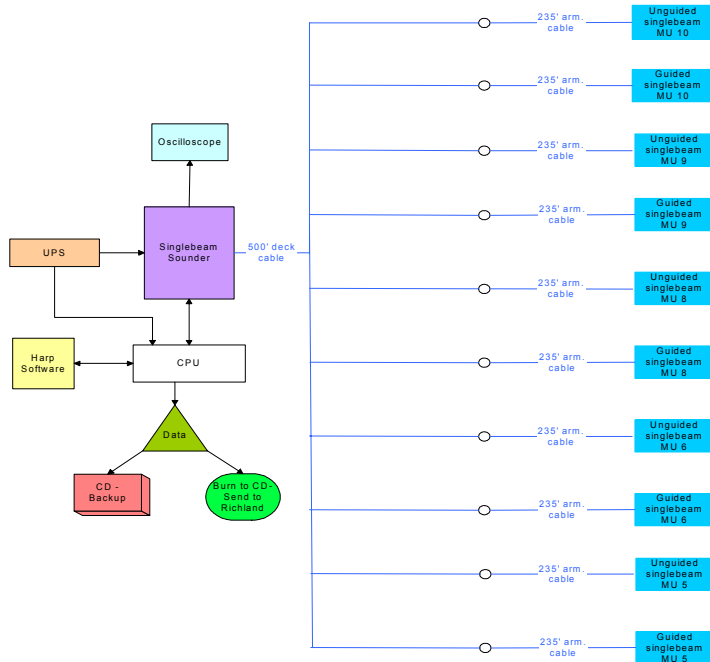


Figure 3. Wiring diagram of System B.

**John Day Dam Powerhouse
Singlebeam System "C" at Units 13-16**

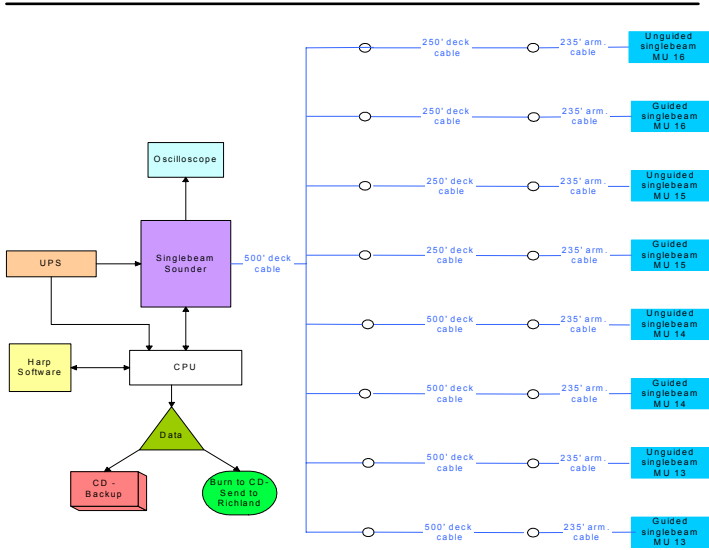


Figure 4. Wiring diagram of System C.

**John Day Dam Powerhouse
Splitbeam System "Y" at Units 11-12**

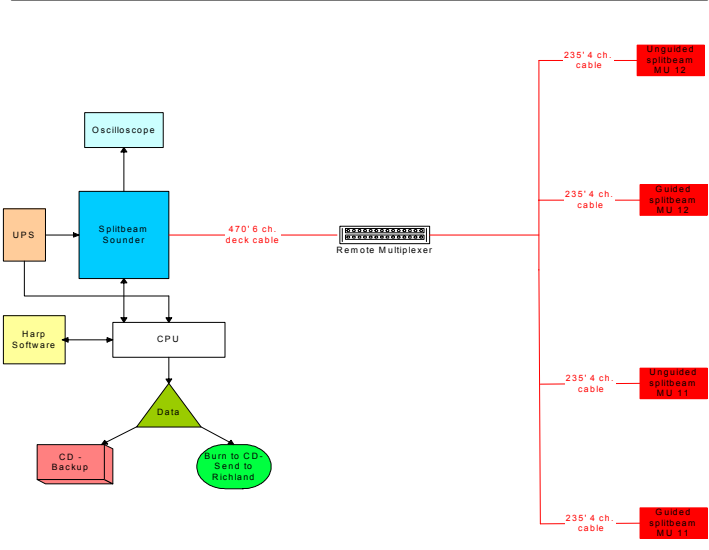


Figure 5. Wiring diagram of System Y.

**John Day Dam Powerhouse
Splitbeam System "X" at Unit 7, ESBS Screen**

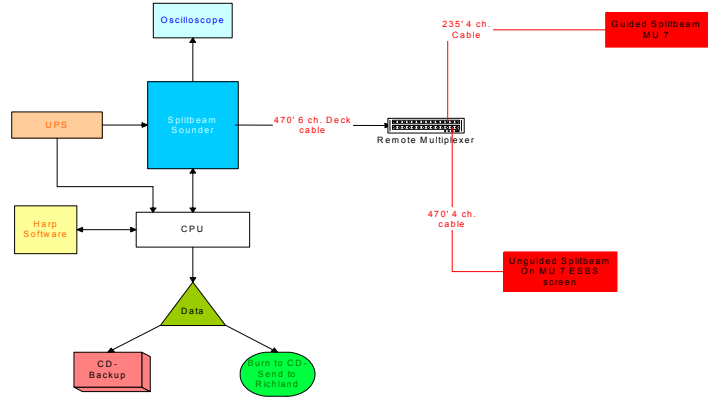


Figure 6. Wiring diagram of System X.

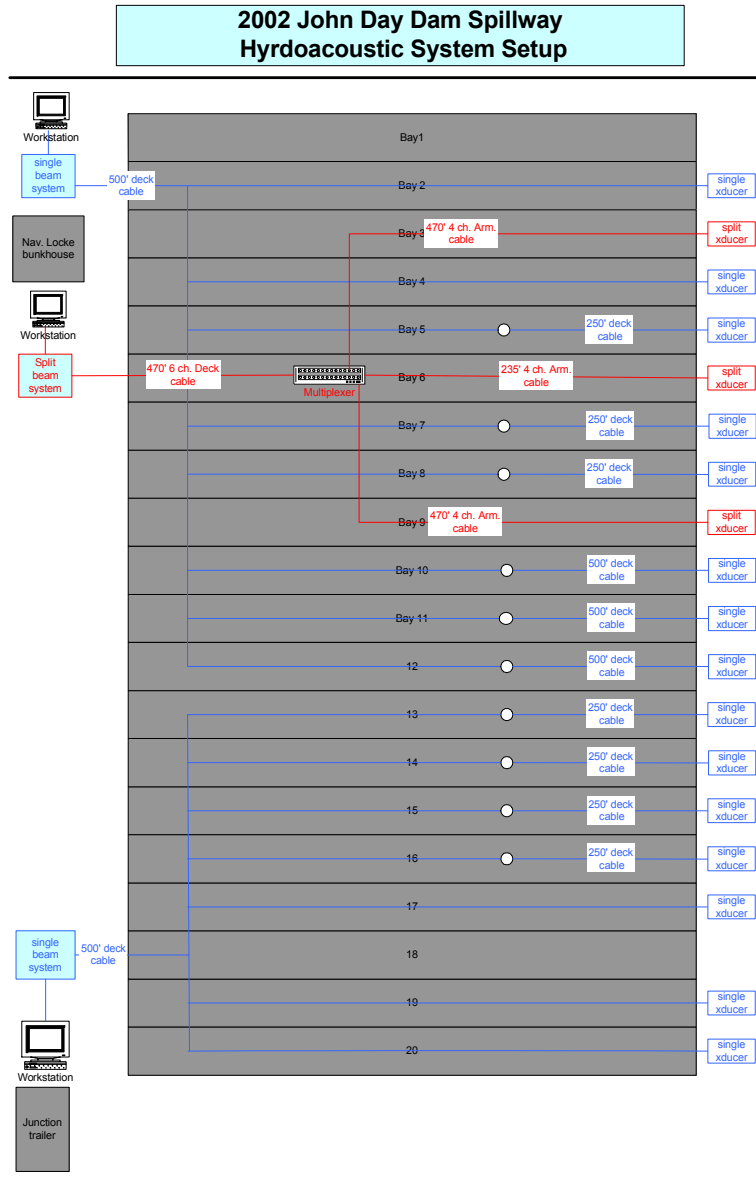


Figure 7. Physical layout of the hydroacoustic deployment at the spillway.

**John Day Dam Spillway
Singlebeam System "E" at Spillbay 2-12**

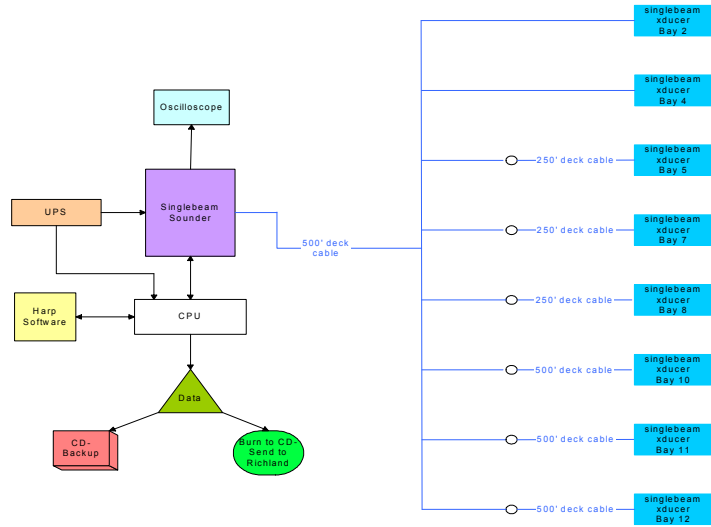


Figure 8. Wiring diagram of System E.

**John Day Dam Spillway
Singlebeam System "D" at Spillbay 13-20**

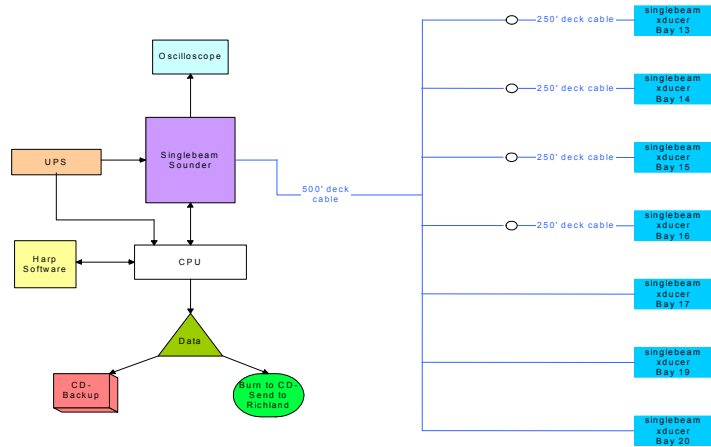


Figure 9. Wiring diagram of System D.

**John Day Dam Spillway
Splitbeam System "Z" at Spillbay 3, 6, and 9**

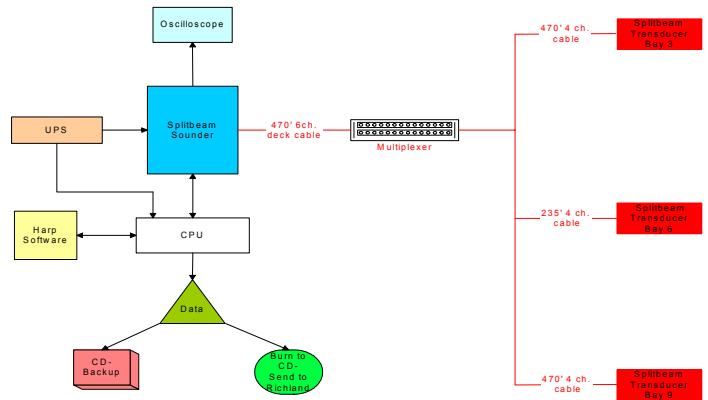


Figure 10. Wiring diagram of System Z.

Appendix C

System Setup and Calibration

Appendix C - System Setup and Calibration

Powerhouse																	
System A																	
System	Description	Channel	S/N	Arm	Deck		Deck	Total	Xducer		Elevation	Type	Ping				
					Cable Lengths			Length	Type				Rate				
					(ft.)	SN	(ft.)	SN	(ft.)	SN	(ft.)			Hr.			
A	SIB Sounder	40	105	235	247	500	563	250	632	985	MU01-A-G	uplooker/guided	40° from plane of trashrack	129 ft.	Slow	25	6
A	SIB xducer_1	0	106	235	252	500	562	250	625	985	MU01-A-U	uplooker/unguided	61° from plane of trashrack	129 ft.	Slow	25	6
A	SIB xducer_2	1	107	235	244	500	571	250	634	985	MU02-B-G	uplooker/guided	42° from plane of trashrack	129 ft.	Slow	25	6
A	SIB xducer_3	2	108	235	250	500	593	250	623	985	MU02-B-U	uplooker/unguided	58° from plane of trashrack	129 ft.	Slow	25	6
A	SIB xducer_4	3	109	235	239	500	564	250	624	985	MU03-C-G	uplooker/guided	42° from plane of trashrack	129 ft.	Slow	25	6
A	SIB xducer_5	4	110	235	251	500	605	250	614	985	MU03-C-U	uplooker/unguided	64° from plane of trashrack	129 ft.	Slow	25	6
A	SIB xducer_6	5	111	235	254	500	561	250	616	985	MU04-C-G	uplooker/guided	39° from plane of trashrack	129 ft.	Slow	25	6
A	SIB xducer_7	6	524	235	255	500	609	250	620	985	MU04-C-U	uplooker/unguided	64° from plane of trashrack	129 ft.	Slow	25	6
A	SIB xducer_8	7															
System B																	
System	Description	Channel	S/N	Arm	Deck		Deck	Total	Xducer		Elevation	Type	Ping				
					Cable Lengths			Length	Type				Rate				
					(ft.)	SN	(ft.)	SN	(ft.)	SN	(ft.)			Hr.			
B	SIB Sounder	41	113	235	248	500	576	735			MU05-A-G	uplooker/guided	34° from plane of trashrack	129 ft.	Slow	25	6
B	SIB xducer_1	0	114	235	236	500	573	735			MU05-A-U	uplooker/unguided	63° from plane of trashrack	129 ft.	Slow	25	6
B	SIB xducer_2	1	115	235	240	500	588	735			MU06-B-G	uplooker/guided	33° from plane of trashrack	129 ft.	Slow	25	6
B	SIB xducer_3	2	116	235	256	500	575	735			MU06-B-U	uplooker/unguided	63° from plane of trashrack	129 ft.	Slow	25	6
B	SIB xducer_4	3	117	235	241	500	572	735			MU08-A-G	uplooker/guided	33° from plane of trashrack	129 ft.	Slow	25	6
B	SIB xducer_5	4	118	235	253	500	567	735			MU08-A-U	uplooker/unguided	63° from plane of trashrack	129 ft.	Slow	25	6
B	SIB xducer_6	5	119	235	263	500	594	735			MU09-C-G	uplooker/guided	33° from plane of trashrack	129 ft.	Slow	25	6
B	SIB xducer_7	6	120	235	245	500	590	735			MU09-C-U	uplooker/unguided	63° from plane of trashrack	129 ft.	Slow	25	6
B	SIB xducer_8	7	533	235	246	500	610	735			MU10-A-G	uplooker/guided	33° from plane of trashrack	129 ft.	Slow	25	6
B	SIB xducer_9	8	122	235	236	500	602	735			MU10-A-U	uplooker/unguided	61° from plane of trashrack	129 ft.	Slow	25	6
B	SIB xducer_10	9															
System C																	
System	Description	Channel	S/N	Arm	Deck		Deck	Total	Xducer		Elevation	Type	Ping				
					Cable Lengths			Length	Type				Rate				
					(ft.)	SN	(ft.)	SN	(ft.)	SN	(ft.)			Hr.			
C	SIB Sounder	42	123	235	238	500	577	500	597	1235	MU13-A-G	uplooker/guided	37° from plane of trashrack	129 ft.	Slow	25	6
C	SIB xducer_1	0	124	235	237	500	560	500	586	1235	MU13-A-U	uplooker/unguided	63° from plane of trashrack	129 ft.	Slow	25	6
C	SIB xducer_2	1	125	235	242	500	565	500	566	1235	MU14-C-G	uplooker/guided	37° from plane of trashrack	129 ft.	Slow	25	6
C	SIB xducer_3	2	126	235	249	500	578	500	570	1235	MU14-C-U	uplooker/unguided	63° from plane of trashrack	129 ft.	Slow	25	6
C	SIB xducer_4	3	127	235	257	500	574	250	613	985	MU15-B-G	uplooker/guided	35° from plane of trashrack	129 ft.	Slow	25	6
C	SIB xducer_5	4	540	235	262	500	569	250	630	985	MU15-B-U	uplooker/unguided	63° from plane of trashrack	129 ft.	Slow	25	6
C	SIB xducer_6	5	541	235	243	500	585	250	617	985	MU16-B-G	uplooker/guided	35° from plane of trashrack	129 ft.	Slow	25	6
C	SIB xducer_7	6	542	235	267	500	596	250	633	985	MU16-B-U	uplooker/unguided	63° from plane of trashrack	129 ft.	Slow	25	6
C	SIB xducer_8	7															
System X																	
System	Description	Channel	S/N	Arm	Deck		Deck	Total	Xducer		Elevation	Type	Ping				
					Cable Lengths			Length	Type				Rate				
					(ft.)	SN	(ft.)	SN	(ft.)	SN	(ft.)			Hr.			
X	SPB Sounder	11	441	235	107	470	106	705			MU07-B-G	uplooker/guided	37° from plane of trashrack	129 ft.	Slow	25	30
X	Remote Mux	16	442	235	108	470	106	705			MU07-B-U	downlooker/unguided	53° from verticle	159 ft.	Slow	25	30
X	SPB xducer_1	0															
X	SPB xducer_2	10															
System Y																	
System	Description	Channel	S/N	Arm	Deck		Deck	Total	Xducer		Elevation	Type	Ping				
					Cable Lengths			Length	Type				Rate				
					(ft.)	SN	(ft.)	SN	(ft.)	SN	(ft.)			Hr.			
Y	SPB Sounder	27	443	235	110	470	109	705			MU11-B-G	uplooker/guided	37° from plane of trashrack	129 ft.	Slow	25	15
Y	Remote Mux	17	444	235	111	470	109	705			MU11-B-U	uplooker/unguided	63° from plane of trashrack	129 ft.	Slow	25	15
Y	SPB xducer_1	0	445	235	112	470	109	705			MU12-C-G	uplooker/guided	37° from plane of trashrack	129 ft.	Slow	25	15
Y	SPB xducer_2	10	446	235	113	470	109	705			MU12-C-U	uplooker/unguided	63° from plane of trashrack	129 ft.	Slow	25	15
Y	SPB xducer_3	20															
Y	SPB xducer_4	30															

Spillway																	
System D																	
System	Description	Channel	S/N	Arm	Cable Lengths	Deck	Deck	Total	Location	Mounting	Xducer	Aiming angle	Elevation	Type	Ping Rate	Min./Hr.	
					(ft.)	SN	(ft.)	SN	(ft.)		Type		(ft.)				
	SIB Sounder		38														
D	SIB xducer_1	0	517		500	592		500	Bay 20n	pole-downlooker	10° single	2° downstream of vertical	258 ft.	Slow	25	6	
D	SIB xducer_2	1	518		500	612		500	Bay 19m	pole-downlooker	10° single	2° downstream of vertical	258 ft.	Slow	25	6	
D	SIB xducer_3	2	519		500	581		500	Bay 18n	pole-downlooker	10° single	2° downstream of vertical	258 ft.	Slow	25	6	
D	SIB xducer_4	3	520		500	606		500	Bay 17n	pole-downlooker	10° single	2° downstream of vertical	258 ft.	Slow	25	6	
D	SIB xducer_5	4	526		500	579	250	628	Bay 16n	pole-downlooker	10° single	2° downstream of vertical	258 ft.	Slow	25	6	
D	SIB xducer_6	5	522		500	604	250	621	Bay 15m	pole-downlooker	10° single	2° downstream of vertical	258 ft.	Slow	25	6	
D	SIB xducer_7	6	523		500	568	250	615	Bay 14s	pole-downlooker	10° single	2° downstream of vertical	258 ft.	Slow	25	6	
D	SIB xducer_8	7	538		500	595	250	622	Bay 13m/n	pole-downlooker	10° single	2° downstream of vertical	258 ft.	Slow	25	6	
System E									Total								
	SIB Sounder		39														
E	SIB xducer_1	0	527		500	598	500	589	1000	Bay 12n	pole-downlooker	10° single	2° downstream of vertical	258 ft.	Slow	25	6
E	SIB xducer_2	1	528		500	600	500	607	1000	Bay 11s	pole-downlooker	10° single	2° downstream of vertical	258 ft.	Slow	25	6
E	SIB xducer_3	2	529		500	583	500	599	1000	Bay 10m/s	pole-downlooker	10° single	2° downstream of vertical	258 ft.	Slow	25	6
E	SIB xducer_4	3	530		500	587	250	622	750	Bay 8s	pole-downlooker	10° single	2° downstream of vertical	258 ft.	Slow	25	6
E	SIB xducer_5	4	531		500	601	250	635	750	Bay 7n	pole-downlooker	10° single	2° downstream of vertical	258 ft.	Slow	25	6
E	SIB xducer_6	5	532		500	603	250	618	750	Bay 5m/n	pole-downlooker	10° single	2° downstream of vertical	258 ft.	Slow	25	6
E	SIB xducer_7	6	534		500	611		500	500	Bay 4s	pole-downlooker	10° single	2° downstream of vertical	258 ft.	Slow	25	6
E	SIB xducer_8	7	535		500	582		500	500	Bay 2m/n	pole-downlooker	10° single	2° downstream of vertical	258 ft.	Slow	25	6
System Z									Total								
	SIB Sounder		12														
Z	Remote Mux		14		470	99											
Z	SPB xducer_1	10	435		470	104		940	Bay 9n	pole-downlooker	10° split	2° downstream of vertical	258 ft.	Slow	25	20	
Z	SPB xducer_2	20	436		235	80		705	Bay 6m/n	pole-downlooker	10° split	2° downstream of vertical	258 ft.	Slow	25	20	
Z	SPB xducer_3	30	437		470	105		940	Bay 3n	pole-downlooker	10° split	2° downstream of vertical	258 ft.	Slow	25	20	

System	Channel	Transducer Number and Phase (if split beams)	Location	Calibrated Cable Length (ft)	Source Level (dB) - 6 dB Static Transmit	Max. Output Voltage (dB)	Voltage On Largest axis target at 20 dB per Volt (V)	40 logR Receiver Sensitivity (dB)	Target Strength of largest on-axis target of interest (db)	Calculated Receiver gain (dB)	Installed Cable Length (ft)	Difference in Cable Length Between Calibrated Cable and Installed Cable (ft)	Receiver Gain Adjusted for Difference in Cable Length (dB)	Source Level Adjusted for Difference in Cable Length (dB)	Receiver Sensitivity Adjusted for Difference in Cable Length (dB)	Target Strength of Smallest On-axis Target (dB)	Voltage of Smallest On-axis Target (dB)
A	0		MU1A-G	750	213.33	90	4.5	-104.66	-26	7.33	750	0	7.33	213.33	-104.66	-56	60
A	1		MU1A-UG	750	213.68	90	4.5	-104.56	-26	6.88	750	0	6.88	213.68	-104.56	-56	60
A	2		MU2B-G	750	213.32	90	4.5	-104.82	-26	7.30	750	0	7.30	213.32	-104.62	-56	60
A	3		MU2B-UG	750	213.32	90	4.5	-104.82	-26	7.50	750	0	7.50	213.32	-104.82	-56	60
A	4		MU3C-G	750	213.24	90	4.5	-104.82	-26	7.58	750	0	7.58	213.24	-104.82	-56	60
A	5		MU3C-UG	750	213.57	90	4.5	-104.74	-26	7.17	750	0	7.17	213.57	-104.74	-56	60
A	6		MU4C-G	750	213.46	90	4.5	-104.72	-26	7.26	750	0	7.26	213.46	-104.72	-56	60
A	7		SPARE	750	213.48	90	4.5	-104.70	-26	7.22	750	0	7.22	213.48	-104.70	-56	60
A	7		MU4C-UG	750	214.76	90	4.5	-103.22	-26	4.46	750	0	4.46	214.76	-103.22	-56	60
D	0		SB 20S	500	210.77	80	4.0	-107.32	-26	2.55	500	0	2.55	210.77	-107.32	-56	50
D	1		SB 19M	500	210.94	80	4.0	-107.20	-26	2.26	500	0	2.26	210.94	-107.20	-56	50
D	2		SB 18N	500	211.6	80	4.0	-106.74	-26	1.14	500	0	1.14	211.60	-106.74	-56	50
D	3		SB 17N	500	211.77	80	4.0	-106.64	-26	0.87	600	-100	1.51	211.26	-106.77	-56	50
D	D		SPARE(?)	500	211.57	80	4.0	-106.84	-26	1.27	600	-100	1.91	211.06	-106.97	-56	50
D	5		SB 15M	750	211.12	80	4.0	-109.24	-26	4.12	750	0	4.12	211.12	-109.24	-56	50
D	6		SB 14S	750	210.91	80	4.0	-109.34	-26	4.43	750	0	4.43	210.91	-109.34	-56	50
D	7		SB 13M	750	210.87	80	4.0	-109.38	-26	4.51	750	0	4.51	210.87	-109.38	-56	50
D	D		SPARE	500	211.61	80	4.0	-106.56	-26	0.95	500	0	0.95	211.61	-106.56	-56	50
D	4		SB 16S	750	211.10	80	4.0	-109.02	-26	3.92	700	50	3.60	211.36	-108.96	-56	50
E	0		SB 12N	1000	207.37	80	4.0	-111.14	-26	9.77	1000	0	9.77	207.37	-111.14	-56	50
E	1		SB 11S	1000	208.73	80	4.0	-109.76	-26	7.03	1000	0	7.03	208.73	-109.76	-56	50
E	2		SB 10M	1000	208.57	80	4.0	-109.88	-26	7.31	1000	0	7.31	208.57	-109.88	-56	50
E	3		SB 8S	750	211.13	80	4.0	-109.38	-26	4.25	750	0	4.25	211.13	-109.38	-56	50
E	4		SB 7N	750	211.32	80	4.0	-109.26	-26	3.96	750	0	3.96	211.32	-109.28	-56	50
E	5		SB 5M	750	211.58	80	4.0	-109.06	-26	3.48	750	0	3.48	211.58	-109.06	-56	50
E	6		SB 4S	500	211.43	80	4.0	-107.04	-26	1.61	500	0	1.61	211.43	-107.04	-56	50
E	7		SB 2M	500	212.03	80	4.0	-106.68	-26	0.65	700	-200	1.93	211.01	-106.94	-56	50
E	E		SPARE	1000	208.87	80	4.0	-109.56	-26	6.69	1000	0	6.69	208.87	-109.56	-56	50
E	E		SPARE	750	211.38	80	4.0	-108.96	-26	3.58	750	0	3.58	211.38	-108.96	-56	50
C	0		MU13A-G	985	213.28	90	4.5	-105.20	-26	7.92	1235	-250	9.52	212.01	-105.53	-56	60
C	1		MU13A-UG	985	213.33	90	4.5	-104.88	-26	7.55	1235	-250	9.15	212.06	-105.21	-56	60
C	2		MU14C-G	985	213.24	90	4.5	-105.00	-26	7.76	1235	-250	9.36	212.01	-105.33	-56	60
C	3		MU14C-UG	985	213.28	90	4.5	-105.00	-26	7.72	1235	-250	9.32	212.01	-105.33	-56	60
C	4		MU15B-G	985	213.40	90	4.5	-104.66	-26	7.26	985	0	7.26	213.40	-104.66	-56	60
C	5		MU15B-UG	985	214.58	90	4.5	-103.42	-26	4.84	985	0	4.84	214.58	-103.42	-56	60
C	6		MU16B-G	985	214.75	90	4.5	-103.38	-26	4.63	985	0	4.63	214.75	-103.38	-56	60
C	7		MU16B-UG	985	214.56	90	4.5	-103.36	-26	4.80	985	0	4.80	214.56	-103.36	-56	60
C	C		SPARE	985	213.56	90	4.5	-103.84	-26	6.28	985	0	6.28	213.56	-103.84	-56	60
B	0		MU5A-G	750	213.11	90	4.5	-104.42	-26	7.31	750	0	7.31	213.11	-104.42	-56	60
B	1		MU5A-UG	750	213.24	90	4.5	-104.38	-26	7.14	750	0	7.14	213.24	-104.38	-56	60
B	2		MU6B-G	750	213.57	90	4.5	-104.10	-26	6.53	750	0	6.53	213.57	-104.10	-56	60
B	3		MU6B-UG	750	213.16	90	4.5	-104.90	-26	7.74	750	0	7.74	213.16	-104.90	-56	60
B	4		MU8A-G	750	213.52	90	4.5	-104.28	-26	6.76	750	0	6.76	213.52	-104.28	-56	60
B	5		MU8A-UG	750	213.05	90	4.5	-104.78	-26	7.73	750	0	7.73	213.05	-104.78	-56	60
B	6		MU9C-G	750	213.50	90	4.5	-104.06	-26	6.56	750	0	6.56	213.50	-104.06	-56	60
B	7		MU9C-UG	750	213.15	90	4.5	-104.48	-26	7.33	750	0	7.33	213.15	-104.48	-56	60
B	B		SPARE	750	213.09	90	4.5	-104.90	-26	7.81	750	0	7.81	213.09	-104.90	-56	60
B	9		MU10A-UG	750	213.47	90	4.5	-104.38	-26	6.91	750	0	6.91	213.47	-104.38	-56	60
B	8		MU10A-G	750	214.79	90	4.5	-102.98	-26	4.19	750	0	4.19	214.79	-102.98	-56	60
B	B		SPARE	750	214.81	90	4.5	-102.76	-26	3.95	750	0	3.95	214.81	-102.76	-56	60

Appendix D
Autotracker Parameters

Appendix D

Autotracker Parameters

Setup information is needed to process raw sonar data files into appropriate samples. The parameter file contains information about the setup of the sounder and the sampling scheme. These parameters allow the raw files to be processed into a usable echogram. The parameters of Blocksize, MaxRange, MinRange, MaxEchoStrength and MinEchoStrength are parameters that allow the raw files to be translated into blocks of echos that represent a sample period. The parameter Structurethreshold, BottomStartRange, BottomCtThold, BottomAmplThold, and Noise are used to identify structure, the bottom (or surface), and noisy areas of the echogram before identifying traces. The autotracker must be calibrated for each deployment type to effectively identify traces whose characteristics are a function of the fish, the flow environment, and angle of view. RangeNoise, Gatesize, DKMax, and Alpha control how trace segments are constructed. LinkGate and LinkDKMax determine which segments will be connected into a single trace. The location indicates the general sampling location, such as a dam or river mile. It does not affect the operation of the autotracker, but is useful for differentiating among data sets (Table 1).

The values used in this study are reported as follows. Table 2 reports the values of parameters that were constant across all deployments. Table 3 reports the values that varied by deployment type. Table 4 reports the values of parameters that varied among individual transducers.

Table 1. Processing parameters and definitions

Parameter	Definition
Name	The channel Name. 1st character is the system letter. The 2nd and 3rd characters are the Mux_Channel
BlockSize	The max number of pings processed for a channel within 1 sample. Generally \geq the ping rate/ second * 60 seconds.
MaxRange:	The maximum range (in meters) for echo processing.
MinRange	The minimum range (in meters) for echo processing.
StructureThreshold	The proportion of a range that must be occupied by echoes to be marked as structure. (0 –1)
RangeNoise	The amount of fuzziness used in assigning echoes to range bins to find linear features (decimeters).
GateSize	The maximum range difference the autotracker will check to find the next ping in a track segment
DKMax	The max ping difference the autotracker will check to find the next ping in a track segment
Alpha	The alpha value for the alpha- beta tracking algorithm, beta is computed
LinkGate	The max range difference the autotracker will check to link segments into a track
LinkDKMax	The maximum ping difference the autotracker will span to link segments into a track
MaxEchoStrength	The maximum echo strength (in decibels) that will be processed.
MinEchoStrength	The minimum echo strength (in decibels) that will be processed.
NOISE	The number of dilates and erodes used to identify noise regions (>0)(-1 means do not do noise for a channel)
BottomStartRange	The range (in centimeters) to begin the routine to identify the surface or bottom range (should be between min and max range) (if bottom identification is not needed, set value > max range)
BottomCtThold	Proportion of a range that must be occupied by echoes > bottom amplitude threshold to be marked as bottom. (0 –1)
BottomAmplThold	The minimum echo strength (in decibels) above which echoes will be tallied as bottom or surface echoes
Location	Text describing the general sampling area

Table 2. Parameter values held constant across all deployments.

Parameter	Value
MinRange	1.00
StructureThreshold	0.075
RangeNoise	0
DKMax	4
Alpha	0.3
LinkGate	0.2
LinkDKMax	12
MaxEchoStrength	-26
MinEchoStrength	-56
Noise	5
BottomStartRange	36
BottomCtThold	0.3
BottomAmplThold	-26
Location	John Day

Table 3. Parameter values held constant within each deployment type.

	Spill	Turbine
GateSize	0.14	0.15

Table 4. Parameter values specific to each deployment

DamOpsXRef	Location	Horizontal Position	Type	BlockSize	MaxRange
MU1	Powerhouse	A	Guided	1851	18.87
MU1	Powerhouse	A	Unguided	1851	18.22
MU2	Powerhouse	B	Guided	1851	18.87
MU2	Powerhouse	B	Unguided	1851	18.27
MU3	Powerhouse	C	Guided	1851	18.87
MU3	Powerhouse	C	Unguided	1851	18.27
MU4	Powerhouse	C	Guided	1851	18.85
MU4	Powerhouse	C	Unguided	2026	18.27
MU5	Powerhouse	A	Guided	1481	19.09
MU5	Powerhouse	A	Unguided	1481	18.35
MU6	Powerhouse	B	Guided	1481	19.01
MU6	Powerhouse	B	Unguided	1481	18.35
MU7	Powerhouse	B	GuidedESBS	4556	18.72
MU7	Powerhouse	B	UnguidedESBS	4556	16.33
MU8	Powerhouse	A	Guided	1481	18.81

MU8	Powerhouse	A	Unguided	1481	18.37
MU9	Powerhouse	C	Guided	1481	19.01
MU9	Powerhouse	C	Unguided	1481	18.25
MU10	Powerhouse	A	Guided	1481	18.87
MU10	Powerhouse	A	Unguided	1656	18.3
MU11	Powerhouse	B	Guided	2217	18.92
MU11	Powerhouse	B	Unguided	2215	18.14
MU12	Powerhouse	C	Guided	2215	19.08
MU12	Powerhouse	C	Unguided	2340	18.03
MU13	Powerhouse	A	Guided	1851	18.86
MU13	Powerhouse	A	Unguided	1851	18.3
MU14	Powerhouse	C	Guided	1851	18.95
MU14	Powerhouse	C	Unguided	1851	18.18
MU15	Powerhouse	B	Guided	1851	18.95
MU15	Powerhouse	B	Unguided	1851	18.22
MU16	Powerhouse	B	Guided	1851	19.1
MU16	Powerhouse	B	Unguided	2026	18.3
SP20	Spillway	S	Spill	2115	15.16
SP19	Spillway	M	Spill	2115	15.41
SP18	Spillway	N	Spill	2115	15.5
SP17	Spillway	N	Spill	2115	15.33
SP16	Spillway	S	Spill	2115	15.28
SP15	Spillway	M	Spill	2115	15.18
SP14	Spillway	S	Spill	2115	15.33
SP13	Spillway	M	Spill	2290	15.25
SP12	Spillway	N	Spill	1851	15.41
SP11	Spillway	S	Spill	1851	15.41
SP10	Spillway	M	Spill	1851	15.31
SP9	Spillway	N	Spill	3079	15.18
SP8	Spillway	S	Spill	1851	15.43
SP7	Spillway	N	Spill	1851	15.24
SP6	Spillway	M	Spill	2953	15.38
SP5	Spillway	M	Spill	1851	15.22
SP4	Spillway	S	Spill	1851	15.31
SP3	Spillway	N	Spill	3078	15.16
SP2	Spillway	M	Spill	2026	15.13

Appendix E
Post Tracking Filters

Appendix E - Post Tracking Filters

The following filters were imposed after the data was autotracked.

Table 1. Fields used in filtering traces.

Field Name	Explanation
ECHO_COUNT	Number of echoes in track
LAST_RANGE	Range in m of last echo
LINEARITY1	Root mean squared error for a straight line fit
MAX_RUN	Maximum number of contiguous echoes
MEAN_ECHO_STRENGTH	Mean echo strength
NOISE_COUNT_AVERAGE	Noise Count / Track echo count
PLUNGE	Angle relative to a tangent of the beam axis in the YZ plane (split beams only)
SLOPE	(last range- first range)/(last relative ping- first relative ping)
SPEED	Speed of the target m per sec (split beams only)
TRACK_TYPE	0 if normal, 1 if flat track near clutter
XANGLE1	X phase angle of first echo
XANGLE2	X phase angle of last echo
YANGLE1	Y phase angle of first echo
YANGLE2	Y phase angle of last echo

Table 2. Operators used in filtering traces.

Operator	Function
=	Equal
<>	not equal
>	greater than
<	less than
>=	greater than or equal
<=	less than or equal
Abs(value)	The filter will use absolute value of the variable in parenthesis.

Table 3. Trace filters by deployment type.

Deployment	Filter
All deployments	$(Track_Type = 0 \text{ or } ABS(\text{Last_Range} - \text{First_Range}) > 0.2)$ $((\text{Noise_Count_Average} * \text{Echo_Count}) / ((\text{Echo_Count} + 10) * 5)) < 0.35 \text{ or } (\text{Noise_Index} > 2)$ $((\text{Last_Ping} + 1 - \text{First_Ping}) / \text{Group_Size}) > 5 \text{ or } \text{Max_Run} > 4$ $\text{Mean_Pulse_Width} > 180$ $\text{Mean_Pulse_Width} < 250$ $\text{Linearity1} / \text{Echo_Count} < 0.5$ $\text{Linearity1} / \text{Echo_Count} > 0$
Turbine	$((\text{Last_Ping} + 1 - \text{First_Ping}) / \text{Group_Size}) < 80$
Guided	$\text{Slope} > 0.17$ $\text{Slope} < 1$ $\text{Last_Range} \geq 14.6$ $\text{Last_Range} < 18.60$ $(\text{Last_Range} > 14.94 \text{ or } \text{F.Channel} \neq \text{'A06'})$ $(\text{Last_Range} > 14.85 \text{ or } \text{F.Channel} \neq \text{'A02'})$ $(\text{Last_Range} < 18.40 \text{ or } \text{Season} = \text{'Sp'})$
Unguided	$\text{Slope} > 0.5$ $\text{Slope} < 2.5$ $\text{First_Range} < 15.0$ $(\text{First_Range} > 6.50 \text{ or } \text{F.Channel} \neq \text{'A01'})$ $(\text{First_Range} < 13.50 \text{ or } \text{F.Channel} \neq \text{'A01'})$ $(\text{First_Range} < 12.50 \text{ or } \text{F.Channel} \neq \text{'A03'})$ $(\text{First_Range} < 13.00 \text{ or } \text{F.Channel} \text{ not in } (\text{'B01'}, \text{'B03'}, \text{'C05'}, \text{'C07'}))$ $(\text{First_Range} < 14.00 \text{ or } \text{F.Channel} \text{ not in } (\text{'B05'}, \text{'B09'}, \text{'C01'}))$ $(\text{First_Range} < 12.50 \text{ or } \text{F.Channel} \neq \text{'C05'} \text{ or } \text{Season} = \text{'Sp'})$ $(\text{First_Range} < 12.60 \text{ or } \text{F.Channel} \neq \text{'Y01'})$ $(\text{First_Range} < 12.25 \text{ or } \text{F.Channel} \neq \text{'Y01'} \text{ or } \text{Season} = \text{'Sp'})$

GuidedESBS

Slope >0
Slope < 1.0
((mean_echo_strength>-54.0Mean_Pulse_Width <230 and speed >0.5Slope>0.1)
or Last_Range >8.10 or Last_Range<6.68)
Last_Range >9.16
Last_Range <18.5
((Last_Range>18.5 or Last_Range<18.44) or (First_Range>18.5 or
First_Range<18.44))

UnguidedESBS

Slope <-0.21
(((Last_Range+First_Range)/2 <8.56 or (Last_Range+First_Range)/2 >11.33) or
((Slope<-0.29 or (Echo_Count>10 and Slope<-0.17))Noise_Index >2))
First_Range <16.24

Spill

(((Last_Ping + 1 - First_Ping) / Group_Size) < 120)
linearity2/Echo_Count <0.23
(Slope>0.5)
Slope<3.6
(((Last_Range>14.55 or Last_Range<13.4) or (First_Range>14.55 or
First_Range<13.4)) or (Noise_Index>2 or Slope >0.5))
standard_deviation_pulse_width <100
Last_Range >=6
(Last_Range >=9 or Flow >9)
Last_Range <14.90
(Last_Range <14.50 or F.Channel<>'Z01')
(Last_Range <14.75 or F.Channel<>'E05')
Last_Range >=9 when gate open >=6 FT
Last_Range >=6 when gate open <6 FT

Appendix F
Effective Beam Widths

Appendix F

Effective Beam Widths

The effective beam width is calculated from a detectability model. Inputs to this model include fish speeds and trajectories as well as the sensitivity and beam pattern of each transducer. These come from split beam data of actual fish paths and from the equipment calibration process, respectively. The output forms the basis for expanding the fish counts. As shown below, the effective beam width varies by range, diel, and season. The charts below show the effective beam width used in this study.

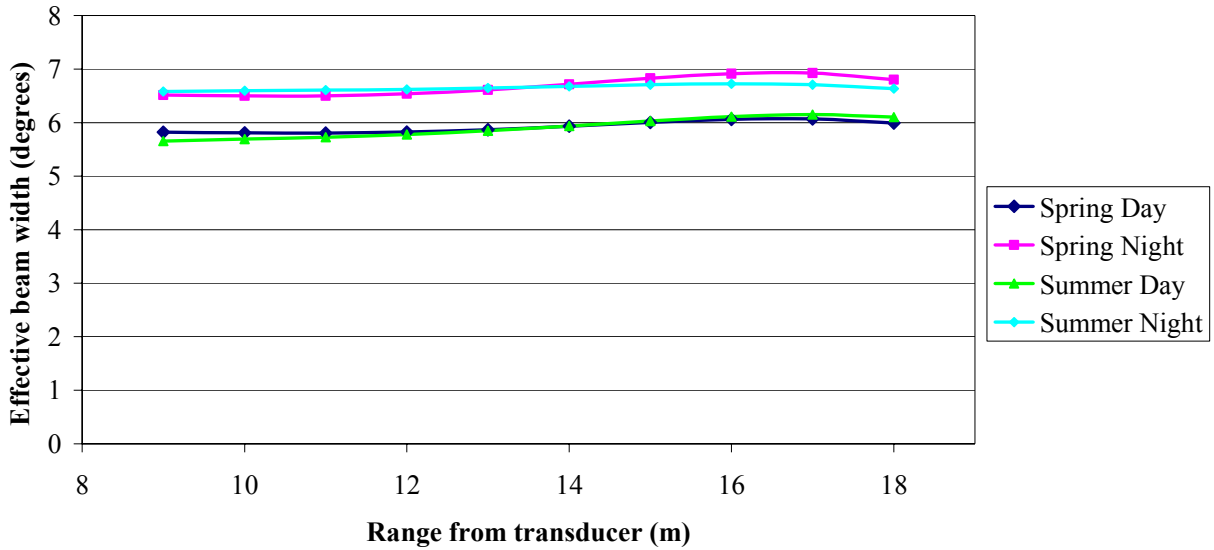


Figure 1. Guided ESBS.

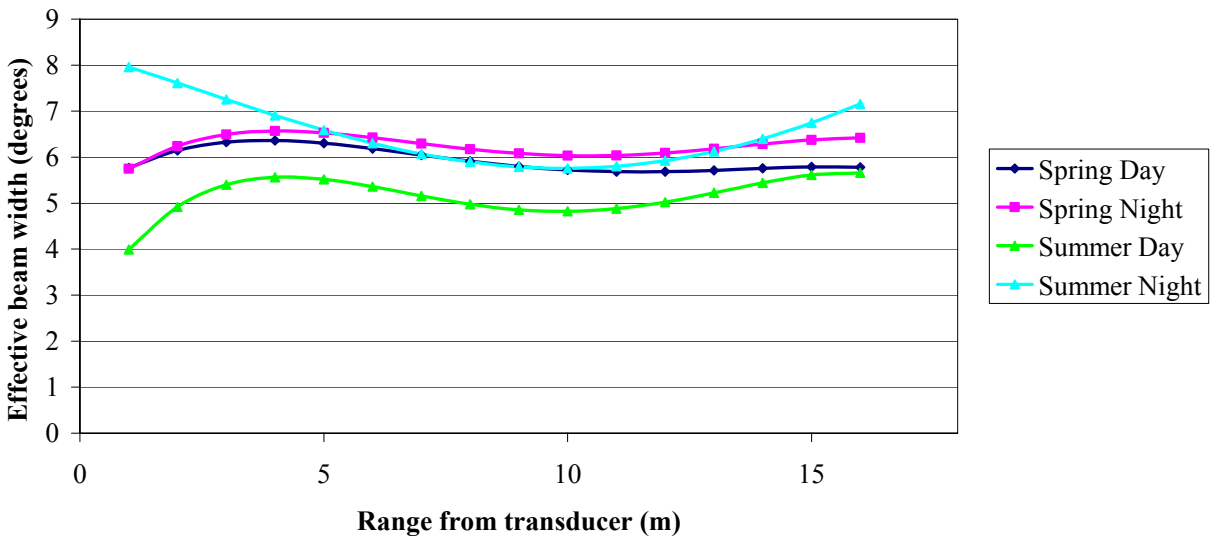


Figure 2. Unguided ESBS.

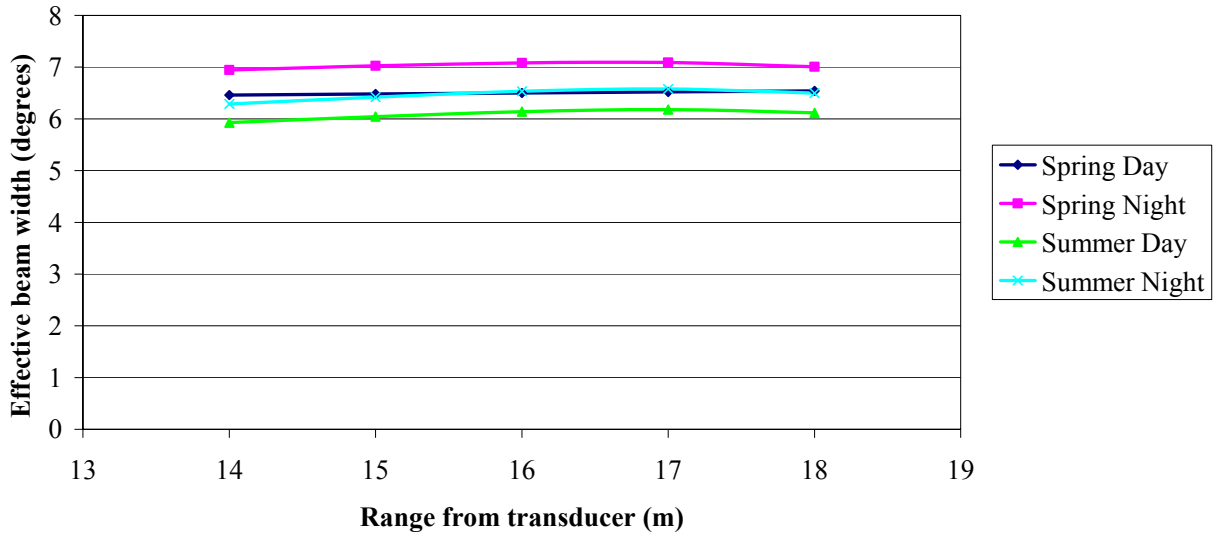


Figure 3. Guided STS.

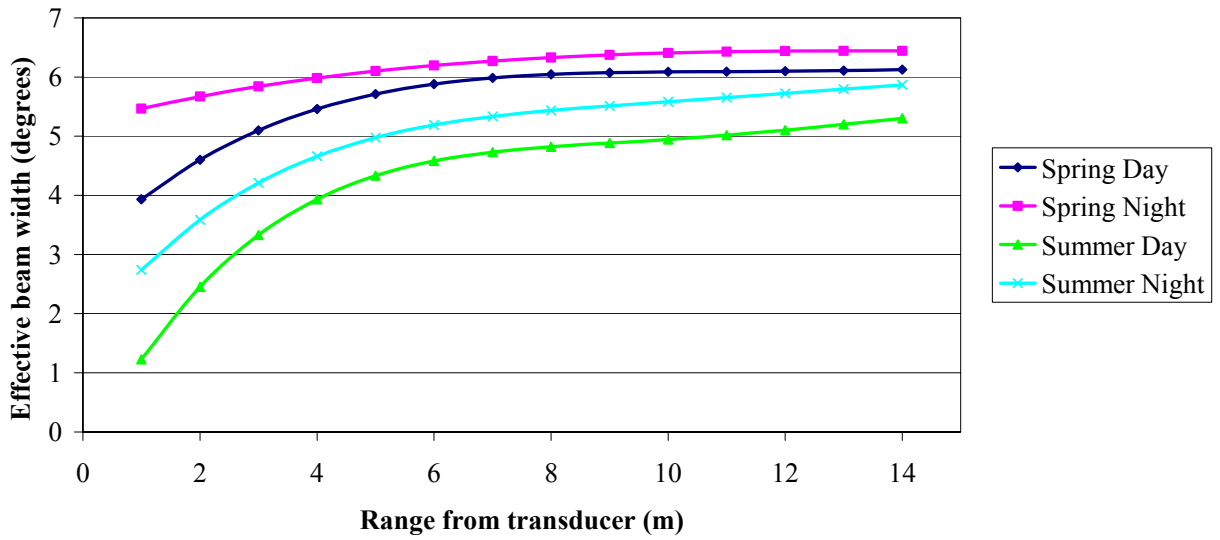


Figure 4. Unguided STS.

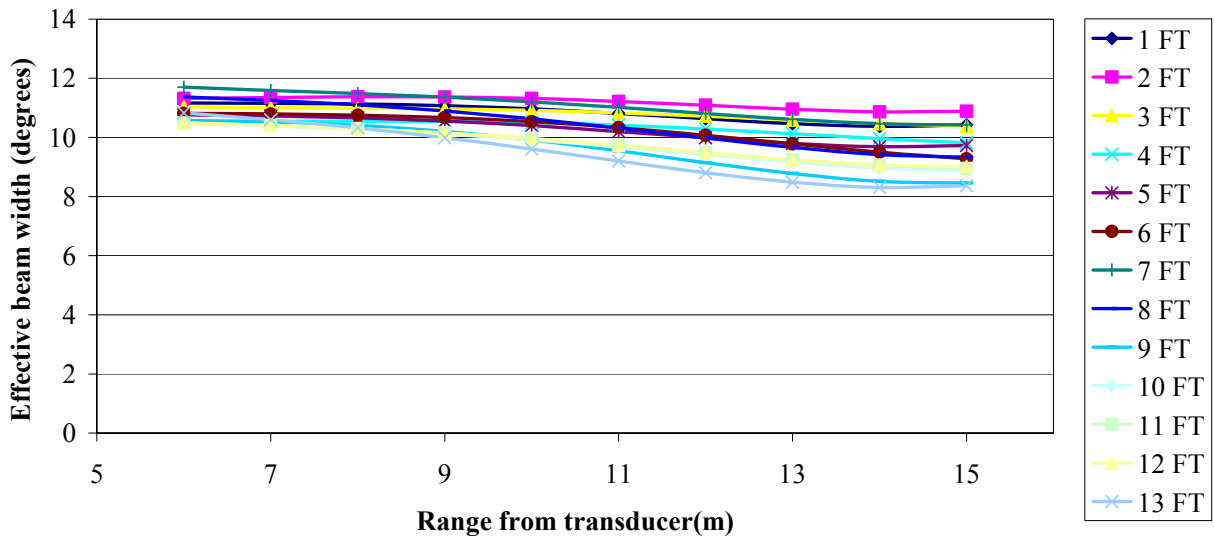


Figure 5. Spring day spill.

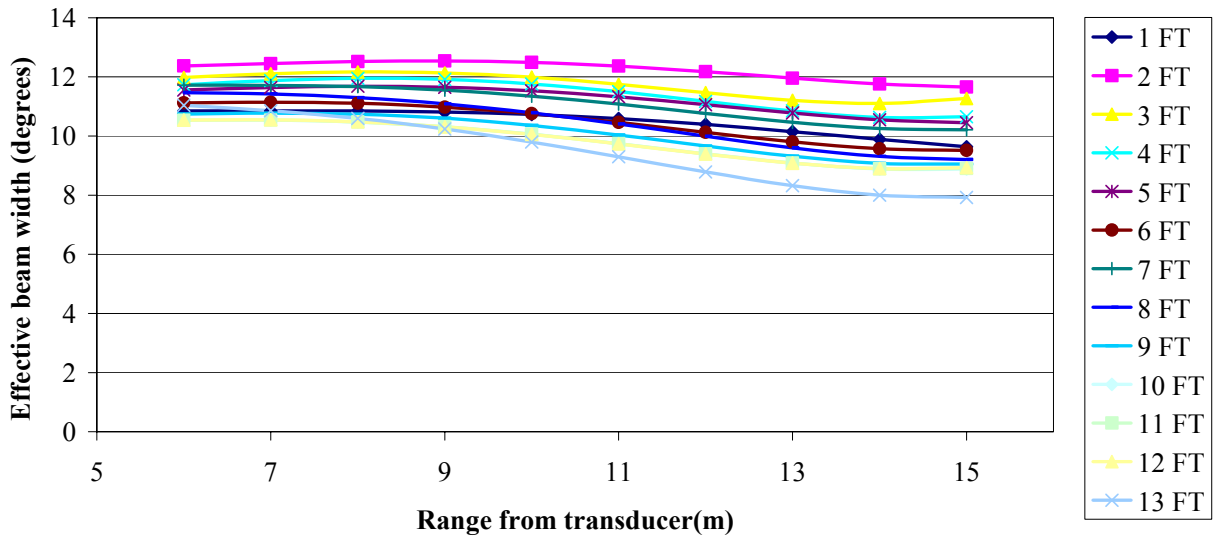


Figure 6. Spring night spill.

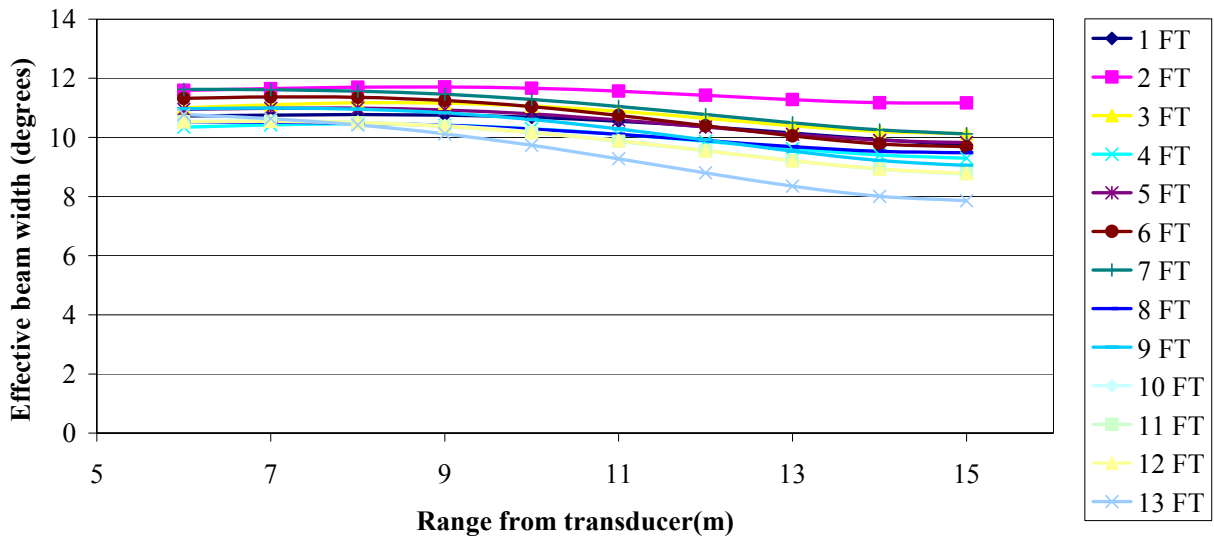


Figure 7. Summer day spill.

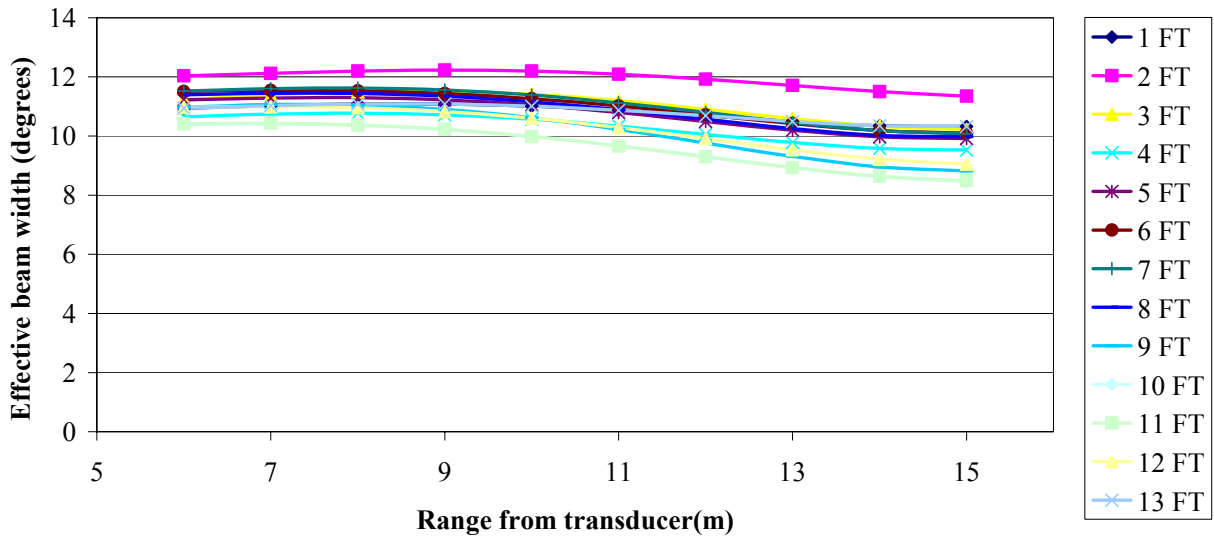


Figure 8. Summer night spill.

Appendix G
Spill Bay Hydraulics

Appendix G

Spill Bay Hydraulics

Detailed spillway hydraulic data were based on a computational fluid dynamics model. A dynamic flow model (Flow3D™) was run for each spill gate opening. The model runs were completed by PNNL based on hydraulic modeling work previously funded by the U.S. Army Corps of Engineers, Portland District. The flows used to calibrate the model were based on a rating curve developed by the Corps in 2002 (Table 1). The median forebay elevation during the hydroacoustic study was 263.3 ft MSL. The flow field output for each model run and the transducer sampling volume are shown below (Figure 1 through Figure 10).

These data are valuable for fish passage studies in a variety of circumstances. Having this type of information *a priori* allows researchers to design and deploy equipment prior to costly field deployments. Instrument performance can be predicted; and, in the case of hydroacoustics, the detectability of fish passing through the beam can be estimated for the deployment location. This type of information is also useful *a posteriori*. For example, to verify predictions made pre-season. Another use is to compare fish and hydraulic data numerically, as has been done in the body of the report. However, this is useful only when sufficient split-beam data is collected because of the additional trajectory information collected with each fish.

Table 1. Flows for vertical gate openings based on the 2002 rating curve and a forebay elevation of 263.3 ft.

Vertical Gate Opening (ft)	Q (cfs)
1	1,569
2	3,384
3	5,190
4	7,001
5	8,795
6	10,596
7	12,393
8	14,185
9	15,971
10	17,750

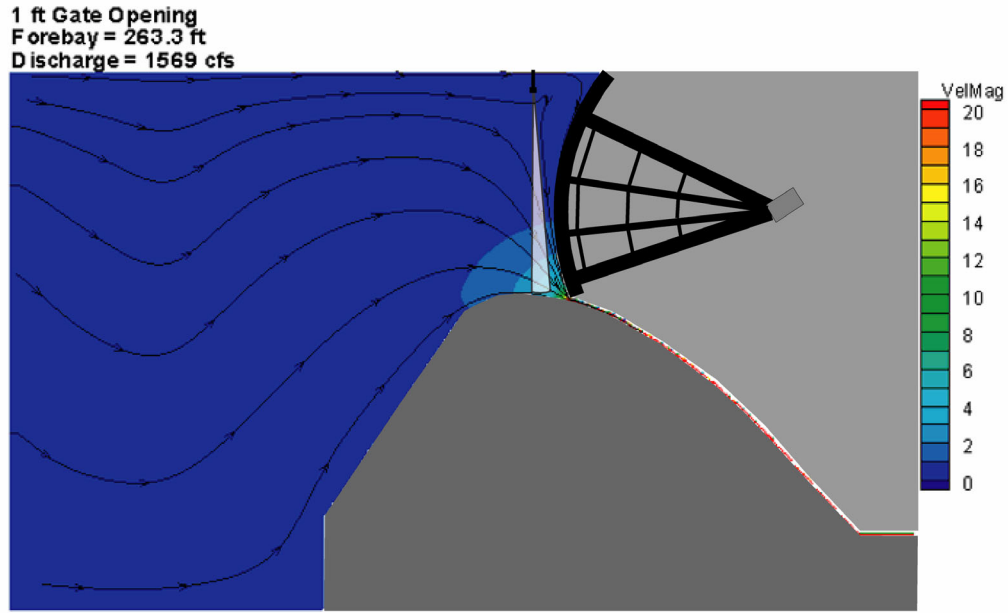


Figure 1. Spill bay with a 1 ft gate opening. Velocities shown are in ft/s. The transducer sampling volume is also shown for reference.

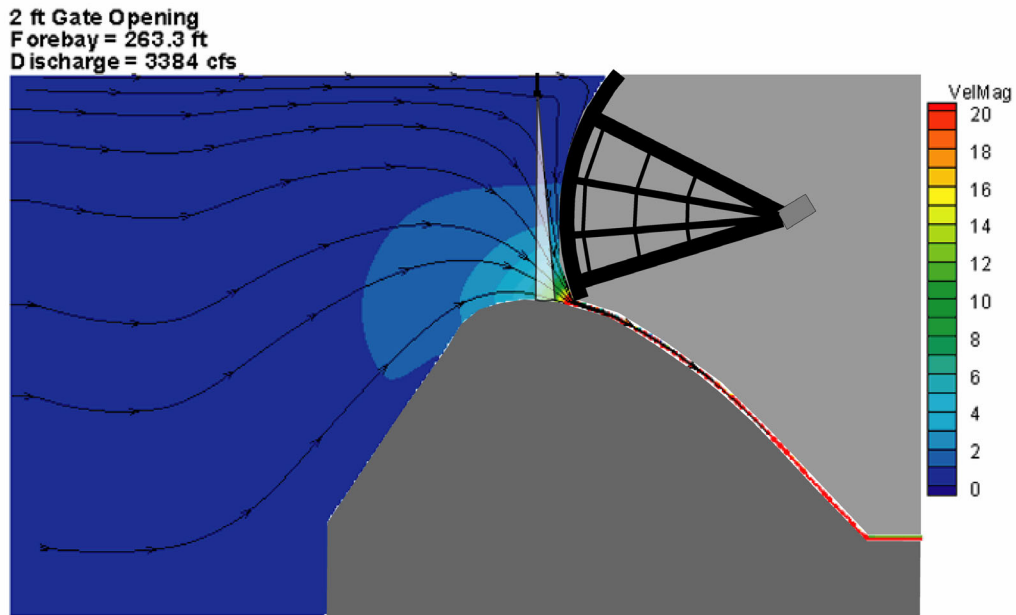


Figure 2. Spill bay with a 2 ft gate opening. Velocities shown are in ft/s. The transducer sampling volume is also shown for reference.

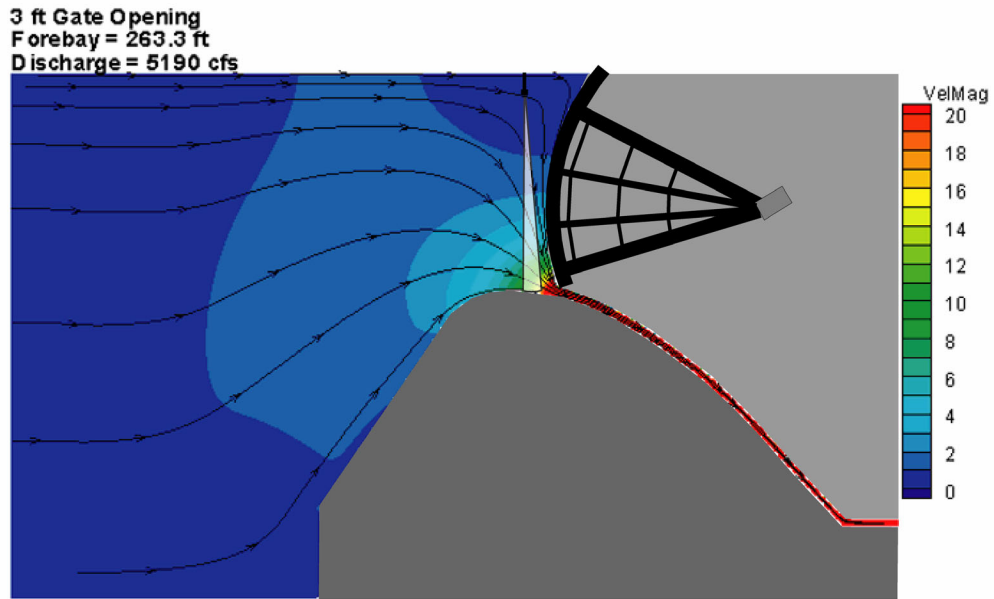


Figure 3. Spill bay with a 3 ft gate opening. Velocities shown are in ft/s. The transducer sampling volume is also shown for reference.

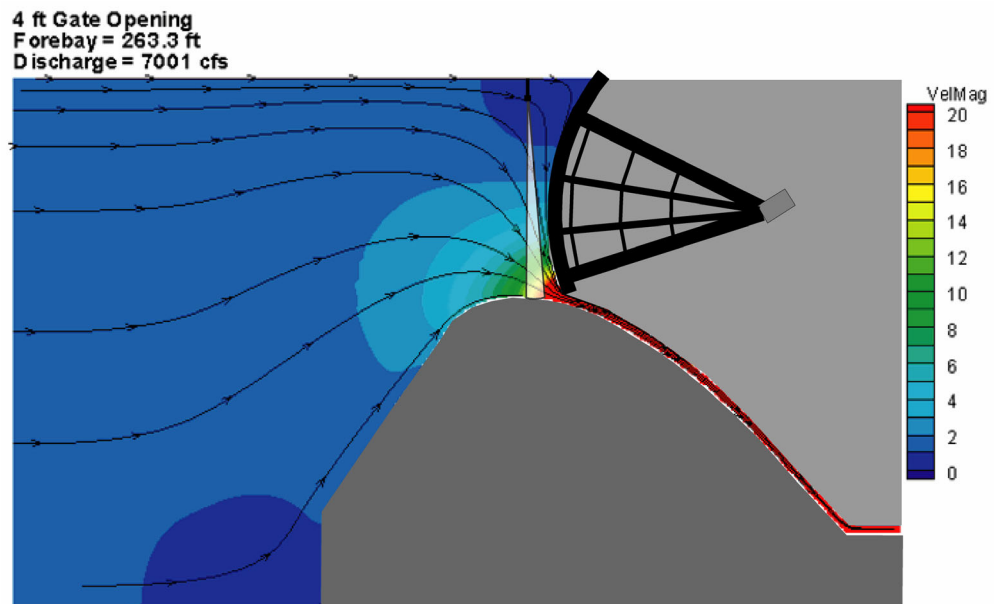


Figure 4. Spill bay with a 4 ft gate opening. Velocities shown are in ft/s. The transducer sampling volume is also shown for reference.

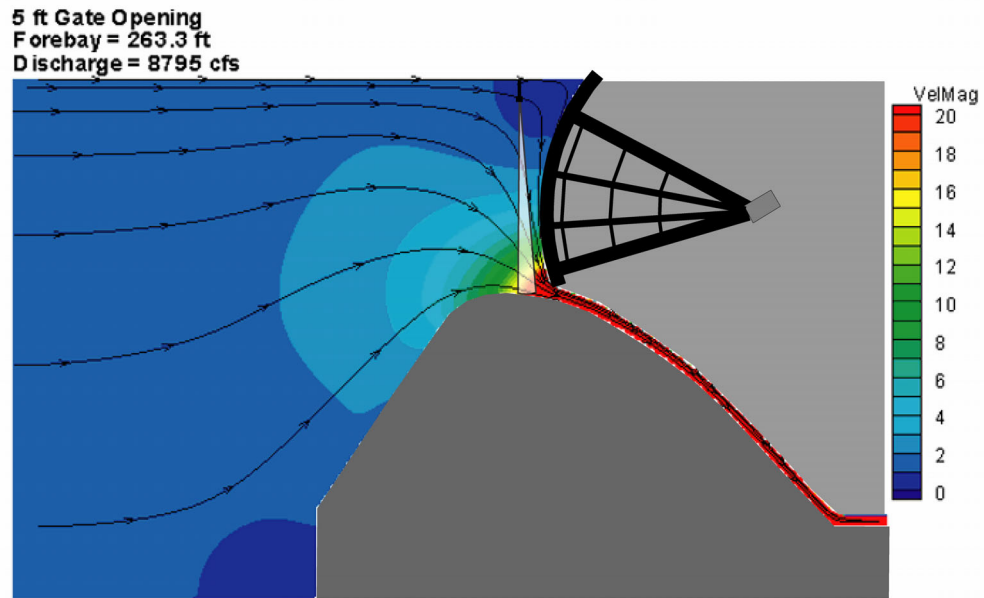


Figure 5. Spill bay with a 5 ft gate opening. Velocities shown are in ft/s. The transducer sampling volume is also shown for reference.

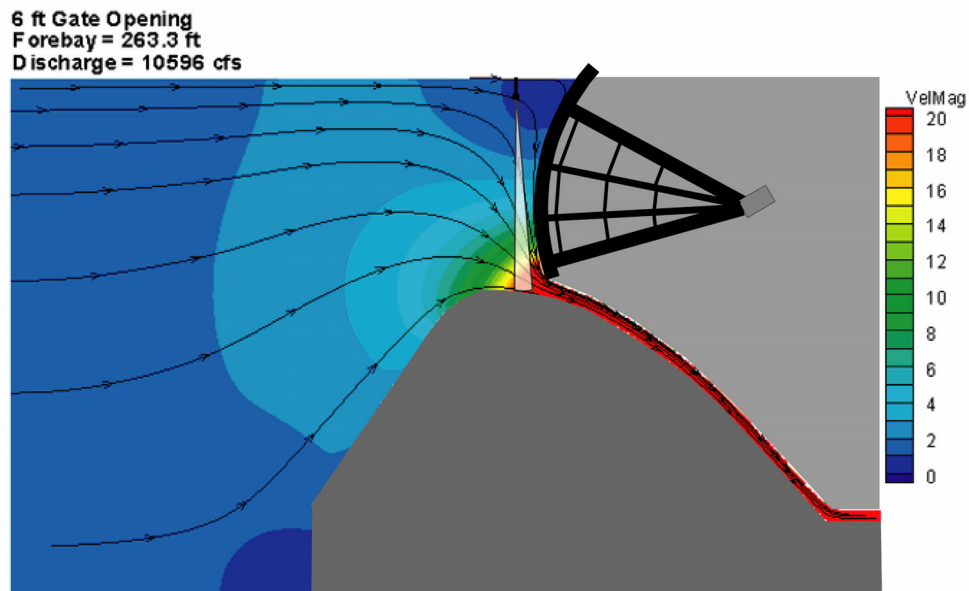


Figure 6. Spill bay with a 6 ft gate opening. Velocities shown are in ft/s. The transducer sampling volume is also shown for reference.

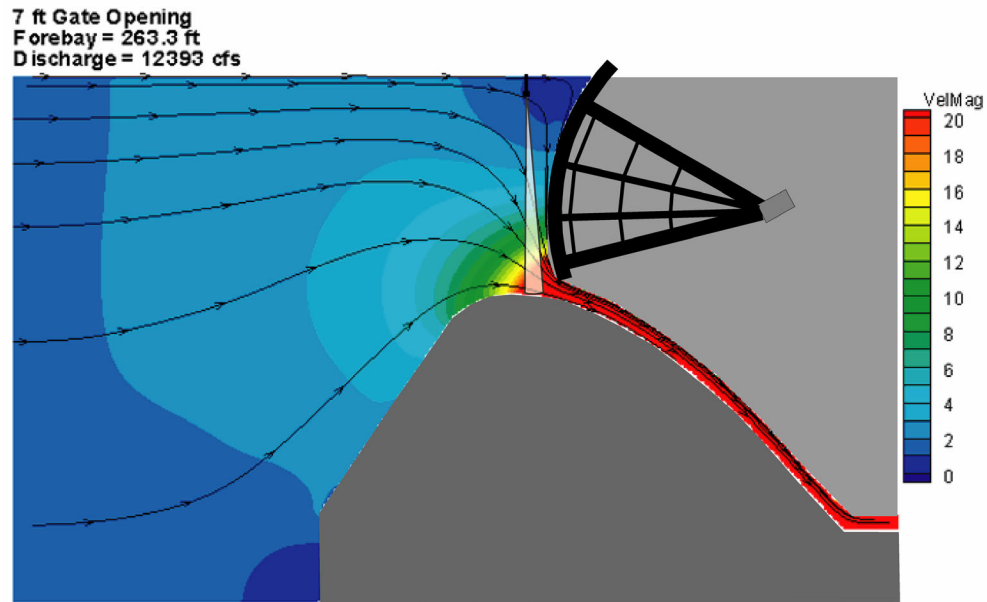


Figure 7. Spill bay with a 7 ft gate opening. Velocities shown are in ft/s. The transducer sampling volume is also shown for reference.

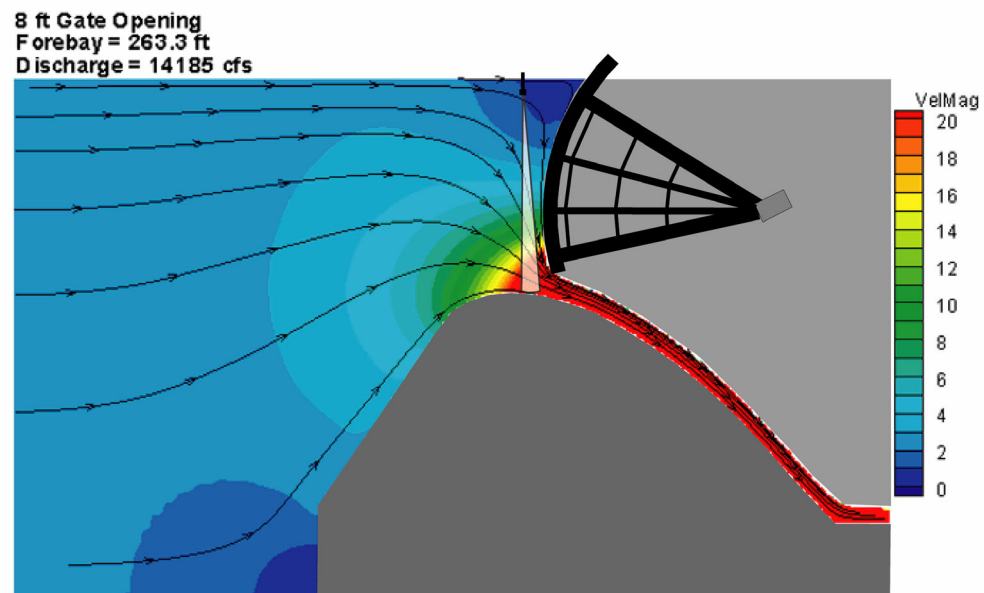


Figure 8. Spill bay with a 8 ft gate opening. Velocities shown are in ft/s. The transducer sampling volume is also shown for reference.

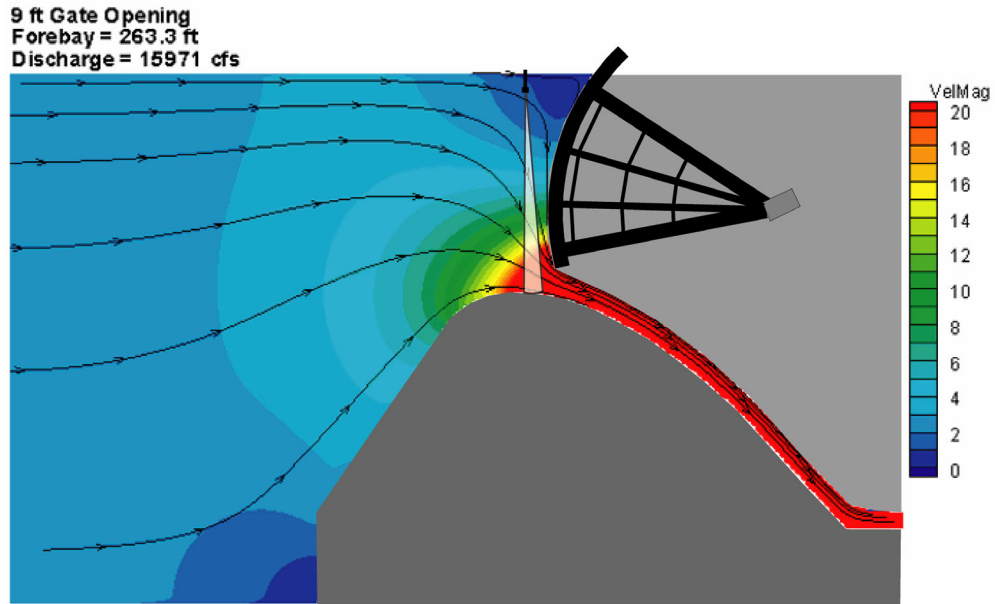


Figure 9. Spill bay with a 9 ft gate opening. Velocities shown are in ft/s. The transducer sampling volume is also shown for reference.

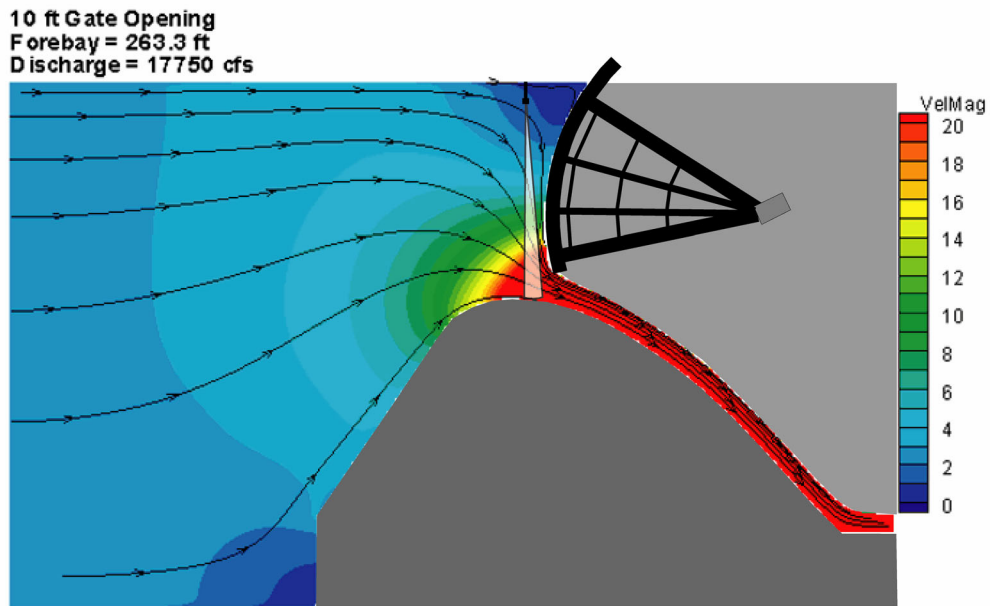


Figure 10. Spill bay with a 10 ft gate opening. Velocities shown are in ft/s. The transducer sampling volume is also shown for reference.

Appendix H
Hourly Spill by Block

Appendix H

Hourly Spill by Block

The following series of graphs show the hourly spill proportion by each four-day block of this study. These graphs illustrate how close the actual dam operations came to the preseason treatment goals.

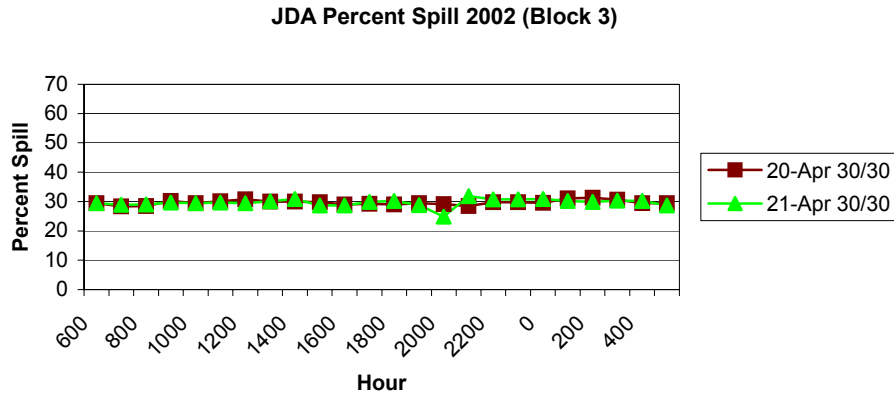


Figure 1. Block 3, spring, censored.

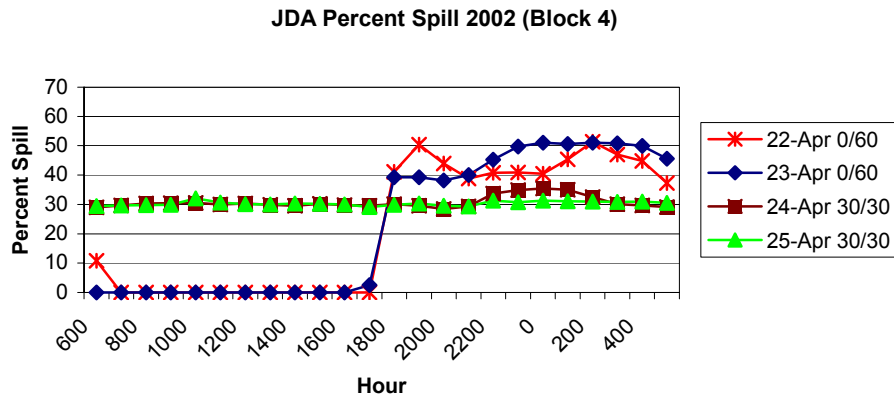


Figure 2. Block 4, spring, censored.

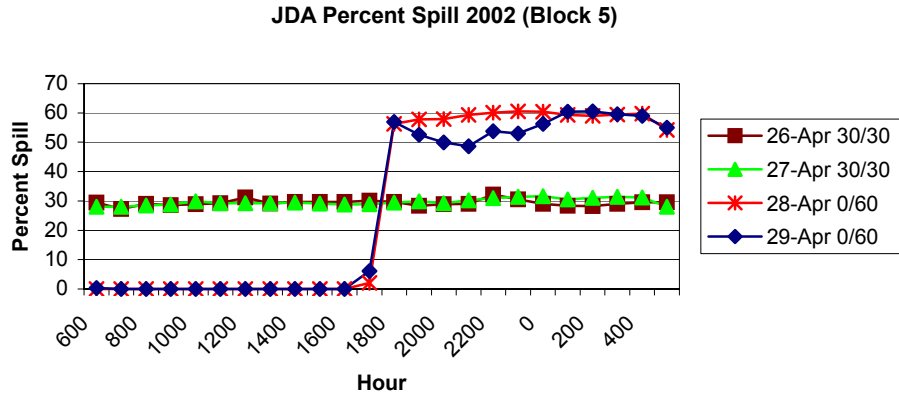


Figure 3. Block 5, spring, accepted for ANOVA.

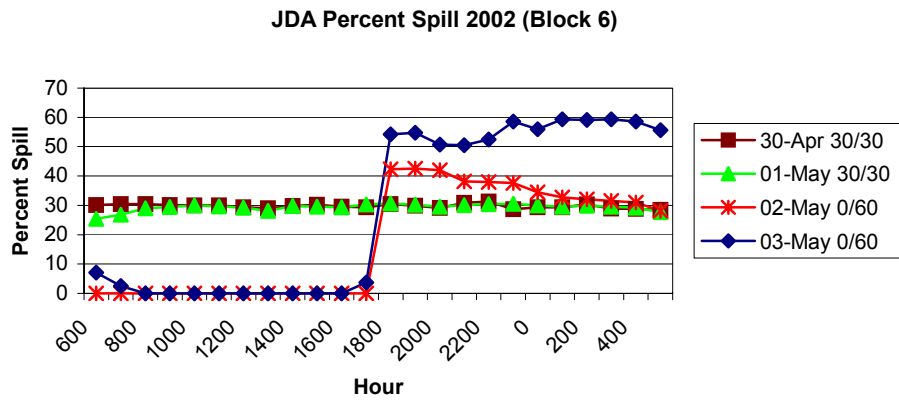


Figure 4. Block 6, spring, accepted for ANOVA.

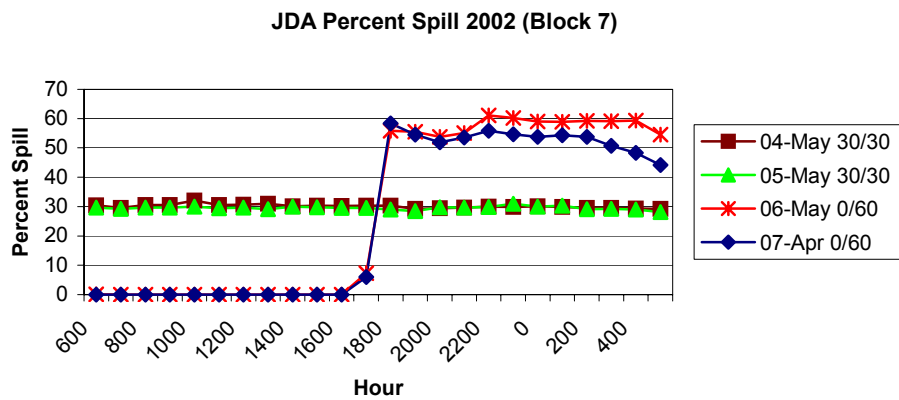


Figure 5. Block 7, spring, accepted for ANOVA.

JDA Percent Spill 2002 (Block 8)

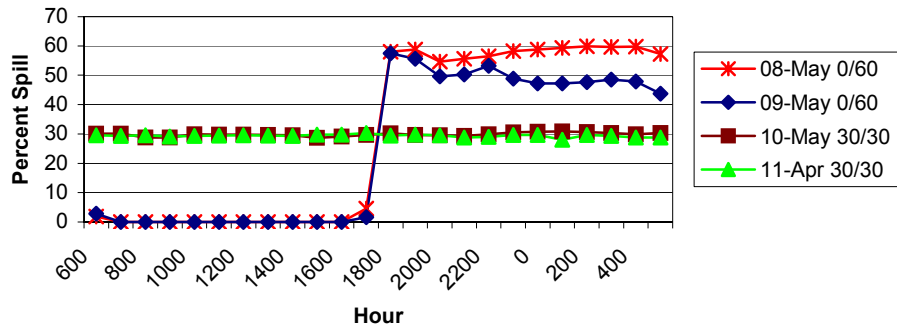


Figure 6. Block 8, spring, accepted for ANOVA.

JDA Percent Spill 2002 (Block 9)

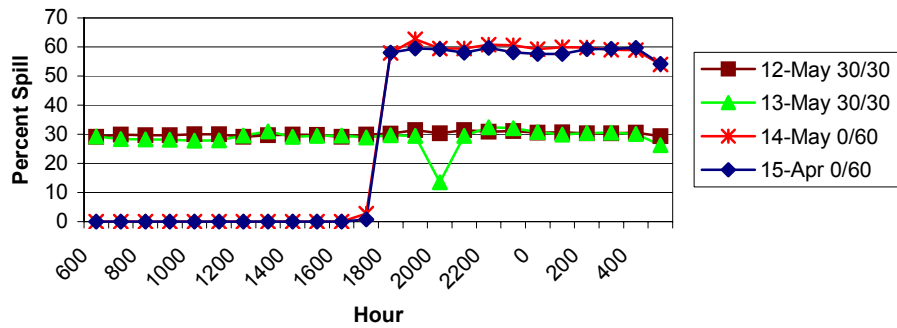


Figure 7. Block 9, spring, accepted for ANOVA.

JDA Percent Spill 2002 (Block 10)

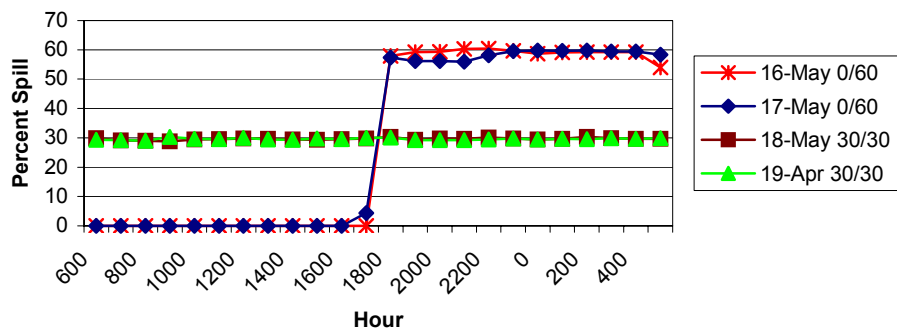


Figure 8. Block 10, spring, accepted for ANOVA.

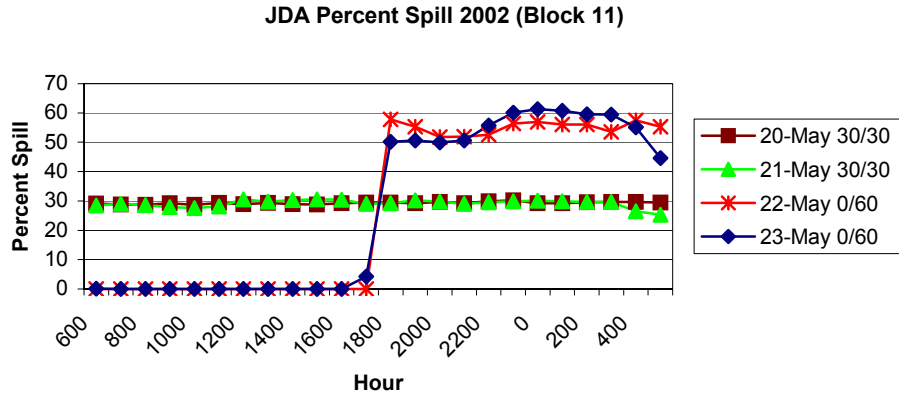


Figure 9. Block 11, spring, accepted for ANOVA.

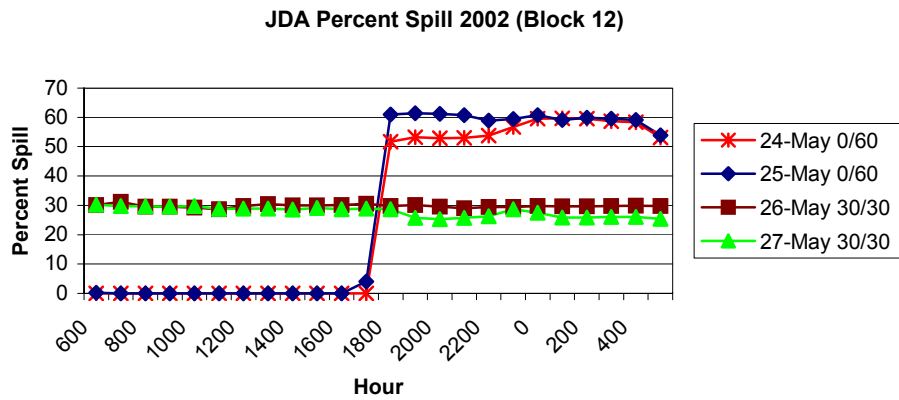


Figure 10. Block 12, spring, accepted for ANOVA.

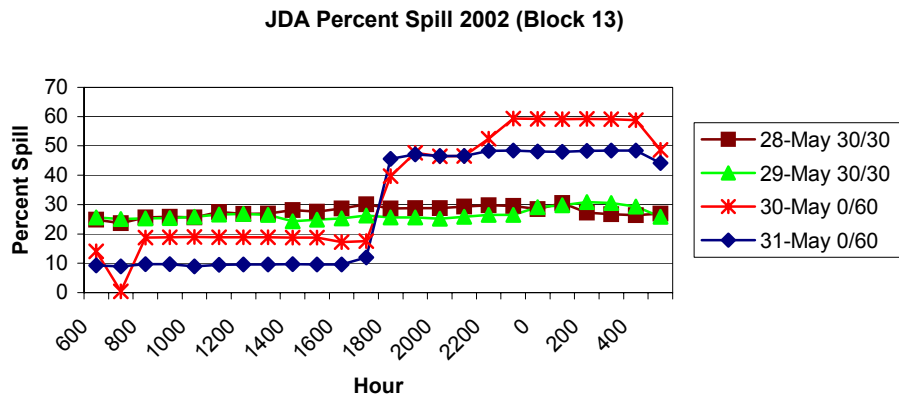


Figure 11. Block 13, spring, accepted for ANOVA.

JDA Percent Spill 2002 (Block 14)

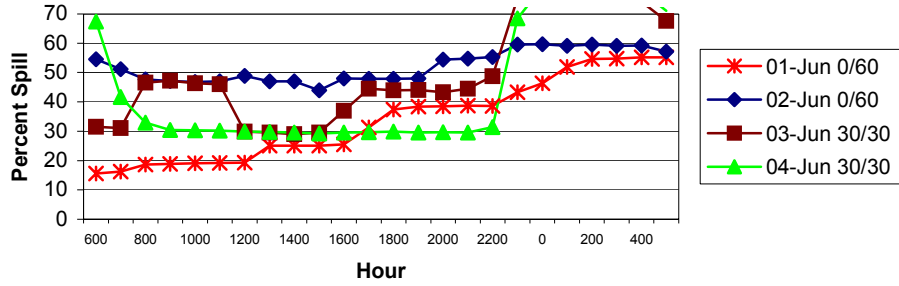


Figure 12. Block 14, spring, censored.

JDA Percent Spill 2002 (Block 15)

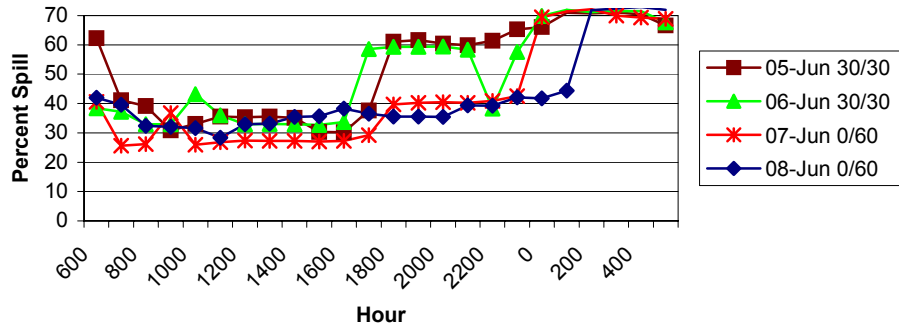


Figure 13. Block 15, summer, censored.

JDA Percent Spill 2002 (Block 16)

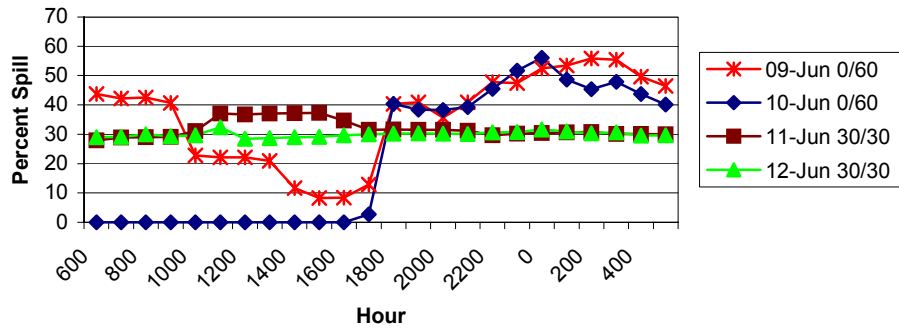


Figure 14. Block 16, summer, censored.

JDA Percent Spill 2002 (Block 17)

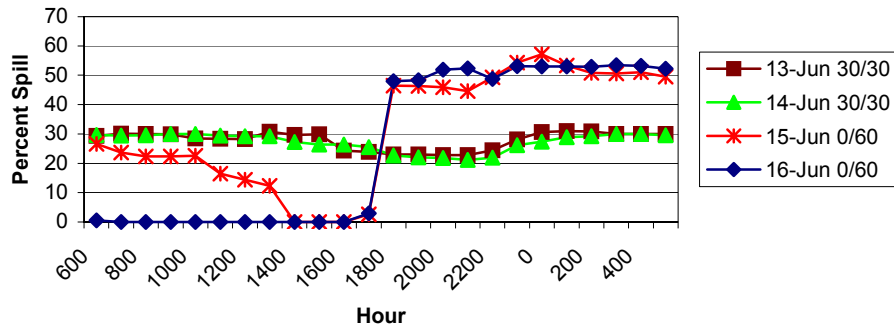


Figure 15. Block 17, summer, accepted for ANOVA.

JDA Percent Spill 2002 (Block 18)

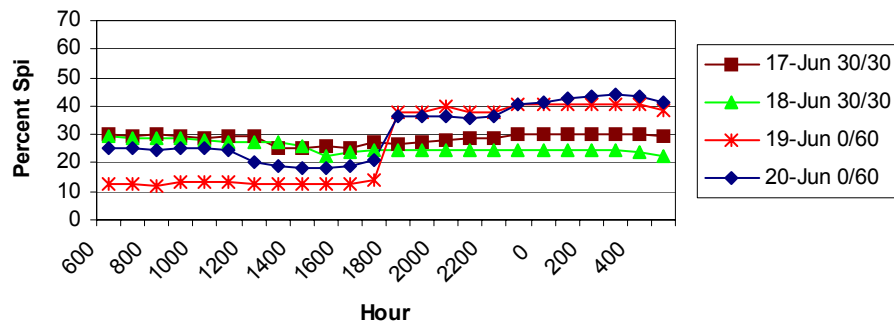


Figure 16. Block 18, summer, accepted for ANOVA.

JDA Percent Spill 2002 (Block 19)

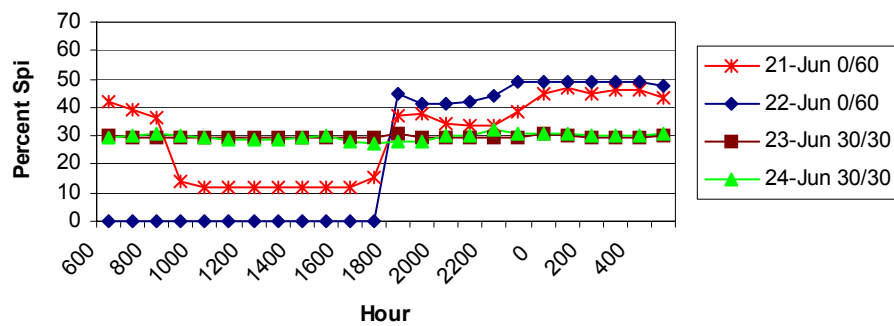


Figure 17. Block 19, summer, accepted for ANOVA.

JDA Percent Spill 2002 (Block 20)

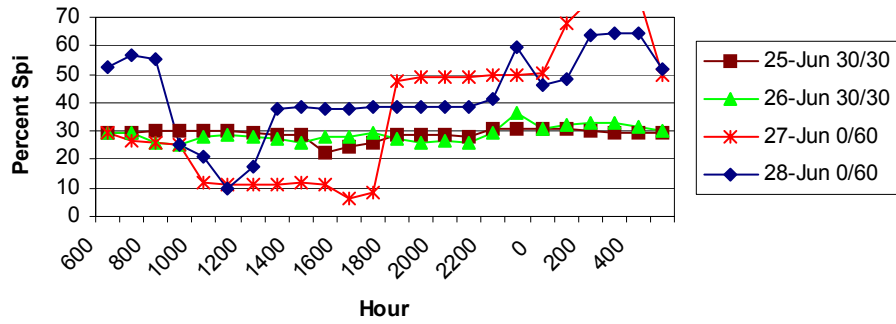


Figure 18. Block 20, summer, censored.

JDA Percent Spill 2002 (Block 21)

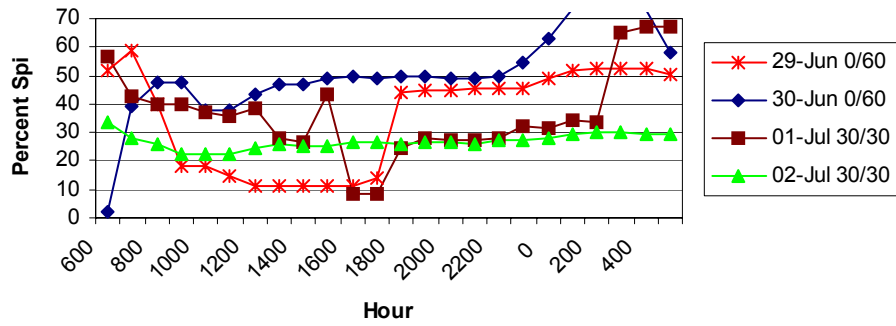


Figure 19. Block 21, summer, censored.

JDA Percent Spill 2002 (Block 22)

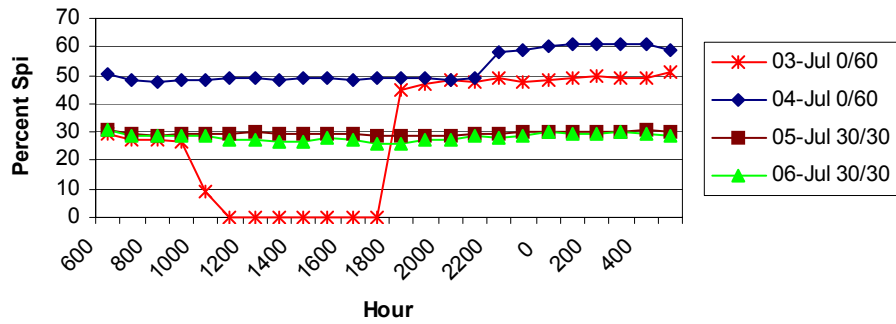


Figure 20. Block 22, summer, censored.

JDA Percent Spill 2002 (Block 23)

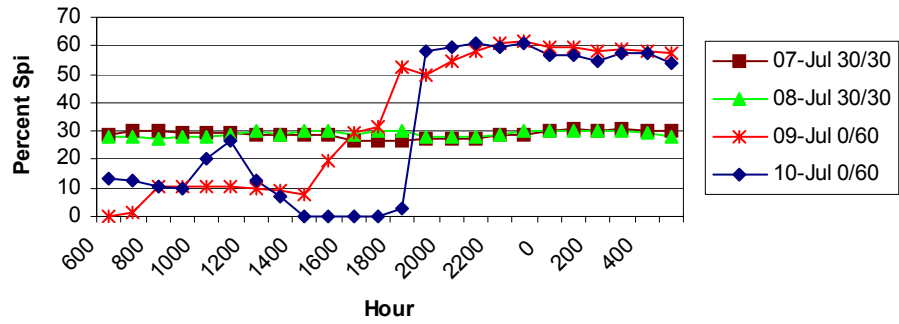


Figure 21. Block 23, summer, accepted for ANOVA.

JDA Percent Spill 2002 (Block 24)

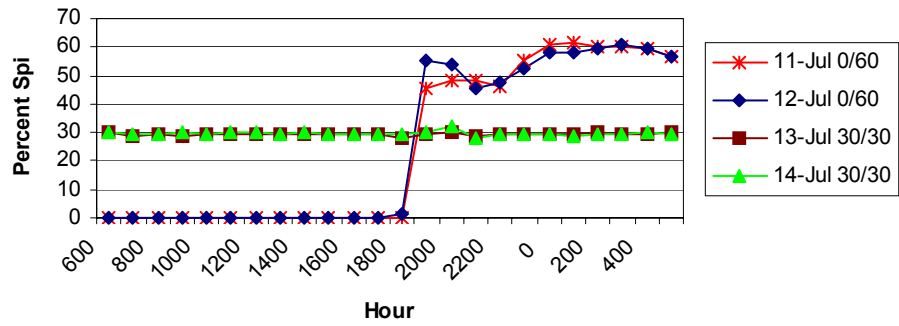


Figure 22. Block 24, summer, accepted for ANOVA.